NAVAL POSTGRADUATE SCHOOL

MONTEREY, CALIFORNIA

THESIS

DESIGN AND ANALYSIS OF A HYDROGEN COMPRESSION AND STORAGE STATION

by

Edward A. Fosson

December 2017

Thesis Advisor: Anthony Gannon
Co-Advisor: Andrea Holmes

THIS PAGE INTENTIONALLY LEFT BLANK

REPORT DOCUMENTATION PAGE			*Form Approved OMB No. 0704–0188*

1. AGENCY USE ONLY ***(Leave blank)***	**2. REPORT DATE** December 2017	**3. REPORT TYPE AND DATES COVERED** Master's thesis

4. TITLE AND SUBTITLE DESIGN AND ANALYSIS OF A HYDROGEN COMPRESSION AND STORAGE STATION	**5. FUNDING NUMBERS**
6. AUTHOR(S) Edward A. Fosson	
7. PERFORMING ORGANIZATION NAME(S) AND ADDRESS(ES) Naval Postgraduate School Monterey, CA 93943-5000	**8. PERFORMING ORGANIZATION REPORT NUMBER**
9. SPONSORING /MONITORING AGENCY NAME(S) AND ADDRESS(ES) Project supported by the Office of Naval Research's (ONR) Energy Systems Technology Evaluation Program (ESTEP), supported by Dr. Richard Carlin and under the technical monitoring of Marissa Brand.	**10. SPONSORING / MONITORING AGENCY REPORT NUMBER**

11. SUPPLEMENTARY NOTES The views expressed in this thesis are those of the author and do not reflect the official policy or position of the Department of Defense or the U.S. Government. IRB number ____N/A____.

12a. DISTRIBUTION / AVAILABILITY STATEMENT Approved for public release. Distribution is unlimited.	**12b. DISTRIBUTION CODE**

13. ABSTRACT (maximum 200 words)

This research investigates the use of an electrochemical hydrogen compressor in an energy storage station. The electrochemical hydrogen compressor, as a solid-state device, offers the ability to continuously operate for long periods without the need to replace mechanical seals, lubricants, or filters. The two-part study consists of station design and performance testing of a commercial-off-the-shelf electrochemical hydrogen compressor. Station design used American Society of Mechanical Engineers (ASME), National Fire Protection Association (NFPA), and Compressed Gas Association (CGA) standards for risk mitigation and determination of feasibility for Department of Defense (DOD) and Navy application. Analysis of the compressor includes a comparison of actual field performance to ideal isothermal and adiabatic compression of hydrogen. Performance characteristics are investigated over a range of variable inputs for use during future optimization of the compression and storage station.

The hydrogen compression and storage station is one subsystem of a multi-system demonstration of solar energy storage using hydrogen as the primary storage medium. The larger system integrates commercial-off-the-shelf photovoltaic solar panels, solid-state hydrogen electrolyzers, solid-state electrochemical compressors, and proton exchange membrane fuel cells to demonstrate renewable energy storage. The compression and storage station design allows for reconfiguration and further research in hydrogen technologies. Similar systems could be used on Navy shore installations, on expeditionary bases, and at sea to increase resiliency and reduce logistical demand for fuels.

14. SUBJECT TERMS electrochemical hydrogen compressor, hydrogen compression, hydrogen storage, energy storage, renewable energy storage	**15. NUMBER OF PAGES** 139
	16. PRICE CODE

17. SECURITY CLASSIFICATION OF REPORT	**18. SECURITY CLASSIFICATION OF THIS PAGE**	**19. SECURITY CLASSIFICATION OF ABSTRACT**	**20. LIMITATION OF ABSTRACT**
Unclassified	Unclassified	Unclassified	UU

NSN 7540–01-280-5500 Standard Form 298 (Rev. 2–89)
Prescribed by ANSI Std. 239–18

THIS PAGE INTENTIONALLY LEFT BLANK

Approved for public release. Distribution is unlimited.

DESIGN AND ANALYSIS OF A HYDROGEN COMPRESSION AND STORAGE STATION

Edward A. Fosson
Lieutenant Commander, United States Navy
B.S., United States Naval Academy, 2005

Submitted in partial fulfillment of the
requirements for the degree of

MASTER OF SCIENCE IN MECHANICAL ENGINEERING

from the

NAVAL POSTGRADUATE SCHOOL
December 2017

Approved by: Anthony Gannon
Thesis Advisor

Andrea Holmes
Co-Advisor

Garth Hobson
Chair, Department of Mechanical and Aerospace Engineering

THIS PAGE INTENTIONALLY LEFT BLANK

ABSTRACT

This research investigates the use of an electrochemical hydrogen compressor in an energy storage station. The electrochemical hydrogen compressor, as a solid-state device, offers the ability to continuously operate for long periods without the need to replace mechanical seals, lubricants, or filters. The two-part study consists of station design and performance testing of a commercial-off-the-shelf electrochemical hydrogen compressor. Station design used American Society of Mechanical Engineers (ASME), National Fire Protection Association (NFPA), and Compressed Gas Association (CGA) standards for risk mitigation and determination of feasibility for Department of Defense (DOD) and Navy application. Analysis of the compressor includes a comparison of actual field performance to ideal isothermal and adiabatic compression of hydrogen. Performance characteristics are investigated over a range of variable inputs for use during future optimization of the compression and storage station.

The hydrogen compression and storage station is one subsystem of a multi-system demonstration of solar energy storage using hydrogen as the primary storage medium. The larger system integrates commercial-off-the-shelf photovoltaic solar panels, solid-state hydrogen electrolyzers, solid-state electrochemical compressors, and proton exchange membrane fuel cells to demonstrate renewable energy storage. The compression and storage station design allows for reconfiguration and further research in hydrogen technologies. Similar systems could be used on Navy shore installations, on expeditionary bases, and at sea to increase resiliency and reduce logistical demand for fuels.

THIS PAGE INTENTIONALLY LEFT BLANK

TABLE OF CONTENTS

LIST OF FIGURES

THIS PAGE INTENTIONALLY LEFT BLANK

LIST OF TABLES

THIS PAGE INTENTIONALLY LEFT BLANK

LIST OF ACRONYMS AND ABBREVIATIONS

ASME	American Society of Mechanical Engineers
C4ISR	Command, Control, Communications, Computers, Intelligence, Surveillance, and Reconnaissance
CAISO	California Independent System Operator
CFR	United States Code of Federal Regulations
CGA	Compressed Gas Association
DOD	Department of Defense
EHC	electrochemical hydrogen compressor
ESTEP	Energy Systems Technology Evaluation Program
EXWC	Engineering and Expeditionary Warfare Center
HAZCOM	hazard communication standard
HMC&M	hazardous material control and management
ISD	inherently safer design
NAVFAC	Naval Facilities Engineering Command
NFPA	National Fire Protection Association
OEM	original equipment manufacturer
OSHA	Occupational Safety and Health Administration
PEM	proton exchange membrane
psig	pounds per square inch gauge
PSM	process safety management
RMP	risk management program
slpm	standard liters per minute
TTPs	tactics, techniques, and procedures
UAV	unmanned aerial vehicle

THIS PAGE INTENTIONALLY LEFT BLANK

ACKNOWLEDGMENTS

First and foremost, I thank my beautiful, loving, patient, and inspiring wife. She has sacrificed her career and time spent with friends and family to accompany me during my own pursuit of happiness.

I also owe a debt of gratitude to the Naval Postgraduate School's Mechanical and Aerospace Engineering Department and Energy Academic Group staff and faculty for providing unparalleled leadership, instruction, and support during my project.

I would like to specifically thank Professor Anthony Gannon for his inspiration and dedication to helping students and supporting the Navy and Department of Defense energy mission. I am very grateful for your wisdom and guidance and wish you the very best as you continue tackling the Navy's engineering, administrative, and acquisition challenges. I also thank Professor Garth Hobson for his enthusiastic support of my research and steadfast pursuit of excellence in the MAE department. Your sound leadership and genius are displayed through all the brilliant students who pass through the department, and I am grateful to have been among them. I also thank Professor Maximilian Platzer and Professor Christopher Brophy for their encouragement and kindness as well as the Turbopropulsion Laboratory staff, Andrea Holmes and John Gibson, for their direct support and guidance during all stages of my project. I could not have completed this project without your help and I am truly grateful to have worked with you. And lastly, many thanks to the Rocket Propulsion Laboratory staff, Bobby Wright and David Dausen, who provided invaluable expertise, material, advice, and time to help in getting the station running. Thank you, gentlemen.

THIS PAGE INTENTIONALLY LEFT BLANK

I. INTRODUCTION

The purpose of this research is to design, build, and test a renewably powered hydrogen gas compression and storage station incorporating an electrochemical hydrogen gas compressor. The research, funded through the Office of Naval Research Engineering Systems Technology Evaluation Program, is intended to further the ongoing efforts to develop low-cost hydrogen infrastructure in the Navy. Potential applications of this research include energy storage at shore installations with renewably generated power, expeditionary microgrids, and sea-based hydrogen harvesting.

A. WHY IS A COMPRESSION AND STORAGE STATION NECESSARY?

Generating renewable and sustainable energy is the cornerstone of the ongoing Department of Defense (DOD) drive for increasing resiliency at shore installations. There are several methods of generating power from renewable energy sources, but most of these are limited in their reliability due to existing energy storage options. Significant investments have been made in developing advanced batteries and superconductors as a solution. Currently, supply chains are developing to provide grid-scale electrical power storage using batteries and supercapacitors. With a high gravimetric energy density, hydrogen gas offers an enticing alternative. Hydrogen could serve as either an alternative to batteries and supercapacitors or a supplementary storage medium within a portfolio of several storage technologies.

Previous research by Aviles at the Naval Postgraduate School demonstrated the feasibility of using solar photovoltaic electricity to extract water from ambient air and then use the water to make hydrogen gas [1]. This project also used the hydrogen gas in a fuel cell to produce electricity. Adding a hydrogen compression and storage station to this system will enable electrical power generation during times when the photovoltaic array cannot operate. Once compressed hydrogen gas is made readily available onsite, other systems can make use of the fuel such as generators, fuel cell powered vehicles, and unmanned vehicles.

The DOD has traditionally focused its alternative fuel investments in drop-in alternative fuels for existing platforms. The DOD and Navy define alternative fuels as those derived from materials other than fossil fuels [2]. Renewably generated hydrogen gas, such as the hydrogen station demonstrated at NPS, falls into this category of alternative fuels. Current DOD policy is to "diversify and expand energy supplies and sources, including renewable energy sources and alternative fuels" [3]. By analyzing hydrogen storage technologies, this research is helping to achieve the DOD's "policy to enhance military capability, improve energy security, and mitigate costs in its use and management of energy" [3].

B. WHAT ARE ELECTROCHEMICAL COMPRESSORS AND WHY USE THEM?

Electrochemical hydrogen compressors (EHCs) are solid-state devices that use direct current electricity to transport hydrogen through a proton exchange membrane and build pressure into a pressure vessel. Their physical construction, operation, and theory are very similar to that of a proton exchange membrane fuel cell. There are numerous potential advantages to using EHCs as opposed to traditional mechanical compressors; most notably, the solid-state EHCs are not subject to the same mechanical friction and thermodynamic losses of their mechanical counterparts. The EHC is also designed to follow an isothermal compression process which requires less energy than the adiabatic process of mechanical compressors. A third core advantage is the inherent purification process that happens as hydrogen gets transported through the membranes.

Figure 1 illustrates the process of hydrogen transfer through the membrane. As low-pressure hydrogen is supplied to the inlet (anode), it oxidizes due to the electrical potential. Each hydrogen atom loses an electron at the anode, and this electron gets transported via the electrical power supply to the cathode. Since the former hydrogen atom is now missing an electron, it becomes a proton which is attracted to the cathode and pulled through the membrane. At the cathode, each proton receives an electron, becomes a hydrogen atom, bonds with another hydrogen atom, and exits through the compressor outlet. As hydrogen flows out of the compressor outlet, it fills the storage

vessel and increases the vessel pressure until the power supply is turned off, a relief valve is opened, or the compressor reaches its maximum compression.

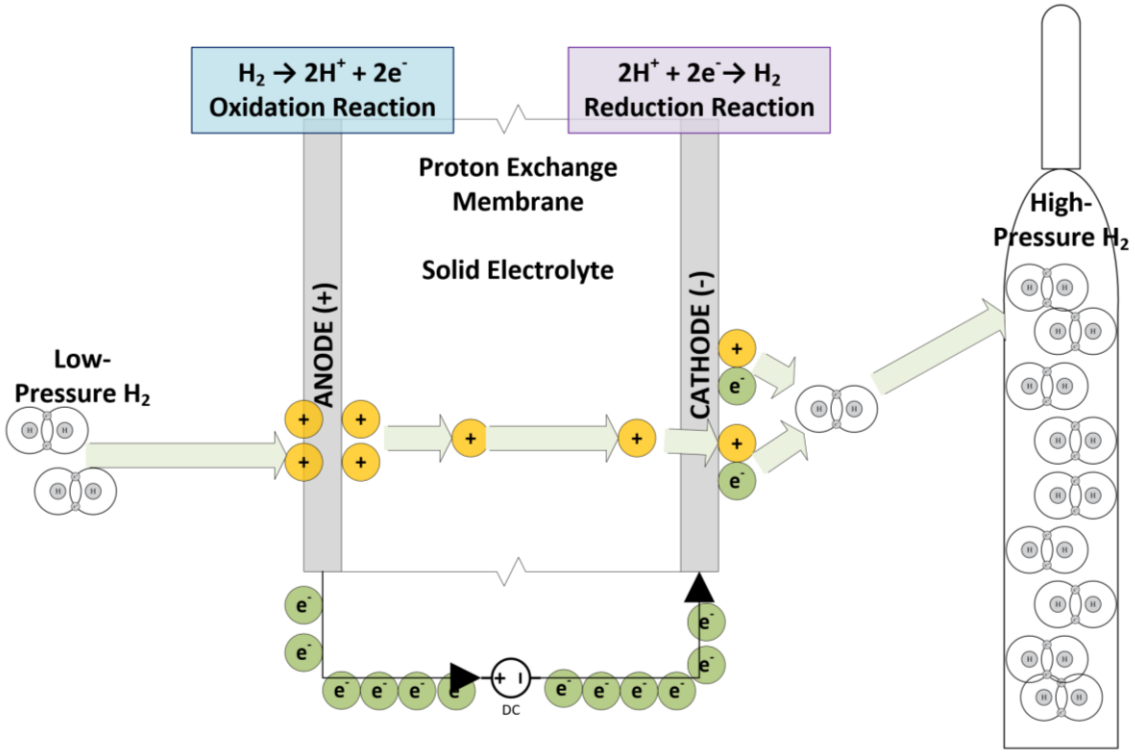

Figure 1. Electrochemical Hydrogen Compression Half-Cell Reactions

One half-cell consists of the oxidation of hydrogen along the anode, $H_2 \rightarrow 2H^+ + 2e^-$. The other consists of its reduction along the cathode, $2H^+ + 2e^- \rightarrow H_2$. Together, these reactions are governed by the Nernst Equation (1), which can provide the theoretical cell potential needed from the power supply to drive the reactions:

$$V_{theoretical} = \frac{R \cdot T}{n \cdot F} \ln\left(\frac{P_2}{P_1}\right) \quad (1)$$

This theory and governing equation will be discussed later along with the results from testing the EHC.

Most hydrogen compressors used today are mechanical diaphragm or piston compressors. Mechanical compression systems have relatively simple construction, maintenance, and repair procedures. Several major manufacturers offer mechanical compressors with a wide range of inlet and outlet pressure configurations, with and without integrated cooling, lubricated or unlubricated, and several other options that must be considered when selecting a compressor. While the technology for mechanical compression is mature, they have several inherent drawbacks.

Mechanical compressors are limited to how much compression they can achieve. Piston compressors are limited to a single stage compression ratio of 4–6:1 while diaphragm compressors can achieve 15–20:1 ratios in a single stage. EHCs, however, are scalable to achieve a desired flow rate and have demonstrated compression ratios of 300:1 [4].

Mechanical compressors are also expensive both in up-front capital expenditure requirements and operation and maintenance. Figure 2 demonstrates the high cost of compression using traditional mechanical compressors. The cost breakdown comes from a study conducted by the National Renewable Energy Laboratory in 2014 and includes initial capital expenditure, as well as, operation and maintenance costs. The study noted that the compressors had wide ranges of reliability and efficiency, making it more difficult to break down the relative costs of compression.

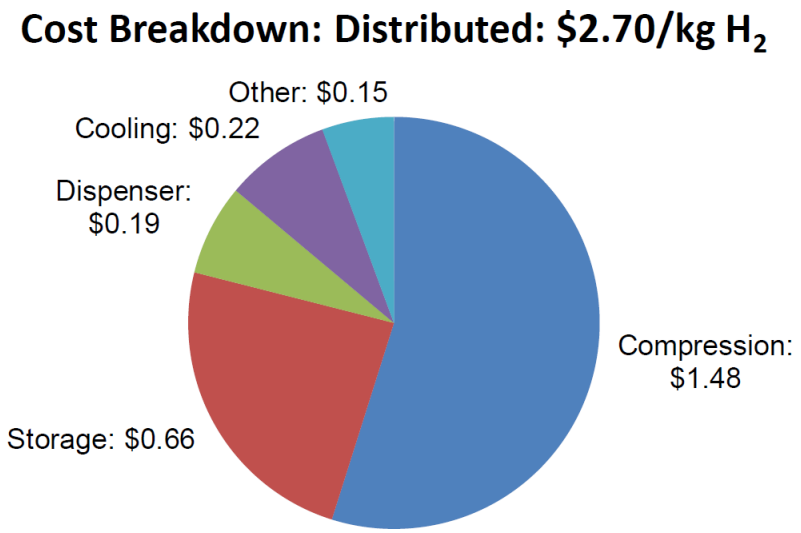

Figure 2. Cost Breakdown for Hydrogen Generation Station. Source: [5].

Mechanical compressors are also large, heavy, loud, and usually, require several hazardous materials to operate efficiently. 'Small' mechanical compressors can weigh as much as 200–400 kg. The smallest mechanical compressor found on the market was 170 kg and 0.5 m3 while it could only compress to 51 Bar. Operating this compressor would require hearing protection and handling of hydraulic fluid and lubricants. EHCs, on the other hand, are silent, compact, and do not require handling hazardous materials. The small compression and storage station designed and tested for this research would not be feasible without the EHC. Neither the space available, budget, or gas generator could support using a mechanical compressor.

C. WHY COMPRESS HYDROGEN GAS?

Hydrogen is considered an energy storage medium and not an energy source. Hydrogen is the third most abundant element on Earth, but it is not found naturally in large and concentrated quantities. Energy sources such as fossil fuels, solar, and wind can be found naturally in both useable form and quantities. Hydrogen, on the other hand, must be extracted from other molecules. Hydrogen can be generated as a byproduct in chemical and biological processes, from electrolysis, or extracted from hydrocarbon molecules, but it cannot be mined, drilled, or captured from the atmosphere in significant quantities.

Once extracted, hydrogen can provide heat and electricity through combustion or reaction in a fuel cell. The oxidation of hydrogen follows the reaction: $2H_2 + O_2 \rightarrow 2H_2O$. The enthalpy of combustion for hydrogen is approximately 141 megajoules per kilogram when the product is liquid water, otherwise known as the higher heating value (HHV). The enthalpy of combustion drops to 121 megajoules per kilogram when the product is water vapor, otherwise known as the lower heating value (LHV). The enthalpy of combustion for hydrogen is nearly triple that of natural gas, propane, gasoline, diesel fuel, and jet fuel. Table 1 provides a brief gravimetric energy comparison of some competing energy sources and storage mediums. The table is listed in descending order of potential gravimetric energy density. Hydrogen offers the best gravimetric alternative to traditional hydrocarbon fuels. However, when the volumetric energy density is considered, hydrogen falls behind many other energy sources and storage mediums. Table 2 provides the volumetric energy comparison, again, sorted in descending order of magnitude. Figure 3 gives a visual reference to the same data and highlights the challenge of making compressed hydrogen gas competitive with liquid hydrocarbon fuels.

Table 1. Gravimetric Energy Densities of Common Energy Sources and Storage Mediums

Energy Source / Storage Medium	Gravimetric Energy Density [MJ/kg]
Gaseous H_2 (g) 1atm	120-142 [6]
Liquid H_2 (l)	120-142 [7]
Compressed Gaseous H_2 (g) 700 Bar	120-142 [7]
Compressed Gaseous H_2 (g) 350 Bar	120-142 [7]
Methane (g)	50.0-55.5 [6]
LNG (l)	49.4-55.2 [8]
LPG Propane (l)	46.0-50.0 [9]
CNG (g)	46.9-49.4 [8]
LPG Butane (l)	45.3-49.13 [9]
Crude Oil (l)	43.1-48.3 [10]
Gasoline (l)	44.5-48.2 [6]
Jet Fuel (l)	42.8-45.7 [6]
Diesel (l)	42.9-45.7 [6]

Energy Source / Storage Medium	Gravimetric Energy Density [MJ/kg]
Biogas Fuel Oil (l)	24.4-41.9 [11]
Commercial by-products (used tires)	38.2 [12]
Coal (s)	16.3-33.5 [11]
Ethanol (l)	26.8-29.7 [6]
Commercial by-products (coffee grounds)	23.8 [12]
Biomass (wood)	19.9-21.3 [11]
Biomass (peat)	8.61-18.6 [11]
Commercial by-products (cow manure)	17.2 [12]
Fuel Cells (2015 Actual)	2.37 [13]
Fuel Cells (2020 Target)	2.34 [13]
Fuel Cells (Ultimate Target)	2.34 [13]
Primary Batteries	0.20-2.12 [14]
Secondary Batteries	0.11-0.72 [14]
Supercapacitors	0.007-0.036 [15]

Values in table are calculated based on physical property values obtained in references listed for each energy source/storage medium.

Table 2. Volumetric Energy Densities of Common Energy Sources and Storage Mediums

Energy Source / Storage Medium	Volumetric Energy Density [MJ/L]
Crude Oil (l)	34.4-47.6 [10]
Jet Fuel (l)	36.0-38.4 [6]
Diesel (l)	36.0-38.4 [6]
Gasoline (l)	33.4-36.2 [6]
Biogas Fuel Oil (l)	17.3-31.4 [11]
Coal (s)	11.0-31.1 [11]
LPG Propane (l)	23.5-25.5 [9]
LPG Butane (l)	23.1-25.1 [9]
Ethanol (l)	23.5 [6]
LNG (l)	22.2 [8]
Biomass (wood)	7.97-21.3 [11]
Commercial by-products (used tires)	14.7-20.2 [12]
Commercial by-products (cow manure)	17.1-17.9 [12]
Biomass (peat)	2.07-17.9 [11]
Liquid H_2 (l)	8.5-9 [7]
CNG (g)	8.44-8.90 [8]
Commercial by-products (coffee grounds)	7.45 [12]

Energy Source / Storage Medium	Volumetric Energy Density [MJ/L]
Primary Batteries	0.5-4.86 [14]
Compressed Gaseous H_2 (g) 700 Bar	4.7 [7]
Fuel Cells (Ultimate Target)	3.06 [13]
Compressed Gaseous H_2 (g) 350 Bar	2.7 [7]
Fuel Cells (2020 Target)	2.34 [13]
Fuel Cells (2015 Actual)	2.304 [13]
Secondary Batteries	0.20-2.05 [14]
Supercapacitors	0.005-0.05 [15]
Methane (g)	0.03-0.04 [6]
Gaseous H_2 (g) 1 atm	0.0098-0.0115 [6]

Values in table are calculated based on physical property values obtained in references listed for each energy source/storage medium.

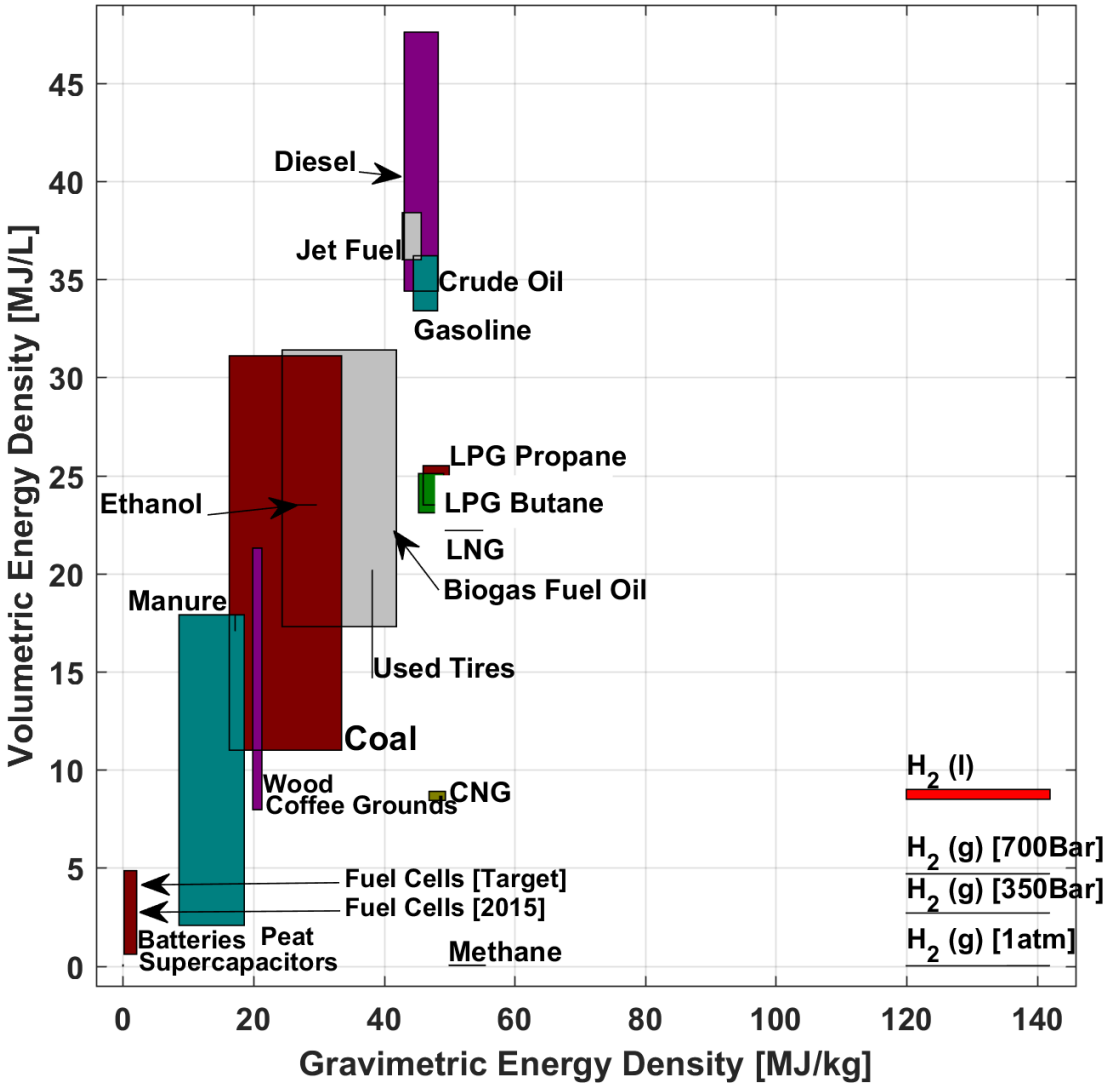

Figure 3. Gravimetric and Volumetric Energy Density Comparison of Common Energy Sources and Storage Mediums

The only way to compensate for the low volumetric energy density of hydrogen is to either compress the gas, liquefy it, or bond hydrogen into another substance. Compression is a straightforward method for increasing the volumetric energy density for short periods of time for two key reasons. First, hydrogen is a gas under practical temperatures and pressures. Its critical temperature, -239.96 °C, and pressure, 12.98 atmospheres, necessitates the use of cryogenic refrigeration to bring hydrogen into liquid form [16]. Second, hydrogen is most commonly used as a fuel under atmospheric

temperatures and pressures. Storage in the same form in which the hydrogen will ultimately be used will not require additional active subsystems to maintain the storage temperature and pressure.

D. CURRENT HYDROGEN STORAGE STRATEGIES

Hydrogen storage technology falls into two broad categories. The first category, physical storage of the hydrogen molecule, is the most common. Physical storage includes compressed hydrogen, liquefied hydrogen, and combined compressed and cooled hydrogen. The second category is material-based storage of hydrogen atoms. Material-based storage includes hydrides, sorbents, and chemical storage. Among the storage methods outlined in Figure 4, physical storage remains the most mature technology and the most economical.

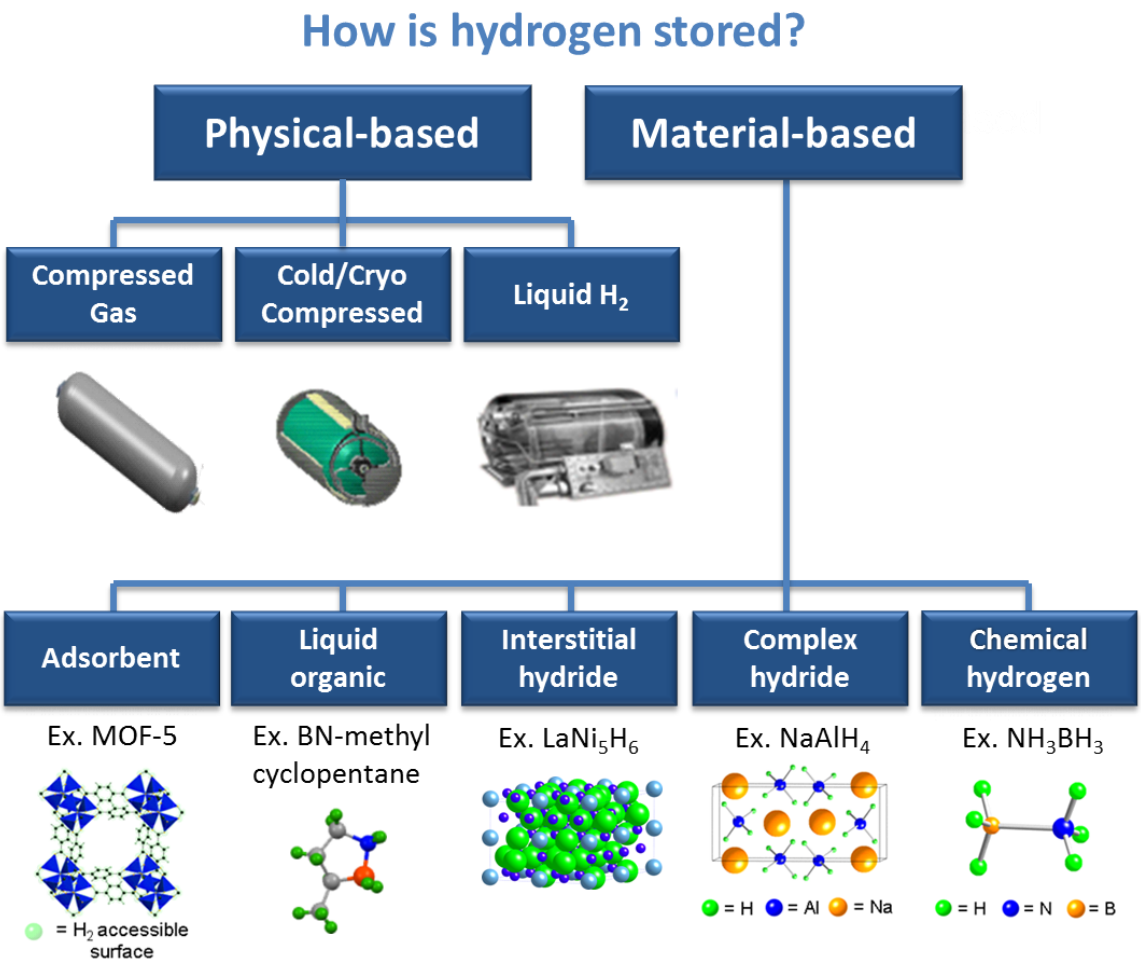

Figure 4. Hydrogen Storage Categories. Source: [17].

Liquid hydrogen storage requires cooling systems that are capable of maintaining temperatures below hydrogen's boiling point, -252.882 °C. The National Aeronautics and Space Administration pioneered the process of liquefying hydrogen to fuel space exploration and has been successfully using liquid hydrogen since the 1950s [18]. Combined compressed/cooled hydrogen storage can be maintained at slightly higher temperatures because compression is used to raise the boiling point. On a volumetric energy density basis, liquefied hydrogen is competitive with compressed natural gas (CNG), but it has significant disadvantages in other areas. Both storage methods require a tremendous amount of energy and large infrastructure investments. This is primarily due to the large amount of energy needed to liquefy hydrogen and store it in liquid form. Any

heat transferred to the hydrogen results in boil-off and venting, reducing the amount of usable fuel and time hydrogen can remain in liquid form without expending energy for cooling.

Material-based storage is one of the fastest growing research areas for increasing hydrogen adoption. The Department of Energy (DOE) budget for hydrogen storage research and development was $15.6M in 2016, and 42% of that went into materials-based storage research programs [19]. Bonding hydrogen with other substances for storage purposes is typically accomplished through the use of metal hydrides, sorbents, or chemical storage. Metal-hydride storage devices have been proven to work for long-term hydrogen storage but are heavy, contain rare and expensive materials, and typically require thermal management systems to absorb and release hydrogen.

Table 3 compares current storage system gravimetric, volumetric, and cost metrics against the DOE's goals for hydrogen storage technologies. The two cheapest systems are compressed gas storage and sorbent-based storage. The 700 Bar storage systems cost roughly the same as the most advanced sorbent-based systems, approximately $15 per kilowatt hour or $54 per megajoule.

Table 3. Hydrogen Storage Technologies, Current Status, and DOE Targets. Adapted from [19].

Current Status	Gravimetric Density	Volumetric Density	Cost
	kWh/kg system (kg H2/kg system)	kWh/L system (kg H2/L system)	$/kWh ($/kg H2)
DOE 2020 Target	1.5 (0.045)	1.0 (0.030)	$10 ($333)
DOE Ultimate Target	2.2 (0.065)	1.7 (0.050)	$8 ($266)
700 bar compressed	1.4 (0.042)	0.8 (0.024)	$15 ($500)
Metal Hydride (MH): NaAlH4	0.4 (0.012)	0.4 (0.012)	$43 ($1,430)
Sorbent: MOF-5, 100 bar, 80 K	1.3 (0.038)	0.7 (0.021)	$15 ($490)
Chemical Hydrogen (CH) Storage Ammonia Borane	1.5 (0.046)	1.3 (0.040)	$17 ($550)

THIS PAGE INTENTIONALLY LEFT BLANK

II. DESIGN

A. REQUIREMENTS DEFINITION

Although no formal requirements documents were drafted before design, the following outlines a few of the performance characteristics and operating elements desired to support ongoing and future hydrogen research at NPS.

1. Previous Research Performed at NPS

The compression and storage station was a necessary addition to the hydrogen generation and fuel cell station demonstrated by Aviles [1] to enable continuous power generation throughout a 24-hour period. While the photovoltaic array could provide useful energy during daylight hours, an energy storage station was needed to provide electrical power during periods of darkness. The 100W Horizon proton exchange membrane (PEM) fuel cell used previously by Aviles [1] would serve as the power source after the photovoltaic array shut down. The PEM requires a steady supply of hydrogen gas at approximately 1.5 bar and uses approximately 1.3 liters of gas per minute at standard temperature and 1.5 bar. The two operating regimes, daytime operations and nighttime operations, are illustrated in Figure 5.

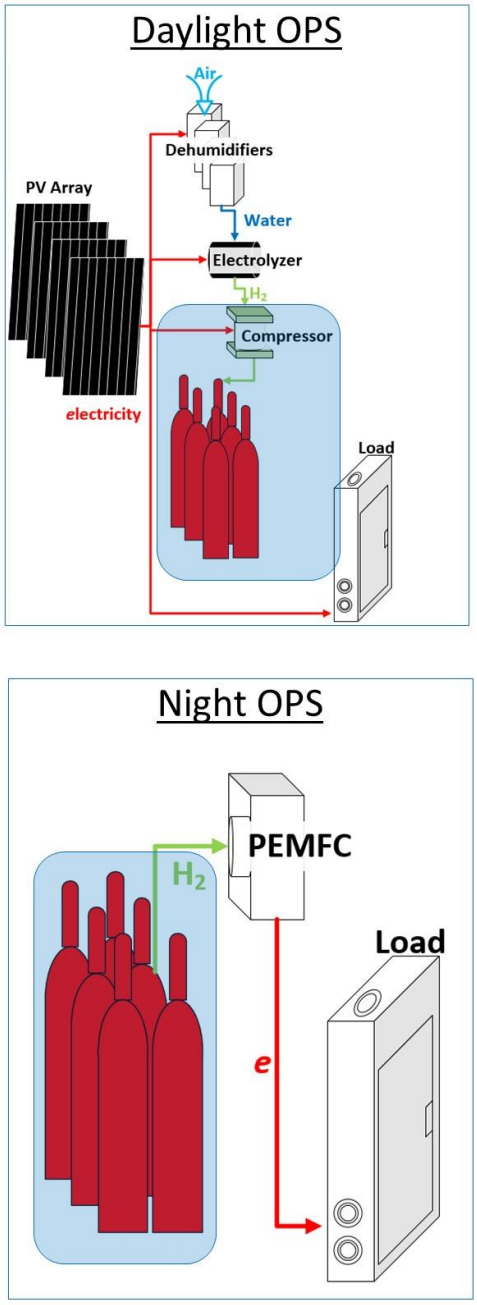

Figure 5. Hydrogen Compression and Storage Station (Highlighted in Blue), Day and Night Operations.

The shortest day of the year in Monterey, CA has roughly 8.5 hours of daylight [20] not including twilight periods. This requires roughly 930 minutes of run time at night from the fuel cell. The volume of hydrogen gas needed becomes:

$$930\,\text{min} \times 1.3\frac{L}{\text{min}} = 1209L@1.5Bar. \tag{2}$$

A total mass quantity is calculated using (3) the Ideal Gas Law (PV=mRT) and the gas constant for Hydrogen (4124.5 J kg^{-1} K^{-1}):

$$\begin{aligned} m &= \frac{PV}{RT} = \frac{1.5Bar \times 1,209L}{4,124.5\frac{L}{kg \cdot K} \times 298.15K} \times \frac{100,000Pa}{1Bar} \times \frac{0.001m^3}{1L} \\ m &= 0.14748kg. \end{aligned} \tag{3}$$

The mass quantity in (3) is the amount of hydrogen gas needed to operate a single 100W PEM fuel cell for the longest night of the year in Monterey. This initial estimate will aid in determining the final size of the storage station.

2. Concurrent Work at NPS

Previous work focused on demonstrating the photovoltaic array, dehumidifiers, electrolyzer, and fuel cell when connected as a system. Concurrent work to this research by Yu [21] focuses on developing realistic performance profiles for the same elements. This work included refining the system design and reconfiguring for a wider range of testing. Therefore, the compression and storage station design, fabrication, assembly, and commissioning could not interfere with the parallel work. Connections to shared power supply, hydrogen pipelines, and test and measurement equipment were required to tie the two stations together. The electrolyzer used previously by LT Aviles produced a maximum of 1.7 standard liters per minute (slpm) of hydrogen. The concurrent research designed replacement of this unit with one rated for four slpm using a 12–14 Vdc power supply. For design purposes, the station would ideally be capable of simultaneous operation with the electrolyzer, compressing the same four slpm using a 12–14 Vdc power supply.

3. Future Work at NPS

Because the hydrogen compression and storage station will be used for future research, it was required to be flexible and scalable in design. Research has already begun to integrate a micro-turbine to test the use of hydrogen gas in small turbine generators. The station needed to deliver hydrogen gas at a flow rate and for a duration useful to collect data and analyze system performance. An initial estimate was made based on a small commercial-off-the-shelf turbine.

In 2016, the DOE began testing hydrogen and synthetic fuel syngas on Capstone microturbines [22]. Although the DOE research has not yet concluded and detailed data is not readily available, Capstone microturbine specifications can provide a starting point for designing a hydrogen storage station. The smallest Capstone C30 microturbine was selected as a suitable example, and its specifications were used to make an initial estimate for required hydrogen fuel flow characteristics.

A Capstone C30 requires a nominal fuel flow of approximately 444,000-457,000 kJ/hr [23]. Using Hydrogen's Higher Heating Value of 141,781 kJ/kg, a mass flow rate of hydrogen can be calculated using (4):

$$\frac{444,000 - 457,000 \frac{kJ}{hr}}{141,781 \frac{kJ}{kg} \times 3,600 \frac{s}{hr}} = 0.000870 - 0.000900 \frac{kg}{s}. \quad (4)$$

At start-up, the flow requirement could be 1.5 times higher than the values in Capstone's published specifications. The values in (4) become approximately 0.00130-0.00134 kg/s for start-up purposes.

An alternative method of determining fuel demand is used to verify these calculations. The Capstone C30 is a 30kW gas turbine with advertised lower heating value efficiency of 25% using approved fuels. An expected efficiency of 18% or less can be assumed when using hydrogen. A second mass flow rate of hydrogen was calculated using (5) and hydrogen's lower heating value of 119,953 kJ/kg:

$$\frac{30kW \times 1,000 \frac{W}{kW}}{18 - 25\% \times 119,953 \frac{kJ}{kg} \times 1,000 \frac{J}{kJ}} =$$
$$= 0.001000 - 0.001389 \frac{W \cdot kg}{J} \tag{5}$$
$$= 0.001000 - 0.001389 \frac{kg}{s}.$$

Therefore, a fuel delivery requirement of 0.0014 kg/s will be used for further design.

A required supply pressure estimate is needed in addition to the required flow rate. The 2015 EPA report on combined heat and power technologies examined six different commercial-off-the-shelf microturbines and the required fuel gas pressure for these turbines ranged from 9.65–3.45 Bar (50–140 psig) [24]. This same range will be used for further design. In summary, the station would need to supply approximately 0.0014 kg/s hydrogen flow rate at 9.65–3.45 Bar (50–140 psig) to support using a commercial-off-the-shelf microturbine during future research.

A project to design a control strategy and controls for the total system comprising of the solar array, charge controller, electrolyzer, dehumidifiers, compressor, and fuel cell will also follow. The design will allow room for installation of additional valves and sensors for automated control. The compression and storage station must be easily modified and reconfigurable to accommodate additional research projects and any others that follow.

B. CODES, STANDARDS, AND EXISTING GUIDANCE

Codes and standards serve to guide the design of safe engineered systems. Once the general requirements were determined, a preliminary list of applicable codes and standards was assembled to aid in further design. Four primary sources of codes, standards, and existing guidance were used to complete the compression and storage station design. Although not all of the standards discussed below applied directly to the

station being designed, they did provide useful information that helped determine the station's capability for future expansion and use.

The American Society of Mechanical Engineers (ASME) serves as an authoritative source for codes and standards relating to pressure vessels, piping, and piping systems. The ASME B31(series) standards provide detailed requirements for piping and piping systems and are adopted in most Federal, State, and Local laws. Specifically, ASME B31.12 "Standard on Hydrogen Piping and Pipelines" provides requirements for the piping used in gaseous hydrogen service. Additionally, ASME B31.3 "Process Piping" provided additional piping design requirements and material specifications. The AMSE Boiler and Pressure Vessel code is also widely adopted and provides detailed requirements for the pressure vessels and auxiliary equipment needed in the compression and storage station.

The National Fire Protection Association (NFPA) codes and standards mitigate risks to people and property by reducing the likelihood and severity of fire. Two of NFPA's codes were consulted during the design of the compression and storage station. First, NFPA 2 Hydrogen Technologies Code provides safety requirements for hydrogen systems. Second, NFPA 70, also known as the National Electric Code, provides safety requirements for electrical wiring and equipment.

The Compressed Gas Association (CGA) prepares standards relating to the production, transportation, handling, and storage of hydrogen gas. Four of CGAs standards were consulted during the design and offered valuable recommendations not found elsewhere. First, CGA G-5 "Hydrogen" provides industry-standard physical and chemical characteristics for hydrogen along with storage requirements. Second, CGA G-5.4 "Standard for Hydrogen Piping Systems at User Locations" guides designing piping systems, system fabrication, start-up, and maintenance. Third, CGA G-5.6 "Hydrogen Pipeline Systems" guides design, fabrication, start-up, maintenance, and shut-down of hydrogen pipelines. Lastly, ANSI/CGA H-5 "Standard for Bulk Hydrogen Supply Systems" provides additional design guidance and outlines regulatory and safety requirements for hydrogen systems.

Daniel Crowl, the American Institute of Chemical Engineers, and the Center for Chemical Process Safety served as the fourth primary source for guidance. Their publications relating to chemical process safety, inerting, purging, and the behavior of flammable materials was invaluable during the design process.

C. SAFETY ANALYSIS

The safety analysis started with determining the applicable regulations and level of effort required for the risk management. Federal, DOD, Department of the Navy, and Naval Postgraduate School regulations and policies were consulted. The hydrogen compression and storage station is intended to be a relatively small and temporary installation to aid in research. Therefore, many of the more stringent safety regulations do not apply.

Title 29 of the U.S. Code of Federal Regulations (29 CFR) Part 1910 contains the Occupational Safety and Health Standards. 29CFR lists hydrogen as a Hazardous Material under Subpart H and Standard Number 1910.103. However, the standard "does not apply to gaseous hydrogen systems having a total hydrogen content of less than 400 cubic feet." Furthermore, hydrogen is not listed in Standard Number 1910.119 Appendix A List of Highly Hazardous Chemicals, Toxics and Reactives and is not subject to the Process Safety Management (PSM) requirements under 29CFR in quantities less than 4,536 kg (10,000 lbs). The station design will not exceed either 11.3 m^3 (400 cubic feet) or 4,536 kg (10,000 lbs). The safety precautions and guidance outlined in 29CFR Standard Number 1910.103 for Hydrogen were followed nonetheless to ensure the system and operators remained safe during research.

Title 40 of the U.S. Code of Federal Regulations (40CFR) Part 68 contains the Chemical Accident Prevention Provisions, also known as the EPA Risk Management Program (RMP). An RMP includes a detailed risk management plan which is published to the general public, submitted to the Environmental Protection Agency, and updated every five years. 40CFR lists hydrogen in its Tables 3 and 4 as a regulated flammable substance in quantities greater than 4,536 kg (10,000 lbs). The station design will not exceed this threshold quantity, and the RMP requirements do not apply.

Since hydrogen is a flammable gas and hazardous material, Navy Occupational Safety and Health Program and Operational Risk Management requirements still apply. Among these requirements include following OPNAVINST 5100.23G Chapter 7 Hazardous Material Control and Management (HMC&M) policies and the 29CFR Section 1910.1200 Occupational Safety and Health Administration (OSHA) Hazard Communication Standard (HAZCOM). These applicable safety regulations are general and contain too many requirements to list here.

The design process incorporated Process Risk Management in addition to following the design requirements, codes, and regulations. Process Risk Management encompasses the design, tactics, techniques, and procedures (TTPs), and overall life cycle approach to managing risk in a process station. The four broad categories of Process Risk Management begin with Inherently Safer Design (ISD) by eliminating hazards through the complete removal of hazardous conditions. The second Process Risk Management strategy is to design passive risk mitigation measures that do not rely on the active operation of a device or person. The third strategy is to use active design elements that continually operate such as controls, detectors, alarms, and automated safety devices. The fourth category of design strategy is to incorporate administrative requirements to mitigate risks such as standard operating procedures, training, certifications, inspections, and process reviews [25]. Three primary safety considerations are discussed in detail along with the measures taken to mitigate risk.

1. Combustion and Explosion Safety

a. Hazards Analysis

Several physical and chemical characteristics of gaseous hydrogen contribute to it being a hazard to personnel, equipment, and facilities. As mentioned earlier, 29CFR classifies hydrogen as a Hazardous Material. Compressed hydrogen gas is also classified as a Class 2, Division 2.1 flammable gas under 49CFR Part 173. NFPA further classifies hydrogen with its highest flammability rating of 4 in NFPA 704 “Standard System for the Identification of the Hazards of Materials for Emergency Response.” Hydrogen is difficult to detect as “a colorless, odorless, tasteless, flammable, nontoxic gas” [26]. It

ignites easily with a minimum ignition energy of “0.02 millijoule, which is an order of magnitude less than the ignition energy for hydrocarbons” [26]. Hydrogen burns with an almost invisible flame and produces only heat and water as combustion products. It will burn in atmospheric air at concentrations ranging from 4% to 75%, a much wider range than most hydrocarbon fuels. In oxygen environments, the limits of flammability for hydrogen gas extend from 4.6% to 93.9% [26]. For these reasons, combustion and explosion of hydrogen gas are considered a high risk and the design for this research mitigated this risk using various methods.

b. Mitigation

The first step in Inherently Safer Design is to remove hazardous conditions completely. For hydrogen gas, this involves purging station components of oxygen and removing all ignition sources. The first goal was designing the system for adequate purging capabilities. The purpose of inerting and purging the system is to ensure there is never a mixture of hydrogen gas (fuel), oxygen (oxidant), and ignition source capable of starting or sustaining combustion. Thoroughly purging the station ensures the fluid remaining is incapable of maintaining a flame and no longer a flammability risk to users or facilities.

When the station was first assembled, it contained atmospheric air, which is roughly 21% oxygen. If one were to simply start pumping compressed hydrogen gas into the station, there would be sufficient oxygen present to support combustion when and if a spark were to ignite the gas. Inert gas was used to mitigate this risk by removing enough oxygen from the station to make combustion impossible. This process is demonstrated on a triangular composition diagram of hydrogen/oxygen/nitrogen in Figure 6. The assembled station starts at position F which is simple atmospheric air. Purging the station to an in-service oxygen concentration of 5.7% O_2 is represented by moving from point F to point G on the figure. This ensures that when hydrogen is added, the fluid composition will never enter the combustible region and will follow the line from point G to point A. Only fluid compositions inside the combustible region will support combustion.

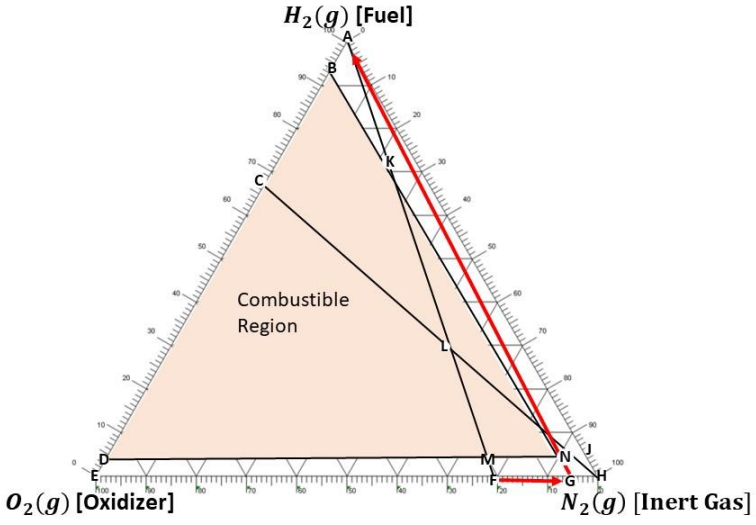

A =Pure Hydrogen Gas, H_2
B = Upper Flammability Limit in Pure O_2 =93.9%
C = Stoichiometric Combustion Point =33.3% O_2 & 66.6% H_2
D = Lower Flammability Limit in Pure O_2 =4.6%
E = Pure Oxygen Gas, O_2
F = Simple Atmospheric Air =21% O_2
G= In-service oxygen concentration (ISOC) ~5.7%
H = Pure Nitrogen Gas, N_2
J = Out-of-service fuel concentration (OSFC) ~5%
K = Upper Flammability Limit in Air =75%
L = Stoichiometric composition in simple air =Intersection of Lines AF and CH
M = Lower Flammability Limit in Air =4%
N = Minimum Oxygen Concentration (MOC) =4% O_2

Figure 6. Purging Process Depicted on Triangular Composition Diagram for Hydrogen/Oxygen/Nitrogen. Adapted from [27].

The Compressed Gas Association Standard for Hydrogen Piping Systems at User Locations specifies using sweep purging, evacuation (vacuum) purging, or pressure purging to residual oxygen levels below 1% [28]. Siphon purging involves using water to displace the combustible gas, it is not included in the standard and therefore was not considered during the design. Sweep-through purging is accomplished by passing the purge gas through the system continuously until residual oxygen levels are acceptable. This method requires large volumes of purge gas and is susceptible to failure due to incomplete mixing of the residual and purge gases. Sweep-through purging requires precise placement of inlet and outlet ports and thorough understanding of the turbulent mixing of gasses. Since the station will use standard commercial steel storage cylinders, which only have one port for both inlet and outlet operations, and conservation of purge gas is desired, sweep-through purging was eliminated as an option during design.

Evacuation (vacuum) purging uses vacuum pumps to remove the air from the tanks. The mechanical vacuum pumps require energy and thereby lower the overall station efficiency. Vacuum pumps also require lubricating fluid to operate, a hazardous

material according to the Navy, and this would add an unwanted burden for researchers. Vacuum pumps also require routine maintenance which adds to the overall cost. The station must also be capable of sustaining a vacuum. All components, tubes, sensors, and the compressor would need to be designed and rated for vacuum service in addition to pressure service. Despite the drawbacks associated with vacuum purging, it can save significant quantities of purge gas over the other methods.

Pressure purging is accomplished by pressurizing the station using pure inert gas, allowing the air/inert gas mixture to mix, and then venting the air/inert gas mixture. Each cycle through the process results in lowering the total amount of oxygen in the station. A combination of vacuum and pressure purging was used for this research to conserve the amount of purge gas needed to reach a safe level of oxygen content in the station cylinders and piping. The ideal gas law was used to determine the minimum number of vacuum/pressure purge cycles needed to reduce the oxygen concentration from atmospheric air to 1% with pure nitrogen gas. The equations are derived and outlined in detail in *Understanding Explosions* by Daniel Crowl, and the result is shown in Appendix A [27].

Purging was accomplished using the four-cylinder pressure purge station shown in Figure 7. After pressurizing, the gasses were given enough time to thoroughly mix by allowing the station to remain pressurized overnight with nitrogen. This also allowed for a 24-hr pressure test to guarantee no leaks were present.

Figure 7. Four-cylinder Pressure Purge Station with Nitrogen Cylinders Connected, 34 atm (500 psig) Pressure Regulator, and Cross-purge Assembly.

Lowering the residual oxygen concentration to below 1% was essential in stopping the combustion process. However, removing potential ignition sources was also required. Combustion requires fuel (hydrogen), oxidizer (oxygen), and ignition. Hydrogen's minimum ignition energy of 0.02 millijoule is orders of magnitude less than that of a spark detectible to touch (20 millijoules) [29]. Two broad strategies were used to mitigate the risk of ignition. First, bonding and grounding were used to reduce the risk of static charge accumulation in station equipment and fluid. Second, electrical wiring and

components were selected that reduce the likelihood of mixing exposed electrical connections with flammable gas.

Bonding and grounding best practices are covered under NFPA 77 Recommended Practice on Static Electricity. For this research, basic grounding paths were established for electrical equipment to reduce the risk of static discharge. Daniel Crowl warns in *Understanding Explosions* that static can build on both the equipment and the process fluid. Grounding of the hydrogen as the process material is required as well as the equipment. If the station were intended to be a permanent installation, a more thorough electrical design based on NFPA 77 recommendations would be necessary to make sure the process fluid is grounded.

NFPA 2 and NFPA 70 provide requirements and standards for electrical wiring of hydrogen stations. According to these standards, electrical components must conform to the provisions of Article 500 of NFPA 70, Hazardous (Classified) Locations. Gaseous hydrogen is designated as Class I, Group B, Division 1 or 2 material by NFPA 70 [30]. The Division 1 or 2 determination depends on the distance to vents or ignitable concentrations of hydrogen. The easiest strategy to eliminate ignition sources is to remove all sources from within the zones specified by NFPA 2, which are reproduced in Figure 8.

Table 7.3.2.3.1.5 Electrical Area Classification

Location	Classification	Extent of Classified Area
Within 3 ft (1 m) of any vent outlet and any points where hydrogen is vented to the atmosphere under normal conditions	Class I, Division 1	Between 0 ft (0 m) and 3 ft (0.9 m) and measured spherically from the outlet
Between 3 ft (1 m) and 15 ft (4.6 m) of any vent outlet and any points where hydrogen is vented to the atmosphere under normal operations	Class I, Division 2	Between 3 ft (0.9 m) and 15 ft (4.6 m) and measured spherically from the vent outlet
Storage equipment excluding the piping system downstream of the source valve	Class I, Division 2	Between 0 ft (0 m) and 15 ft (4.6 m) and measured spherically from the source

Figure 8. Electrical Area Classifications for Hydrogen Systems. Source: [31].

All electrical components were designed to be greater than 1 m from any Class I Division 1 zone. This eliminated some of the more stringent requirements and the risk of ignition during normal conditions. However, some of the electrical components remained within Class I Division 2 zones and were required to meet the requirements of NFPA 70 Article 501. These requirements were not followed for two reasons. First, the initial assembly and testing of the station utilized an alternating current power supply from the adjacent building. These connections were temporary by design and will be removed once the station is ready for connection to the photovoltaic power supply. Second, power connections to the compressor are not enclosed and sealed from potential hydrogen exposure. This is a design deficiency of the compressor. Future compressor designs will need to address this deficiency before they are suitable for permanent installation in a hydrogen station. The deficiency was assessed as a low risk since the manufacturer had not experienced problems after several thousands of hours of work with their product. Future station upgrades will be made when connection to the photovoltaic power supply

is completed that incorporate a redesign of the electrical connections, wiring, and equipment location, alleviating most of the Class I Division 2 deficiencies.

2. High-Pressure Gas Safety

In addition to the flammability and combustion hazard, the use of compressed hydrogen involves several other hazards that had to be mitigated. The risk of unintentional discharge of the compressed gas was also considered as a hazard and addressed during design. Four methods were utilized in reducing the risks associated with high-pressure gas safety. First, the design incorporated overpressure protection to ensure the station could not be pressurized beyond the design limits of the various components and piping. Second, both analog and digital monitoring devices were used to ensure accurate temperature and pressure monitoring regardless of whether the station had electrical power. Third, the materials selected for use in the station are all allowable materials according to the various applicable standards, and they are not susceptible to hydrogen embrittlement at the pressures and temperatures the station will encounter. Lastly, the piping sizes and station components were all selected in accordance with ASME B31.12 Hydrogen Piping and Pipelines to withstand pressures of 200 atm (3,000 psi) or greater, 6–10 times the compressor's expected capability.

a. Overpressure Protection

Overpressure protection was designed for three distinct zones of the station. First, the inlet side of the compressor, which is expected to operate around 1 atm, should not exceed 1.2 atm. Excessively high pressures on the compressor inlet would result in halting hydrogen production by the hydrogen generator and could result in uncontrolled release of hydrogen, oxygen, or both at the generation station. The second zone is the compressor outlet and storage station which is designed to a 200 atm (3,000 psi) working pressure. The third zone is the hydrogen fuel supply line running from the storage station back to the fuel cell. All three zones were designed to have at least two relief devices to ensure redundancy.

The first zone relies on the pressure relief devices installed on the water "bubblers." The pressure relief valve is located at the top of the bubbler and releases the

pressurized gas around 1.2 atm. Figure 9 shows the bubbler installed on the hydrogen generator outlet/compressor inlet line. A second bubbler was used on the oxygen discharge line from the generator. Together, the two bubblers ensured the hydrogen generator and its tanks remained within safe operating pressures. The pressure relief valves that were installed on the bubbler are simple rubber balls with a metal spring backing. While simple, they are not precise in their cracking pressure and were difficult to reset once operated. Their replacement may become necessary if they stop providing a gas-tight seal after operation and should be considered for possible future upgrades.

Figure 9. Hydrogen Bubbler with Pressure Relief Valve

The other two zones incorporated two different relief devices each. First, a spring-loaded and adjustable relief valve was installed. Next, a rupture disc was installed as parallel overpressurization protection. Figure 10 is the proportional safety relief valve

used in the second zone with high-pressure storage. It is rated for service up to 413 Bar (6,000 psi) and will open gradually as the pressure increases above the set pressure. Once the relief valve was adjusted to a desired set pressure of 34 Bar (500 psi), a locking nut was tightened, tamper cover installed, and lock-wire applied to ensure the set pressure adjustment could not be inadvertently changed.

Figure 10. Proportional Safety Relief Valve Set to Operate at 34 Bar (500 psig).

Figure 11 is the proportional relief valve used in the third zone leading to the fuel cell. It is also rated for service up to 413 Bar (6,000 psi) and will open gradually as the pressure increases above the set pressure. However, the spring operating this valve has a narrower operating range and must be replaced based on the desired set pressure. A spring for pressures between 0.7 - 15.5 Bar (10 - 225 psig) was used and set to 1.5 Bar for

service to the fuel cell. If the fuel cell is replaced by a higher capacity unit requiring greater than 15.5 Bar hydrogen, the spring and seals will need to be replaced. Once the relief valve was adjusted to 1.5 Bar set pressure, a locking nut was tightened to ensure the set pressure did not change. This valve does not include a tamper cover, but lock wire was used to prevent inadvertent changing of the set pressure.

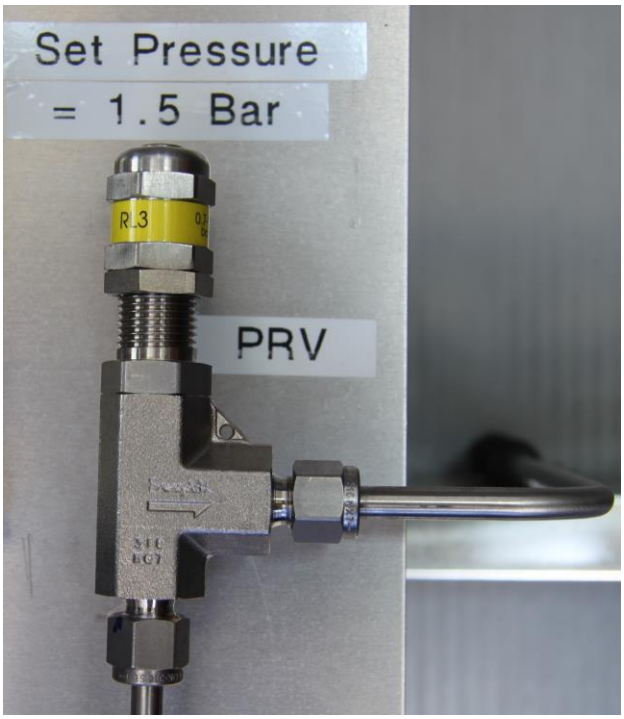

Figure 11. Proportional Relief Valve Set to Operate at 1.5 Bar (22 psig).

Both the second and third zones also received rupture discs manufactured to open at prescribed pressures as redundant overpressure protection. Figure 12 shows one of the two assemblies used including the rupture disc holder, non-fragmenting rupture disc, and muffled outlet port. For the second zone, high-pressure storage area, a Type 316 stainless steel rupture disc designed to burst at 207 Bar (3,000 psig) was used. For the third zone, lower-pressure service to the fuel cell, an aluminum rupture disc designed to burst at 4.5 Bar (65 psig) was used. By using burst discs designed to operate at or below the maximum allowable operating pressures, the risk of over pressurization and uncontrolled release of hydrogen has been reduced. The burst discs and pressure relief valves will

direct any vented hydrogen away from the station, its operators, and sources of ignition through the vent pipes shown in Figure 13.

Figure 12. Screw-Type Rupture Disc Assembly with Muffled Outlet Port

Figure 13. Vent Pipes Located Above Compression and Storage Station, with Mud Dauber Protective End Caps Installed, Turned Down to Prevent Rain Intrusion.

b. System Monitoring

Station monitoring was accomplished using both analog and digital sensors. The analog sensors were necessary to monitor the station temperature and pressure when the data acquisition system was not in use or powered up. The digital sensors provided high-accuracy measurements during data collection and analysis. The pressure gauges used were Type 304 stainless steel, high-accuracy, fluid-filled, vibration and corrosion resistant models designed for use in industrial areas. The digital transducers were heavy duty sensors featuring integrated digital circuits for amplifying the output signal and compensating for temperature fluctuations. Examples of both pressure sensors are shown in Figure 14. Specifications including accuracy and precision of these sensors can be found in Appendix E.

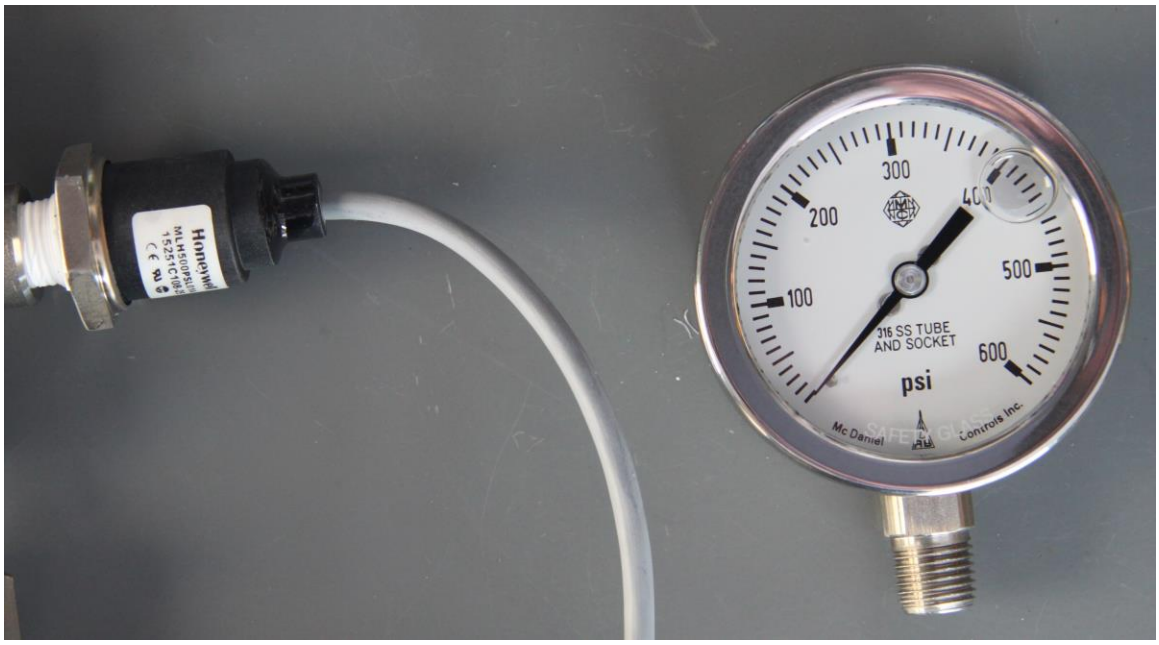

Figure 14. Left: Heavy Duty Pressure Transducer. Right: High-Accuracy Pressure Gauge.

Analog temperature sensing was accomplished using a bimetallic thermometer mounted in a Type 316 stainless steel housing with dampened movement and NIST-traceable calibration certificate. Analog thermometers were installed on the inlet and outlet sides of the compressor to monitor the hydrogen temperature during compressor operations. They also provided station temperatures while the compressor was not in use. Digital thermocouples were also used to monitor station temperatures. The Type K thermocouples were sealed in stainless steel probes and included fiberglass reinforced cables. Figure 15 includes examples of both temperature sensors used. Additional specifications are included in Appendix E.

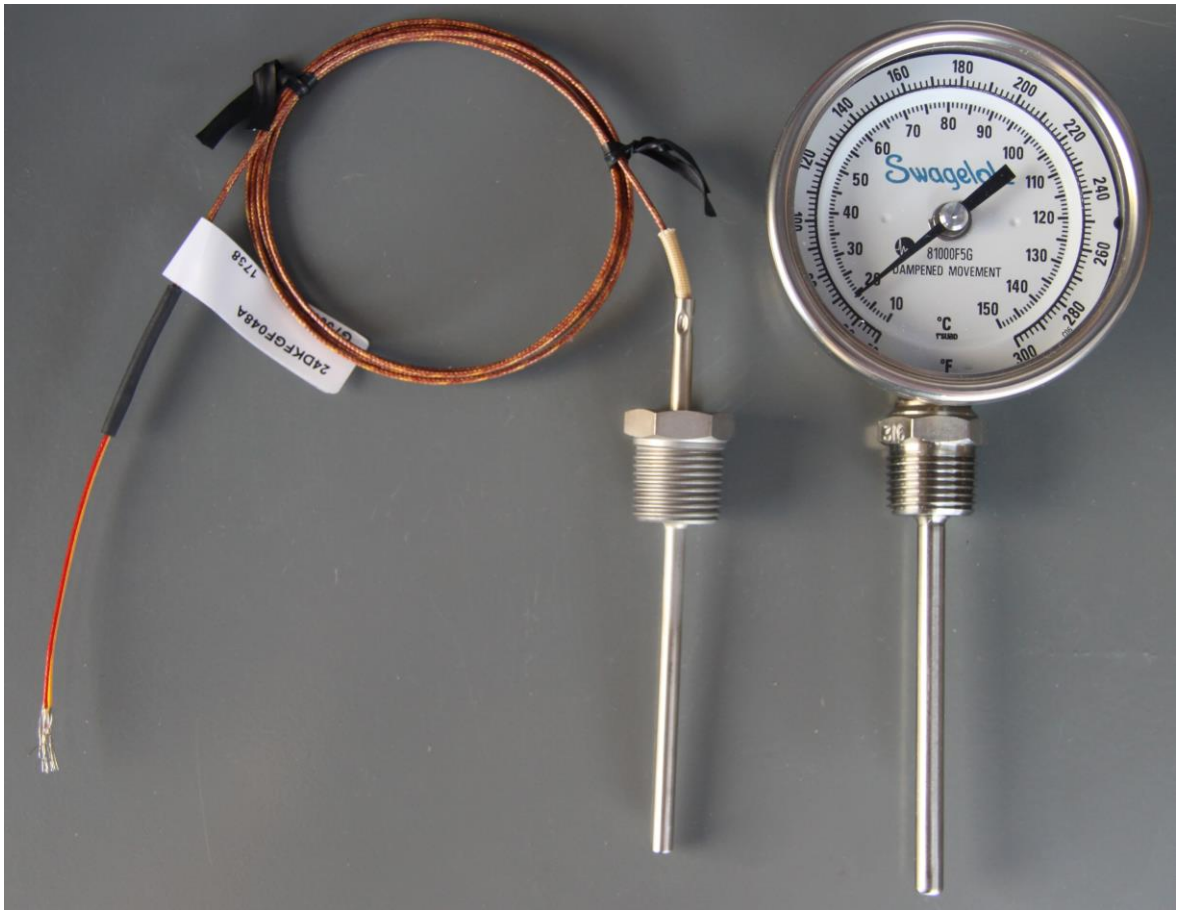

Figure 15. Left: Thermocouple Probe. Right: Bimetallic Thermometer.

c. Materials Selection

ASME B31.12 Hydrogen Piping and Pipelines details the appropriate and allowable materials for pressurized hydrogen service. Specifically, the nonmandatory Appendix A Precautionary Considerations Table A-2-1 "Materials Compatible with Hydrogen Service" was consulted as a starting point. Austenitic stainless steels with greater than 7% nickel are listed as acceptable for gaseous hydrogen service. These include type 304/304L and 316 stainless steels. Other acceptable materials listed include aluminum and aluminum alloys, copper and copper alloys such as brass, and low-alloy steels. Materials not suitable according to this table include nickel and nickel alloys such as Inconel and Monel, gray, ductile, or cast iron, and nickel steels. One of the unacceptable materials is commonly found in commercially available gas handling

equipment, Monel, and care was taken to avoid using these items. ASME B31.12 Chapter GR-2 General Requirements for Materials further defines specific ASME, ASTM, and API materials specifications that are allowable for hydrogen service. The tables and lists provided by ASME were used during market research and equipment selection to make sure all components were compliant and safe to use with hydrogen.

ASME B31.12 lists a very wide range of acceptable materials, but the most specific guidance for materials selection came from CGA G-5.4 Standard for Hydrogen Piping Systems at User Location. The CGA standard states "Austenitic (300 series) stainless steels meeting the temperature limits of ASME B31.12 are recommended for liquid and gaseous hydrogen product piping, tubing, valves, and fittings. The most stable grade is Type 316/316L" [32]. The temperature limits referenced are listed in ASME B31.12 mandatory Appendix IX Allowable Stresses and Quality Factors for Metallic Piping, Pipeline, and Bolting Materials. For Type 316 and Type 316L stainless steel, the temperature limits are between -425 °C and 538 °C. The station designed for this research operates well within these allowable temperatures. Therefore, Types 316 and 316L stainless steels were used when available.

d. Tubing and Tube Fittings

Piping and tubing selection started with determining the appropriate inside diameter for the fluid flow. After an appropriate inside diameter was selected, pipe wall thickness, and outside diameter was determined. A fluid flow analysis was completed for hydrogen flow through a circular pipe to determine an appropriate inside diameter. The volumetric flow expected from the hydrogen generator is four standard liters of hydrogen per minute ($6.6667e^{-5}$ m^3/s). The largest mass flow expected is to a gas turbine at approximately 0.0014 kg/s. At standard temperature and pressure, the volumetric flow to the turbine can be calculated using the ideal gas law and hydrogen density as follows:

$$\frac{0.0014 kg/s}{0.08342 kg/m^3} = 0.0168 \mathrm{m}^3/\mathrm{s}. \quad (6)$$

The two flow regimes allowed the piping to be designed in two sections. The first section extended from the hydrogen generator through the compressor and into the storage tanks. The second section extended from the storage tanks to the turbine. An acceptable inside diameter for the tubing was determined using an iterative process. The fluid analysis outlined in [33] was used along with manufacturer-provided data for various standard tubing sizes. The results for both high-pressure and low-pressure flow are listed in Tables 4 and 5. These results indicated the use of all three tubing sizes would remain in a low Reynold's number regime, and frictional losses were negligible. They also indicate an acceptable pressure drop for service to the turbine through 100 meters of tubing. All three standard tubing sizes are capable of delivery pressure (pressure out) well within the 3.4–9.7 bar (50–140 psig) requirement for a gas turbine. However, use of the smaller diameter tubing would result in fluid flow velocities greater than the recommended 18 meters per second if used at lower pressures. Therefore, the larger diameter tubing was selected for service to the turbine while the smaller diameter tubing was selected for service from the compressor into the storage tanks.

Table 4. Hydrogen Fluid Flow Analysis of Typical Tubing Sizes and 207 Bar (3,000 psig) Starting Pressure

		.0014 kg/s		
		6.35 mm (1/4”) OD, 1.245 mm (0.049”) tube wall thickness	6.35 mm (1/4”) OD, 0.889 mm (0.035”) tube wall thickness	12.7 mm (1/2”) OD, 1.245 mm (0.049”) tube wall thickness
Inputs				
Parameter	Units			
Mass Flow Rate	kg/h	5.0	5.0	5.0
Pressure in (upstream)	kPa (psig)	20,684 (3,000)	20,684 (3,000)	20,684 (3,000)
Viscosity	mPa-s	9.45[a]	9.45[a]	9.45[a]
Pipe Diameter	mm	3.9	4.6	10.2
Equivalent Length of Pipe	m	100.0	100.0	100.0
Density	kg/m3	14.10[a]	14.10[a]	14.10[a]
Temperature	C	25.0	25.0	25.0
Molecular Weight	kg/kgmol	2.00	2.00	2.00
Cp/Cv		1.41	1.41	1.41
Pipe Roughness	m	0.00005[b]	0.00005[b]	0.00005[b]
Results				
Parameter	Units			
Reynolds Number	dimensionless	49	41	18
Average Velocity	m/s	8.89	6.39	1.30
Darcy Friction Factor	dimensionless	1.3101	1.5514	3.4649
Pressure Out	kPa (psig)	13,340 (1,935)	10,892 (1,580)	20,334 (2,949)

(a) Values interpolated from data provided by [34].

(b) Pipe Roughness value derived from material specifications listed in [35].

Table 5. Hydrogen Fluid Flow Analysis of Typical Tubing Sizes and 20.7 Bar (300 psig) Starting Pressure

		.0014 kg/s		
		6.35 mm (1/4") OD, 1.245 mm (0.049") tube wall thickness	6.35 mm (1/4") OD, 0.889 mm (0.035") tube wall thickness	12.7 mm (1/2") OD, 1.245 mm (0.049") tube wall thickness
Inputs				
Parameter	Units			
Mass Flow Rate	kg/h	5.0	5.0	5.0
Pressure in (upstream)	kPa (psig)	2,068 (300)	2,068 (300)	2,068 (300)
Viscosity	mPa-s	8.91[a]	8.91[a]	8.91[a]
Pipe Diameter	mm	3.9	4.6	10.2
Equivalent Length of Pipe	m	100.0	100.0	100.0
Density	kg/m3	1.59[a]	1.59[a]	1.59[a]
Temperature	C	25.0	25.0	25.0
Molecular Weight	kg/kgmol	2.00	2.00	2.00
Cp/Cv		1.41	1.41	1.41
Pipe Roughness	m	0.00005[b]	0.00005[b]	0.00005[b]
Results				
Reynolds Number	dimensionless	52	44	20
Average Velocity	m/s	88.9	63.9	13.0
Darcy Friction Factor	dimensionless	1.2355	1.4631	3.2676
Pressure Out	kPa (psig)	1,334 (193)	1,334 (193)	1,334 (193)

(a) Values interpolated from data provided by [34].

(b) Pipe Roughness value derived from material specifications listed in [35].

ASME B31.12 was used to determine whether the standard tube wall thicknesses were adequate based on corrosion, erosion, joining, and mechanical strength allowances. The three standard tubing sizes used for the fluid analysis are manufactured in accordance with standards listed in ASME B31.12 Table IP-8.1.1-1 Component Standards and are suitable for use at the pressure-temperature ratings specified by their manufacturers. These pressure-temperature ratings are summarized for each tubing size in Table 6. A more rigorous design was completed in accordance with ASME B31.12

Chapter IP-3 Pressure Design of Piping Components for the 12.7 mm (½") OD tubing and is presented in Appendix B.

Table 6. Manufacturer's Allowable Working Pressure for Stainless Steel, Seamless, Type 316/316L. Adapted from [36].

Tube Outside Diameter, mm (in)	Tube Wall Thickness, mm (in)	
	0.889 (0.035)	1.2446 (0.049)
	Maximum Allowable Working Pressure, -28 to 37°C (-20 to 100°F) Bar (psig)	
6.35 (1/4)	352 (5,100)	517 (7,500)
12.7 (1/2)	255 (3,700)	352 (5,100)

Once tubing sizes were determined, appropriate fittings were selected to connect the various pieces of equipment. The use of compression type fittings is allowed per [37]. However, [28] recommends using welded joints when practical. Compression fittings are easier to disconnect and reconnect than welded or flanged fittings. However, compression fittings can develop leaks over time while in hydrogen service due to vibration, corrosion, thermal expansion, or improper installation. Welded connections are less prone to leaks under these conditions but require significantly more effort during fabrication and assembly. Since stainless steel was used for the tubing, the station operates at temperatures well below the limits specified by ASME B31.12, service and testing pressures are below recommended limits, and no external loading was applied to the station tubing, welded connections are not necessary. Therefore, the use compression fittings were maximized to allow easy reconfiguration and station upgrades.

3. Fire Protection Requirements

a. Storage Limits

The compression and storage station limit was established under NFPA 2 Hydrogen Technologies Code. Two criteria were used to determine the maximum allowable station size. First, the Maximum Allowable Quantity of Hydrogen per Control Area outlines the general requirements for indoor areas and is reproduced in Table 7. Additionally, Chapter 16 Laboratory Operations requirements must be met when the amount of gaseous hydrogen exceeds 2.2 standard cubic meters (75 scf). The lower of the two values was used to establish the maximum allowable size of the storage station, 2.2 standard cubic meters, or 0.1832 kg H_2. The minimum amount of hydrogen required to operate a single 100W fuel cell for one night was determined as 0.14748 kg. Therefore, the station was designed to store approximately 0.15-0.18 kg H_2 while under pressure.

Table 7. Maximum Allowable Quantity of Hydrogen. Source: [38].

Table 6.4.1.1 Maximum Allowable Quantity of Hydrogen per Control Area (Quantity Thresholds Requiring Special Provisions)

	Unsprinklered Areas		Sprinklered Areas	
Material	No Gas Cabinet, Gas Room, or Exhausted Enclosure	Gas Cabinet, Gas Room, or Exhausted Enclosure	No Gas Cabinet, Gas Room, or Exhausted Enclosure	Gas Cabinet, Gas Room, or Exhausted Enclosure
LH_2	0 gal (0 L)	45 gal (170 L) †	45 gal (170 L)	45 gal (170 L)
GH_2	1000 ft^3 (28 m^3)	2000 ft^3 (56 m^3)	2000 ft^3 (56 m^3)	4000 ft^3 (112 m^3)

Note: The maximum quantity indicated is the aggregate quantity of materials in storage and use combined.
†A gas cabinet or exhausted enclosure is required. Pressure relief devices or stationary or portable containers shall be vented directly outdoors or to an exhaust hood. *(See 8.1.4.6.)*

b. Station Siting

The location for the construction and operation of the compression and storage station was selected based on several factors. First, the original station prototyped and demonstrated by Aviles [1] was located inside the NPS High-Speed Micro-Propulsion Lab, building number 216. While the original location served well for a small demonstration, it was unsuitable for a larger storage station capable of supporting 24-hr operations. Installing the station inside building 216 would require expensive fire and safety upgrades that would be unnecessary after the research was completed. Second, siting the station outdoors was ideal to minimize the number of required fire protection

and safety subsystems. Lastly, NFPA 2 Section 7 Gaseous Hydrogen details the various setback distances required for hydrogen storage and compression stations. Adherence to these setbacks was a primary goal in the siting process. Table 8 lists several of the setback distances considered during the siting process. A site adjacent to building 216 was selected and ultimately used along with a structure for weather protection (shown in Figure 16).

Figure 16. Compression and Storage Station Facility with Weather Protection and Relocatable Platform

Table 8. Summary of Required Distances to Exposures for Non-Bulk Gaseous Hydrogen Systems. Adapted from [39].

Separation Category	Distance, m	Distance, ft
Gas storage (toxic, pyrophoric, oxidizing, corrosive, unstable)	6.1	20
Group 1 Exposures: Lot lines, air intakes, operable openings in buildings, ignition sources	2	5
Public Thoroughfares	2	5
Buildings with firewall separation	0	0
Group 2 Exposures: Exposed persons, parked cars	1	4
Group 3 Exposures: Combustible Buildings, hazardous materials storage, overhead utilities, combustibles storage, non-openable openings in buildings	2	5

A permanent hydrogen station would be required to meet all of the NFPA 2 requirements along with state and local zoning ordinances and codes. The National Renewable Energy Laboratory H2First Reference Station Design Task report from 2015 [40] describes some of the difficulties in properly siting a hydrogen fueling station. First, the required setback distances for higher density liquid hydrogen storage are so great that any station utilizing liquid hydrogen would be too large to fit into typical city lots. Second, state and local requirements can unintentionally add greater distances than the NFPA standards. Additionally, stations based on compressed hydrogen storage are required to separate compressors, storage cylinders, and fueling points. This also increases the required station size, real estate costs, and could negatively impact future use at Navy installations.

4. Piping and Identification

A piping and identification (P&ID) diagram was used to detail the various equipment, connections, and tubing needed for the compression and storage station. Several of the hydrogen-specific standards discussed earlier provided P&ID templates and examples for compliant systems. The examples were used, along with subject matter expert advice from the NPS Rocket Propulsion Laboratory staff, to design a piping and equipment arrangement that would support testing and evaluation of the various

hydrogen technologies undergoing research. The final result is shown in Appendix C along with the detailed lists of equipment, valves, and piping needed for assembly.

D. EQUIPMENT SELECTION

Selecting appropriate equipment for the compression and storage station was paramount for successful research and safety. The major elements of the station had significant impacts on how the station performed during experiments. Selection results are presented here for three of the major pieces of equipment. Cost, capacity, ruggedness, compliance with standards, and simplicity were among the top criteria for selecting the station components.

1. Compressor Selection

a. Electrochemical Hydrogen Compressors

The primary objective of this research involved the investigation of EHCs. Therefore, only EHCs were considered for the compression cycle. Two companies were discovered during market research that offered commercial-off-the-shelf EHCs. Of these two, one was selected for testing and evaluation. The steady-state hydrogen production rate of the two electrolysis hydrogen generators varied from as little as 0.1 slpm up to 4 slpm. Two EHCs of different flow capacities were selected to use in the station that could handle this range of flow from the electrolysis station. The first compressor purchased, shown in Figure 17, was a small 0.4 slpm compressor that used approximately 10–15 Watts to compress hydrogen up to 21–34 Bar (300-500 psi). The second compressor was rated for 4.0 slpm at a slightly higher power and the same pressure capability, shown in Figure 18.

Figure 17. 0.4 slpm Electrochemical Hydrogen Compressor with 15 Proton Exchange Membranes

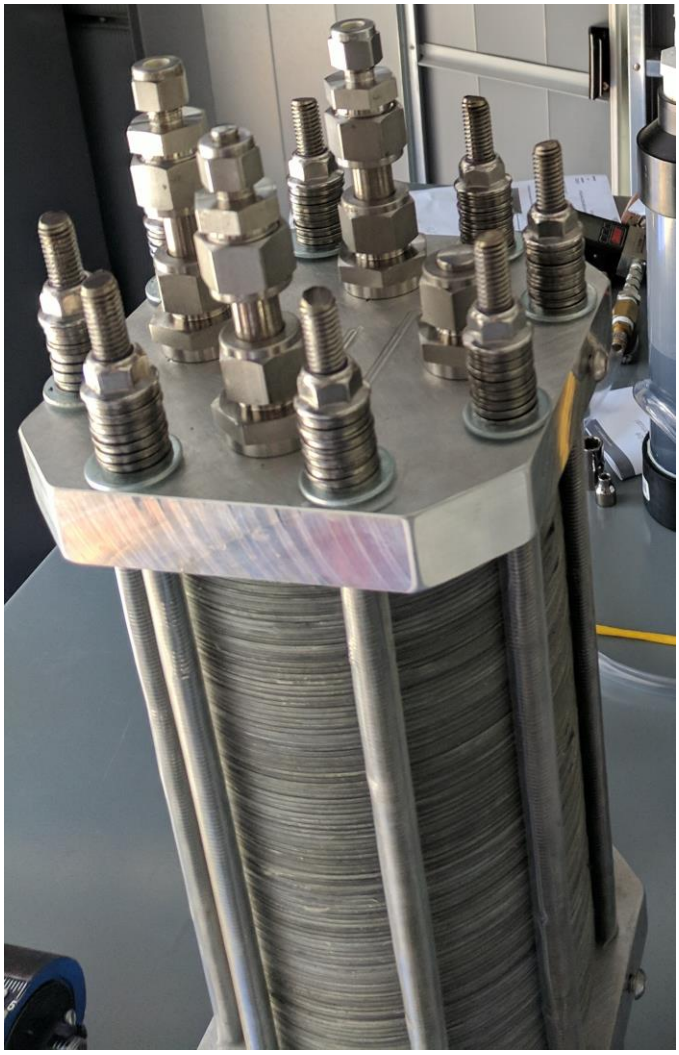

Note the stack of Belleville washers under the tightening nut. The washers are intended to apply constant pressure on the stack as temperature changes and membrane material compresses.

Figure 18. 4.0 slpm Electrochemical Hydrogen Compressor with 120 Proton Exchange Membranes

b. Mechanical Compressors

Almost all hydrogen compression and storage stations worldwide utilize mechanical compressors to achieve higher density hydrogen storage. Although EHCs offer advantages in weight and volume over their mechanical competitors, mechanical compressors are a mature technology with better logistics support. Before the EHCs were purchased for this research, market research was conducted into the mechanical

compressors available and their performance in the field. Figure 19 is a plot of commercially available mechanical compressors rated for hydrogen service based on their maximum outlet pressure and minimum inlet pressure.

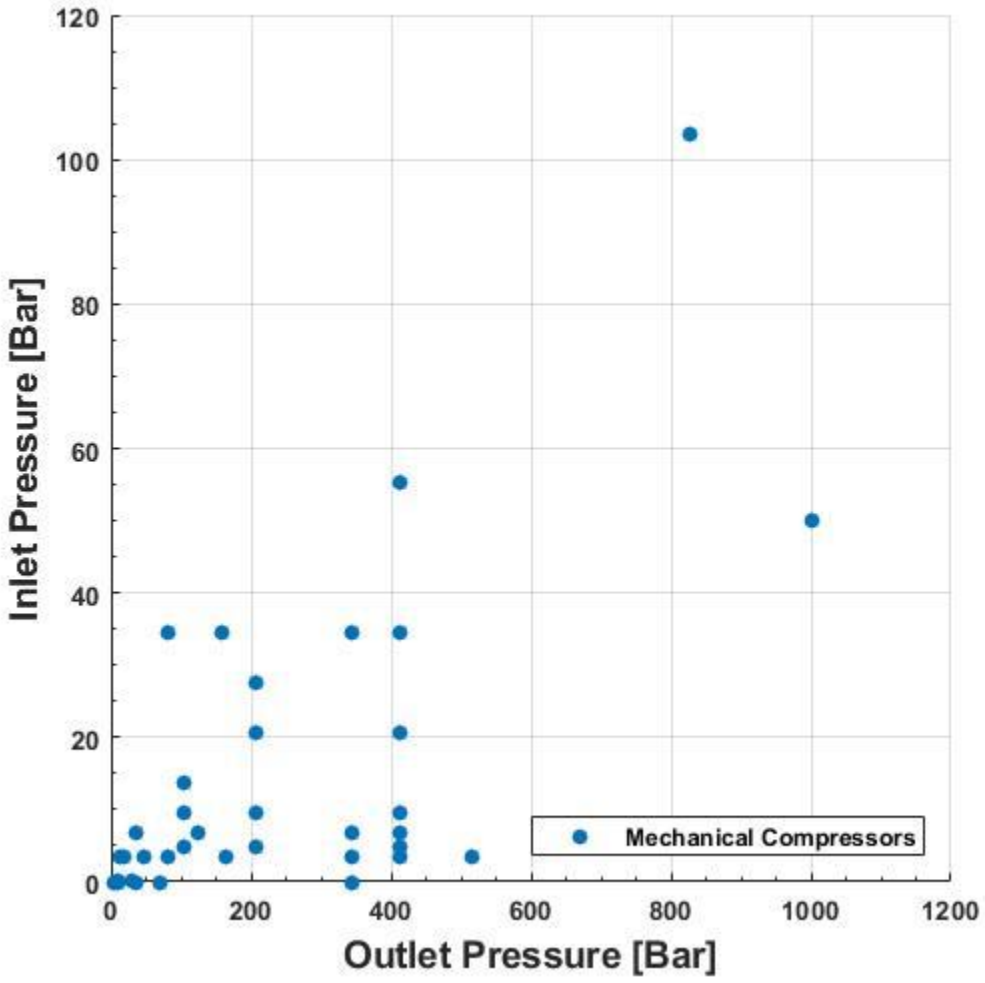

Figure 19. Minimum Inlet Pressure Measured Against Maximum Outlet Pressure for Both Piston and Diaphragm Type Mechanical Hydrogen Compressors. Adapted from [41], [42], [43].

Only five out of 125 mechanical compressors were capable of operating with a 1 atm inlet pressure like the one used during this research. Two more were capable of operating with a 1.2 atm inlet pressure and were added to Figure 20, a plot of the seven

commercially available mechanical compressors found that could support this research. The two compressors rated for 1.2 atm inlet pressures were the smallest of the group at 218 kilograms and 0.35 m^3 with a 3.7 kW motor and 56–850 slpm flow rating (shown in Figure 21). The compressors capable of operating with a 1 atm inlet pressure were more massive, 340 kg and 3 m^3 with a 30 kW motor and 850–5,600 slpm flow rating (shown in Figure 22). These mechanical competitors provided a baseline for comparing the performance of the EHCs.

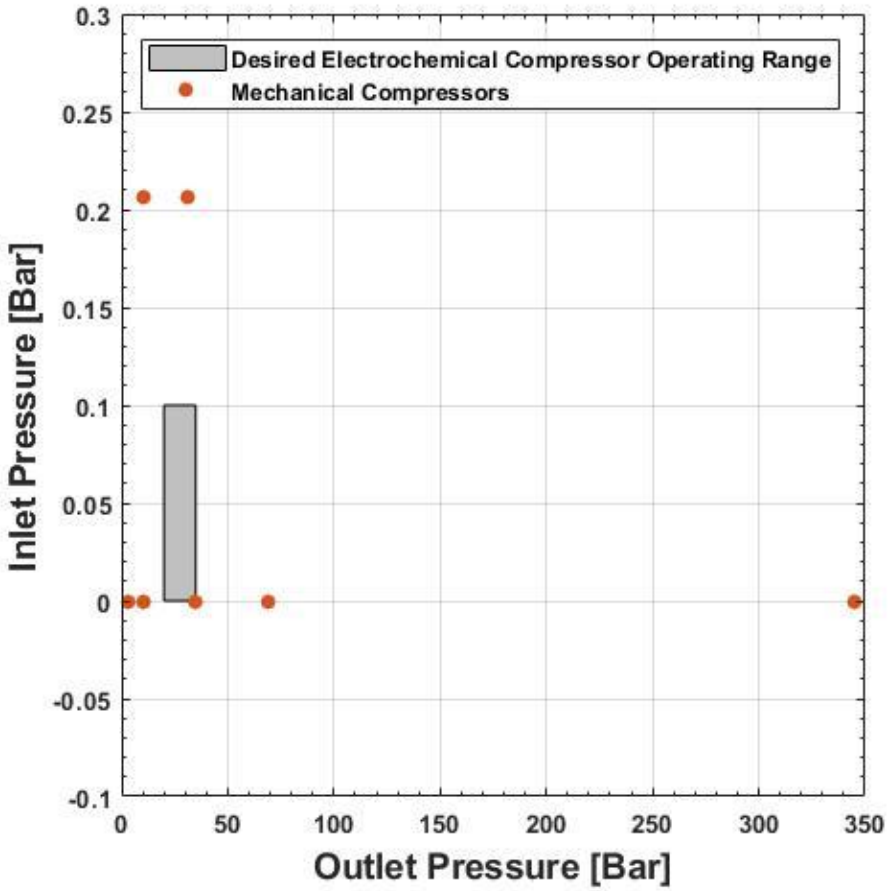

Figure 20. Minimum Inlet Pressure Measured Against Maximum Outlet Pressure for Mechanical Hydrogen Compressors Meeting Research Requirements. Adapted From: [41]

Figure 21. Compact Mechanical Hydrogen Compressor, Piston-Type, Single Stage, Oil-Less, Air Cooled. Source: [41]

Figure 22. Mechanical Hydrogen Compressor, Piston-Type, One–Five Stage, Oil-Less, Air or Water Cooled. Source: [41]

Although the market for mechanical compressors offers a wide range of inlet and outlet pressure ranges, there were no compressors that would sustain low flow rates like the ones expected from the hydrogen generators used during this study. A production rate of 0.1-4.0 slpm was expected, and all of the mechanical compressors surveyed would quickly develop a vacuum suction on the electrolyzer if a buffer tank were not used. A buffer tank is necessary when using a mechanical compressor to 'buffer' fluctuating inlet

pressures due to the cyclical movement of the piston or diaphragm and allow accurate control of the compressor.

2. Storage Device Selection

Storage devices were selected after a compressor was identified for purchase. Compressed hydrogen is typically stored in one of four types of cylinders, listed in Table 9 along with their relative costs. Since the purpose of compressing hydrogen is to increase its volumetric energy density, selecting a lightweight storage device is ideal. The lightest cylinders are Type III and IV composite-wrapped cylinders which are commercially available from several suppliers. The composite cylinders are ideal for applications where reduced weight is a design criterion such as mobile applications, but costly due to their complex manufacturing and certification process.

Several suppliers were queried for pricing and estimated lead times for various cylinder types. Prices for composite-wrapped cylinders ranged from $27.00-$49.00 per liter of storage, and all suppliers required greater than eight weeks for delivery. All-steel cylinders were found already in stock in large quantities, and typical prices were $4.00-$5.00 per liter of storage. In addition to the better price, all-steel cylinders offered higher safety factors, Department Of Transportation compliance, and greater ruggedness. The standard all-steel compressed gas cylinders shown in Figure 23 were selected for this research after considering the designed working pressure, price, and availability of cylinders.

Table 9. High-Pressure Hydrogen Gas Storage Vessels. Adapted from [44].

Type	Description	Relative Cost
I	All-metal cylinder	$
II	Load-bearing metal liner hoop wrapped with resin-impregnated continuous filament	$$
III	Non-load-bearing metal liner axial and hoop wrapped with resin-impregnated continuous filament	$$$
IV	Non-load-bearing, non-metal liner axial and hoop wrapped with resin-impregnated continuous filament	$$$$

The steel cylinders have a DOT service pressure of 156.2 Bar (2,265 psi) and 43.2-liter capacity. The desired storage quantity was previously determined to be between 0.15-0.18 kg H_2. A single cylinder would need to be compressed to 43 Bar (670 psig) to meet the minimum storage requirement. Therefore, six cylinders were used and placed in parallel service with a common manifold. Storage capacity at various pressures is shown in Table 10.

Table 10. Storage Capacity at Various Pressures (at 21°C).

Pressure, Bar (psig)	H_2 Stored, Single-Cylinder, kg	H_2 Stored, 6-Pack, kg
10 (155)	0.036	0.214
20 (310)	0.071	0.427
100 (1,550)	0.356	2.136
200 (3,100)	0.712	4.273

Figure 23. All-Steel, Standard Size, Compressed Gas Cylinders Used for Hydrogen Storage Placed in OSHA, UFC, NFPA, and CGA Compliant Stand with Polypropylene Straps and Steel Chain Straps for Support.

3. Filtration Systems

Two different filtration subsystems were included in the design for the compression and storage station. Particulate filtration was added for safety reasons, and water adsorption was added to protect the steel storage cylinders from corrosion and the fuel cell from poisoning. Tee-type particulate filters, shown in Figure 24, with three different pore sizes were used to protect the safety relief devices, gas regulators, fuel cell, and sensors from damage caused by particles. The tee-type filters allowed filter element replacement without removing the filter housing from the piping system.

Water adsorption was achieved through the use of high-pressure adsorption filters with cleanable and reusable filter elements. The all stainless steel filters and housing bodies, Figure 25, are rated for service up to 414 Bar (6,000 psi) and included drain traps to remove the water from the housing. Two units were purchased with the expectation that they could be tied together in a regenerative cycle arrangement using actuated valves and industrial controllers during station upgrades for future research.

Figure 24. Stainless Steel Tee-type Particulate Filters.

Figure 25. Stainless Steel High-pressure Adsorption Filter. Source: [45].

III. TESTING AND DATA COLLECTION

A. DATA ACQUISITION STRATEGY

Data acquisition was performed using a National Instruments CompactDAQ Model cDAQ-9184 and three analog voltage input modules for temperature, pressure, voltage, and current measurements of the compressor. Figure 26 shows the chassis along with the three modules connected and all mounted to a standard DIN rail assembly. An Alicat M-Series mass flow meter calibrated for service in hydrogen gas was used to measure the hydrogen flow into the compressor. The cDAQ-9184 and flow meter readings were collected through a laptop running the Matlab script found in Appendix D. Specifications for the data acquisition and sensor suite are included in Appendix E.

Figure 26. National Instruments CompactDAQ Model cDAQ-9184 with Analog Thermocouple and Voltage Input modules.

The total suite of sensors was connected according to Figure 27.

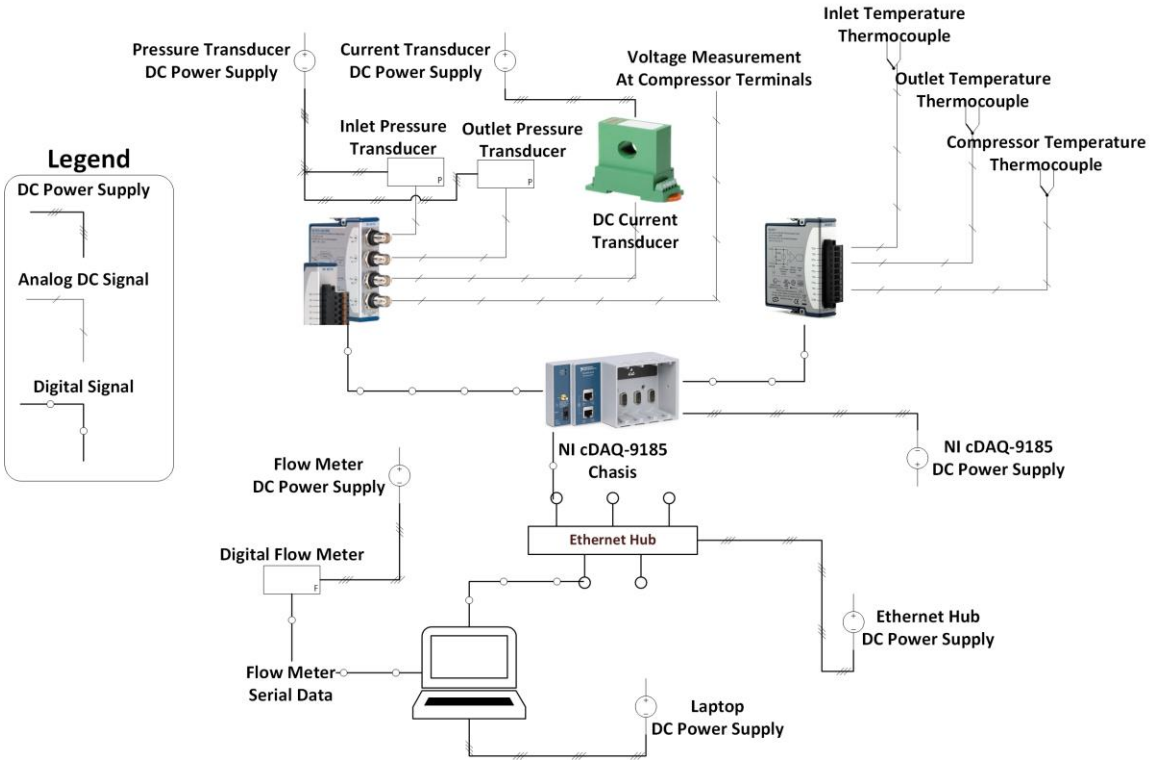

Figure 27. Data Acquisition System Wiring Diagram.

B. TESTS CONDUCTED

1. Specific Power versus Outlet Pressure

The EHCs were expected to be more efficient than mechanical compressors because of their solid state operating principle. Performance was also expected to vary based on inlet pressure, DC voltage applied, and DC current density. Two methods of analysis are presented to compare the EHCs to ideal compression cycles. The first method is a comparison of measured voltage versus the theoretical voltage calculated using the Nernst Equation referenced earlier. The Nernst Equation provides the theoretical cell potential needed from the for each cell to compress the hydrogen from one pressure to the next:

$$V_{theoretical} = \frac{\bar{R} \cdot T}{n \cdot F} \ln\left(\frac{p_2}{p_1}\right), \tag{7}$$

where

$V_{\text{theoretical}}$ = Theoretical potential to compress hydrogen, V

$\bar{R}$ = Universal gas constant, 8.314472 J/(K.mol)

T = Measured Cell Temperature, K

n = number of electrons transferred in the cell reaction, 2

F = Faraday Constant, 9.648533 x 10^4 C/mol

p_1 = Inlet Pressure, Bar

p_2 = Outlet Pressure, Bar.

The equation results in a logarithmic growth of voltage as pressure increases.

Since this equation applies to a single cell, direct comparison of the theoretical voltage versus actual voltage requires monitoring each cell voltage in the compressor stack. The compressor and data acquisition system was not designed for individual cell voltage monitoring and data collection. Therefore, an assumption is made that the

theoretical voltage multiplied by the number of cells in the compressor stack can be reasonably compared to the total voltage across the compressor. Efficiency of the compressor becomes:

$$\eta_{comp,Nernst} = \frac{V_{theoretical} \cdot N_{cells}}{V_{total,measured}}, \tag{8}$$

where

$\eta_{comp,Nernst}$ = Efficiency of the compressor using Nernst Voltage

N_{cells} = Number of cells stacked in the compressor

$V_{\text{total, measured}}$ = Measured total voltage across all cells in the compressor.

The second method of analysis presented is a specific work comparison against ideal compression cycles. Specific work is the work rate divided by the mass flow rate. It provides a convenient analysis of a steady state system in which a control volume can be applied:

where

Work Rate = Power =

$$\dot{W}_{C.V.} = \frac{\delta W_{C.V.}}{dt} kWor \frac{kJ}{s} \tag{9}$$

Mass Flow Rate =

$$\dot{m} = \frac{\delta m}{dt} \frac{kg}{s} \tag{10}$$

and

Specific Work =

$$\frac{WorkRate}{MassFlowRate} = \frac{\frac{\delta W_{C.V.}}{dt}}{\frac{\delta m}{dt}} = \frac{\delta W_{C.V.}}{\delta m} \frac{kJ}{kg} \tag{11}$$

The ideal compression cycles used for analysis were the adiabatic and isothermal compression of an ideal gas. Mechanical compressors are governed by the adiabatic compression cycle while the EHC is governed by the isothermal process. For the adiabatic compression of an ideal gas, the specific work required is calculated as follows:

$$\frac{\dot{W}}{\dot{m}} = \frac{P}{\dot{m}} = {}_1w_2 = \frac{R}{1-\gamma}\left(T_2 - T_1\right). \tag{12}$$

Using the polytropic relationship for an isentropic compression of an ideal gas: $\frac{T_2}{T_1} = \left(\frac{P_2}{P_1}\right)^{\frac{\gamma-1}{\gamma}}$.

Specific work becomes:

$${}_1w_2 = \frac{\gamma}{\gamma-1}RT_1\left[\left(\frac{p_2}{p_1}\right)^{\frac{\gamma-1}{\gamma}} - 1\right], \tag{13}$$

where

γ = the specific heat ratio for hydrogen, 1.4065 [33]

R = hydrogen specific gas constant, 4124.48 J/(K.mol) [33]

and

T_1 = Inlet temperature, [K].

Efficiency of the compressor, compared against the adiabatic process becomes:

$$\eta_{comp,adiabatic} = \frac{{}_1w_{2,ideal}}{{}_1w_{2,actual}} = \frac{\frac{\gamma}{\gamma-1}RT_{1,measured}\left[\left(\frac{p_{2,measured}}{p_{1,measured}}\right)^{\frac{\gamma-1}{\gamma}} - 1\right]}{\left(P_{total,measured} / \dot{m}_{measured}\right)} \tag{14}$$

For the isothermal compression of an ideal gas, the specific work required follows the relationship:

$$\frac{\dot{W}}{\dot{m}} = \frac{P}{\dot{m}} = {}_1w_2 = RT_1 \ln\left(\frac{p_1}{p_2}\right). \tag{15}$$

Where, efficiency of the compressor, compared against the isothermal process becomes:

$$\eta_{comp,isothermal} = \frac{{}_1w_{2,ideal}}{{}_1w_{2,actual}} = \frac{RT_{1,measured} \ln\left(p_{1,measured} / p_{2,measured}\right)}{\left(P_{total,measured} / \dot{m}_{measured}\right)}. \tag{16}$$

The analysis required measurement of the applied DC voltage, DC current, inlet pressure, outlet pressure, inlet temperature, and mass flow rate. Voltage was measured directly from the compressor power supply terminals to the cDAQ-9185 analog voltage input module. Current was measured using a CR Magnetics DC Hall Effect current transducer which was connected to the cDAQ-9185 analog voltage input module. Pressures were measured using sealed gauge pressure transducers connected to the cDAQ-9185 analog voltage input module. Mass flow rate and inlet temperature were both measured using the Alicat Flow Meter. Work rate was calculated from the measured current and voltage using Joule's Law: $Power = Current \times Voltage = IV[AV] or [W]$. Comparisons were made of the actual specific work consumed by the EHC, the ideal isothermal compression process, the ideal adiabatic process, and the advertised performance characteristics for mechanical compressors.

Seven experiments were conducted on the 0.4 slpm EHC before it experienced catastrophic failure. The compressor developed an internal leak that allowed hydrogen to flow from the inlet side of its membranes to the outlet. This leak prevented compression and rendered the compressor useless until repairs could be made. Repairs were attempted in-house following manufacturer's recommendations but were unsuccessful, leading to the eventual return to the manufacturer for repair. This was a significant drawback for the EHC since almost all repairs to mechanical compressors can be made by service technicians in the field and rarely require depot level or original equipment manufacturer (OEM) repairs.

One experiment was conducted with the larger 4.0 slpm compressor. During this experiment, the compressor functioned adequately until it reached around 4.5-5 Bar (65-73 psig) compression. At 4.5 Bar the compressor developed an internal leak, releasing the compressed hydrogen from the storage cylinder, and failed to restart until the system was depressurized entirely. The larger compressor was then shipped back to the OEM for repair.

a. 0.4 SLPM EHC Tested at 1.07 Bar Average Inlet Pressure

The first experiment presented was the last test conducted with of the 0.4 slpm compressor before failure, a 60-minute test with the hydrogen inlet pressure set to 1.07 Bar and DC power supply set to 3 amps in controlled current (CC) mode. This test is presented because it is the closest to real-world conditions when the compressor is connected to the hydrogen gas generator. A cylinder of compressed hydrogen regulated to 1.07 Bar was used to simulate the actual operating conditions. Figure 28 shows the resulting voltage and pressure relationship as a function of time.

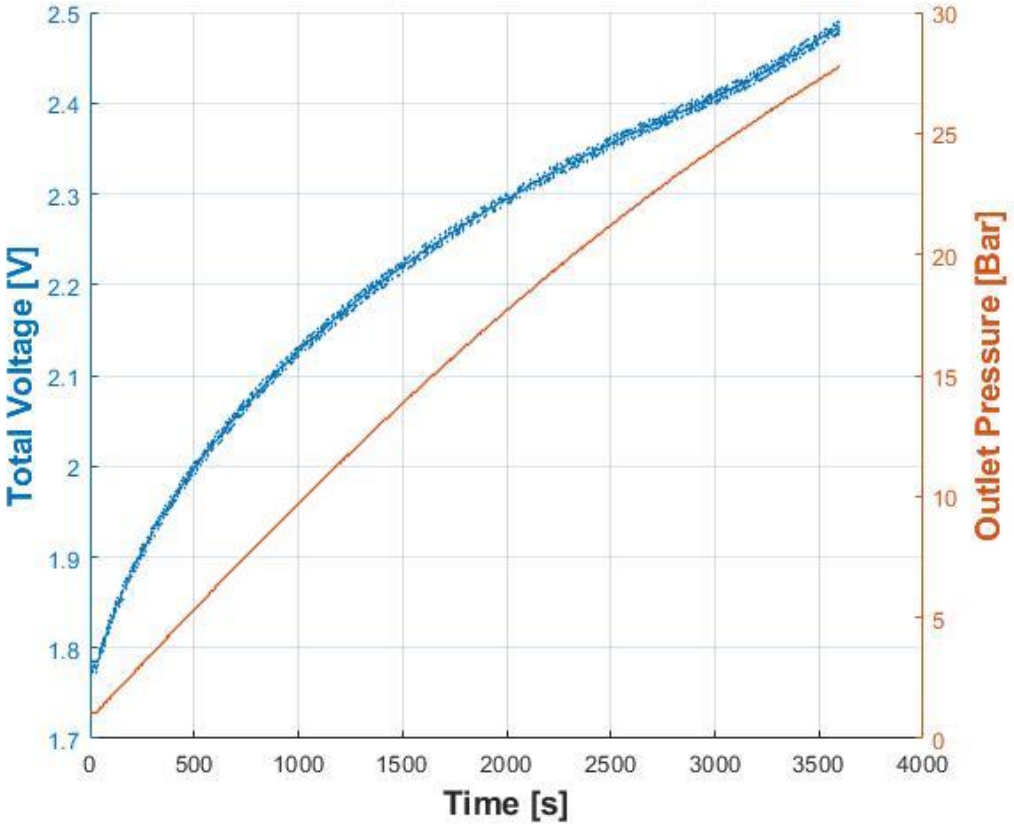

Figure 28. Voltage and Outlet Pressure Characteristics for 0.4 slpm EHC with 1.07 Bar Average Inlet Pressure

Figure 29 shows the total power consumption and volumetric flow rate of the compressor as a function of time.

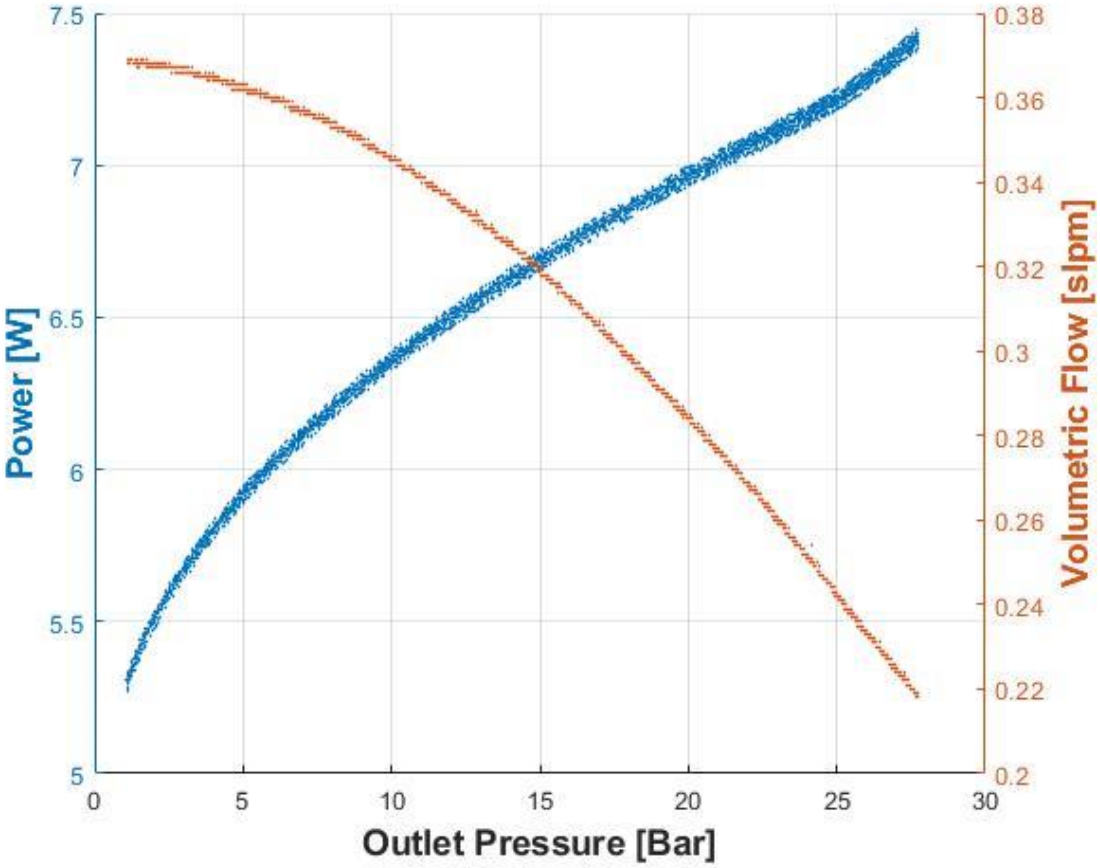

Figure 29. Power Input and Volumetric Flow Characteristics for 0.4 slpm EHC with 1.07 Bar Average Inlet Pressure

The actual voltage, theoretical Nernst voltage, and compressor efficiency are plotted in Figure 30. The efficiency is calculated as: $Efficiency = 100 \times \frac{V_{theoretical}}{V_{actual}}$. There is no evidence of peak efficiency for the compressor over this operating range.

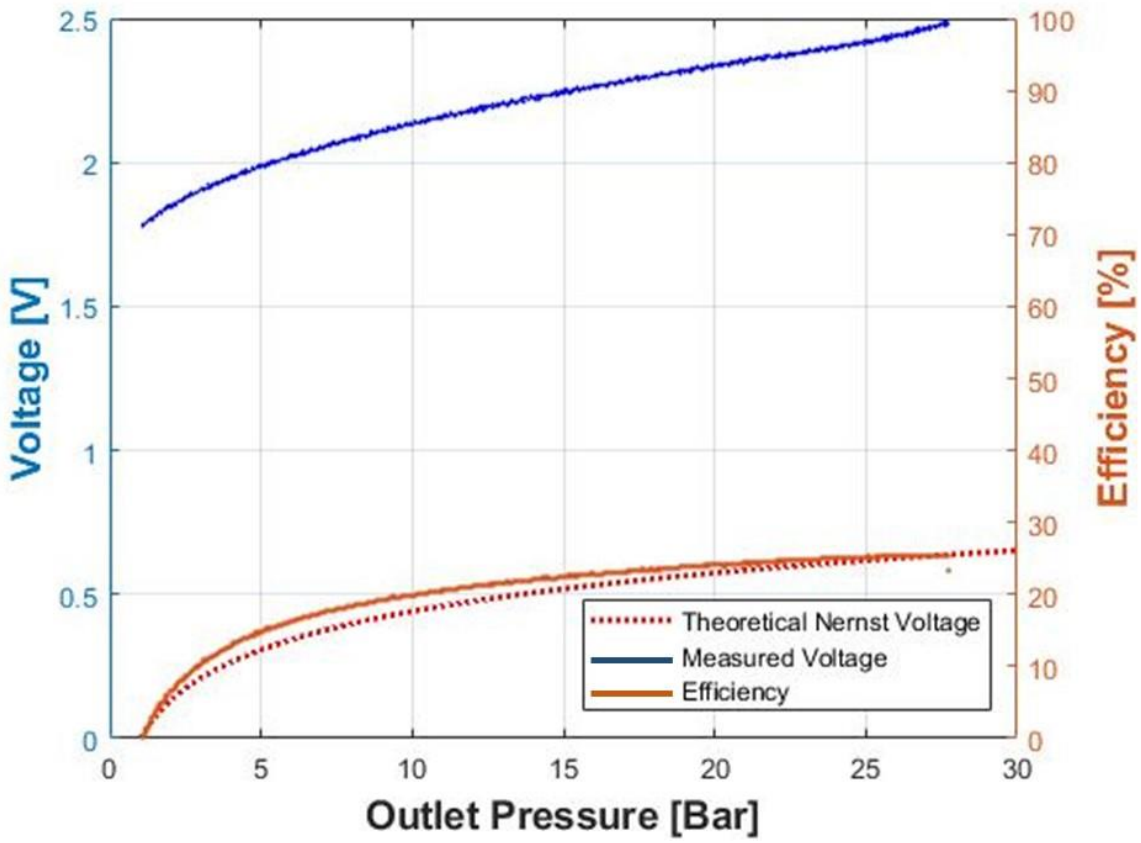

Figure 30. Measured Voltage, Theoretical Voltage, and Efficiency Characteristics for 0.4 slpm EHC with 1.07 Bar Average Inlet Pressure

The measured specific work and calculated ideal adiabatic specific work as a function of outlet pressure is shown in Figure 31. This comparison shows the EHC operating at much higher specific energy consumption than the ideal mechanical compressor.

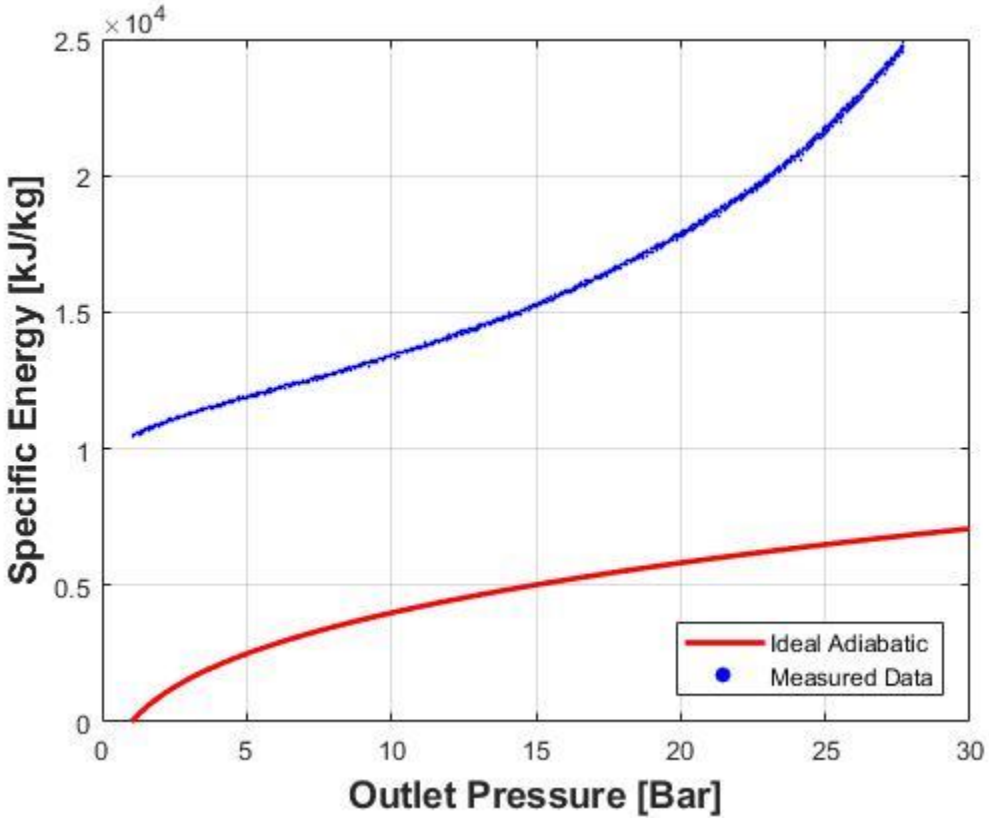

Figure 31. Measured Specific Work vs. Ideal Adiabatic Compression Characteristics for 0.4 slpm EHC with 1.07 Bar Average Inlet Pressure

The calculated efficiency is plotted in Figure 32. Unlike with the Nernst comparison previously, the adiabatic comparison shows a maximum efficiency for the compressor around 17 [Bar].

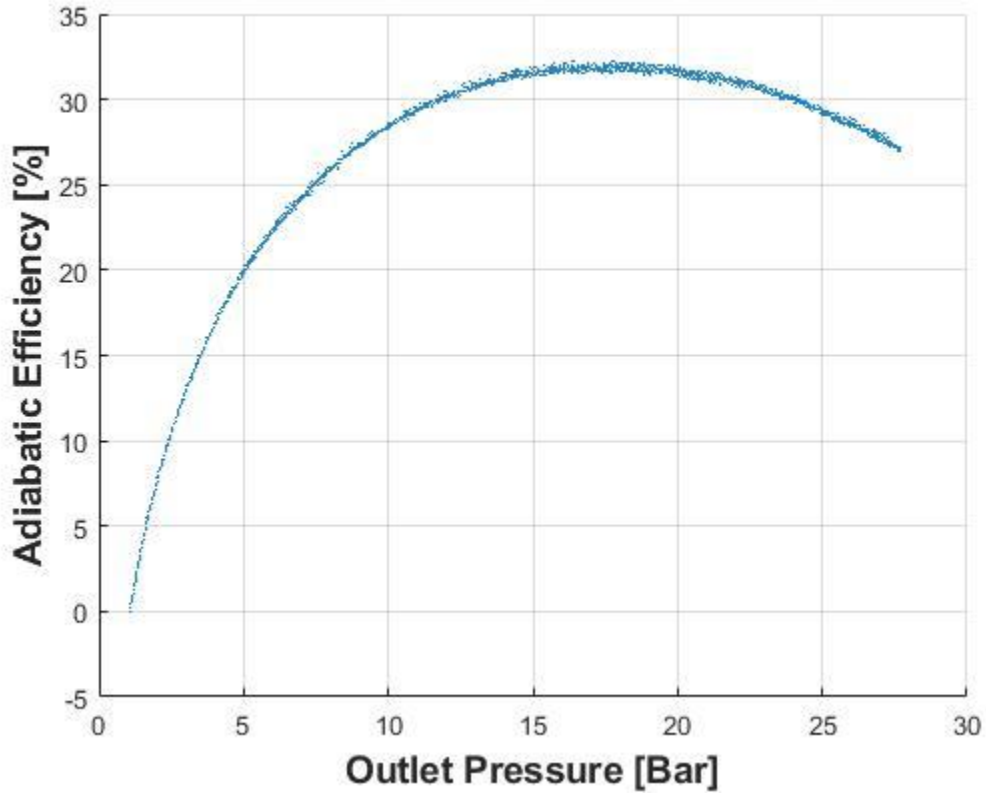

Figure 32. Adiabatic Efficiency Characteristics for 0.4 slpm EHC with 1.07 Bar Average Inlet Pressure

The measured specific energy and calculated ideal isothermal specific energy as a function of outlet pressure is shown in Figure 33. Again, the EHC consumed more energy than the ideal isothermal compression process.

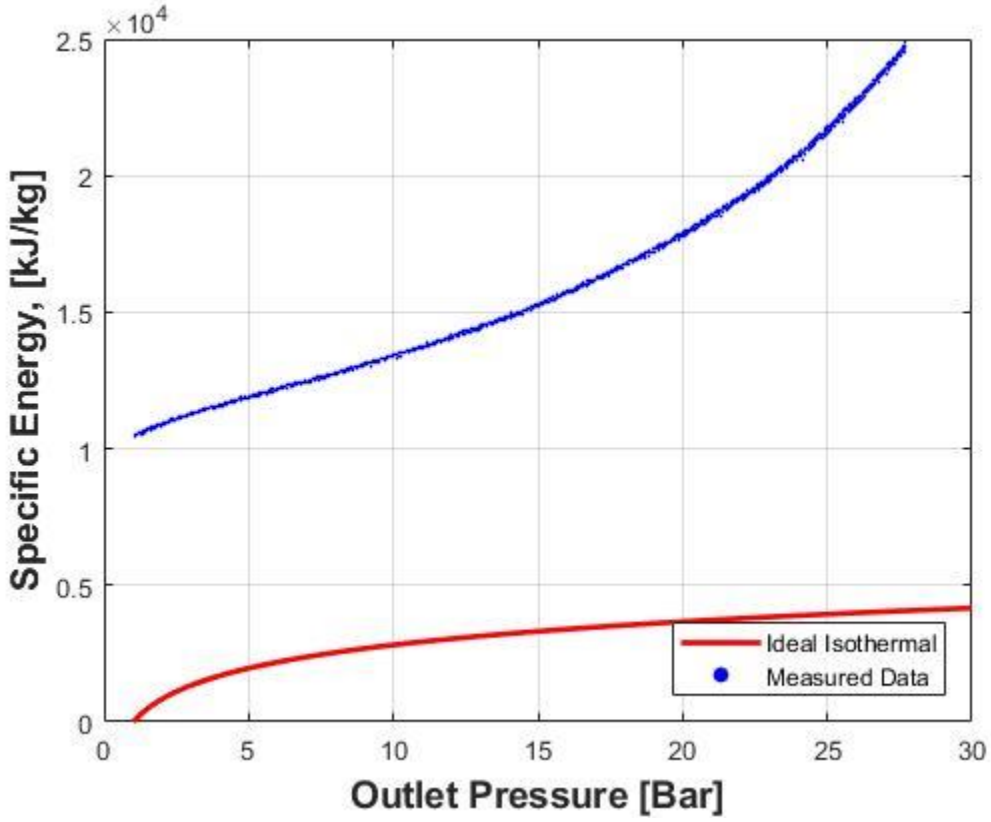

Figure 33. Measured Specific Work vs. Ideal Isothermal Compression Characteristics for 0.4 slpm EHC with 1.07 Bar Average Inlet Pressure

The calculated efficiency is plotted in Figure 34. The isothermal comparison shows a maximum efficiency of the compressor around 14 Bar, slightly lower than the maximum efficiency using adiabatic compression as the comparison.

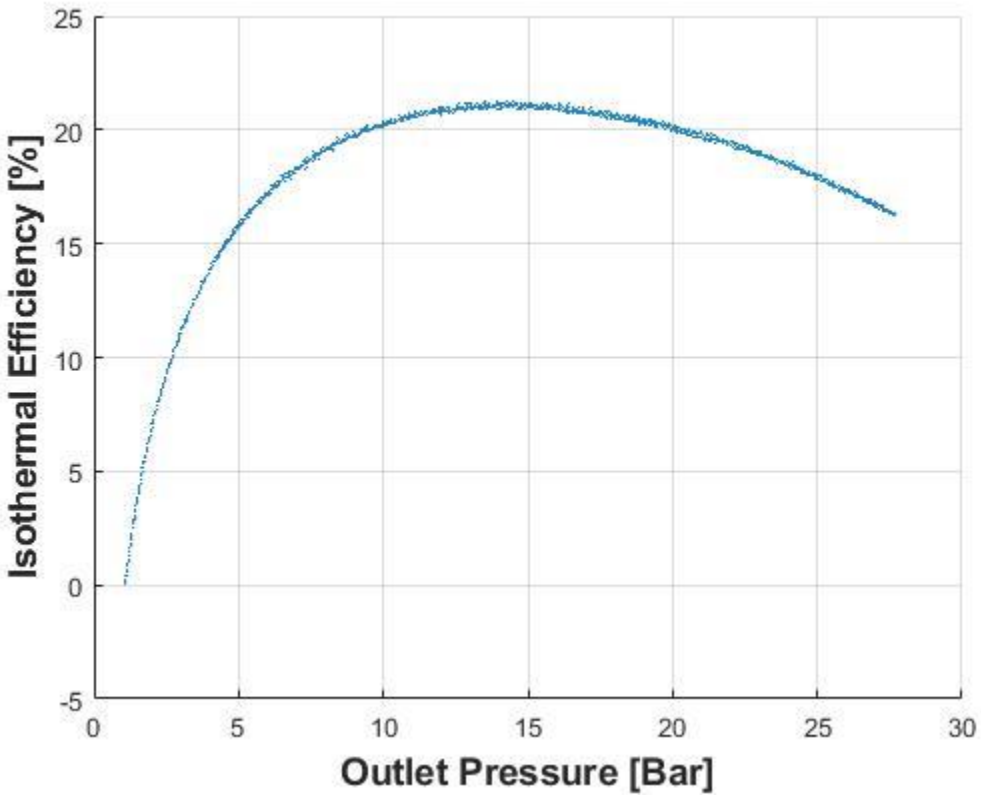

Figure 34. Isothermal Efficiency Characteristics for 0.4 slpm EHC with 1.07 Bar Average Inlet Pressure

The isothermal and adiabatic comparisons show that the compressor peaks in its performance somewhere between 10–20 Bar of compression. This agrees with the start of exponentially increasing work to compress the hydrogen previously shown in Figure 28. The compressor is consuming more energy and producing less work. The voltage continues to increase while the volumetric flow rate goes to zero.

The EHC's performance is compared to a sample of mechanical compressors in Figure 35. The values for the mechanical compressors were calculated using the manufacturer's advertised performance specifications. Since the mechanical compressor values were not verified through testing, they may be subject to error and not representative of actual field performance. Regardless of the uncertainty in the mechanical compressor data, it is clear the EHC does not outperform its mechanical competitors or either ideal cycle.

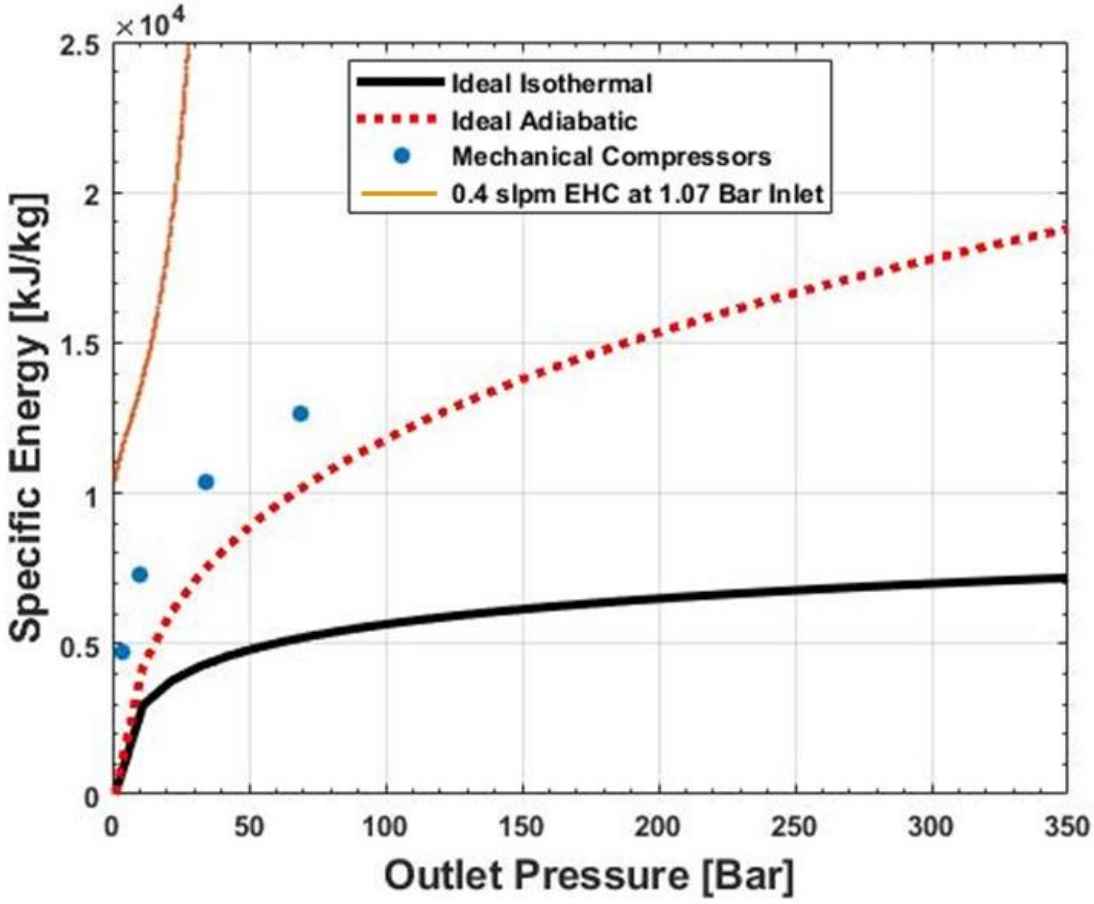

Figure 35. Comparison of 0.4 slpm EHC with 1.07 Bar Average Inlet Pressure to Mechanical Compressors

Figure 36 combines data from all seven experiments conducted with the smaller compressor. There was a wide range of specific energy values from one experiment to the next with minimal changes in the controlled variables. Inlet temperature varied by 3–4 degrees Kelvin and the inlet pressure was varied ± 0.42 Bar (6.1 psi). The compressor followed the same general performance trend through each experiment. It showed logarithmic growth in specific energy consumption during initial stages of compression and transitioned to an exponential growth as the outlet pressure increased. None of the experiments followed the ideal isothermal compression cycle yet the compressor does operate isothermally. The actual cycle includes thermodynamic and electrical losses that prevent the compressor from meeting the ideal cycle efficiencies.

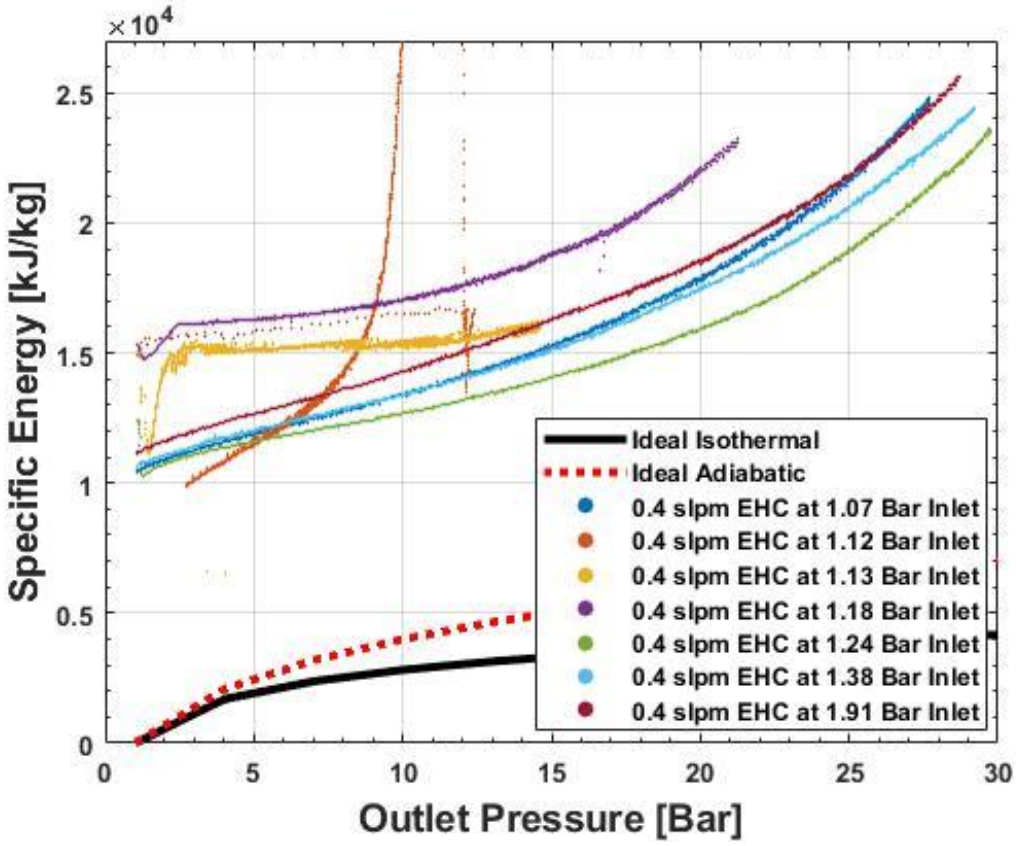

Figure 36. Specific Energy for 0.4 slpm EHC at Various Inlet Pressures

b. 4.0 SLPM EHC Tested at 1.56 Bar Average Inlet Pressure

Figure 37 shows the specific energy used by the larger 4.0 slpm compressor during its first test. The compressor failed around 4.5-5 Bar and was unable to continue the experiment. The data collected was much more scattered, and this could be due to the internal leak that was discovered after the test was concluded. The large compressor showed promising performance for the short time it operated despite the scattered data and inability to continue testing.

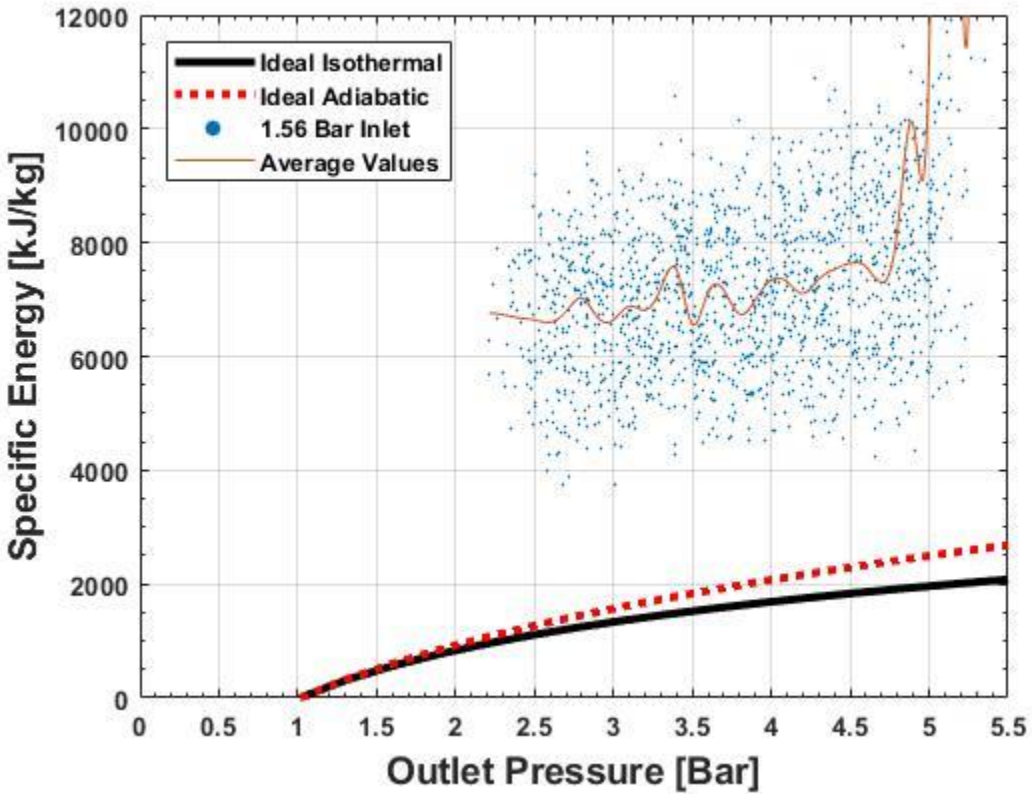

Figure 37. Specific Energy of 4.0 slpm EHC at 1.56 Bar Inlet Pressure

Figure 38 combines data from all eight experiments, including the single experiment conducted on the defective 4.0 slpm compressor. Despite the leak in the larger compressor, its performance far exceeded the smaller compressor over the 0–5 Bar compression range.

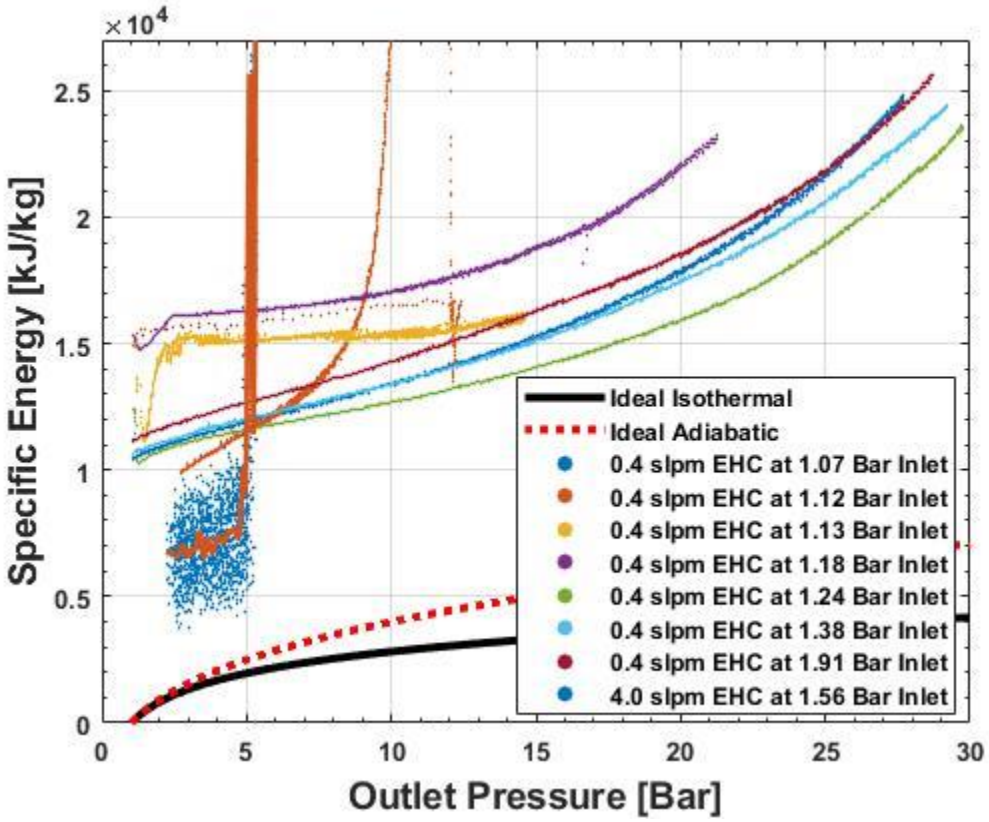

Figure 38. Combined Results of 0.4 slpm and 4.0 slpm Electrochemical Compressors at Various Inlet Pressures

2. Endurance Testing

The EHC, as a solid-state device, offers the ability to continuously operate for extended periods without the need to replace mechanical seals, lubricants, or filters. This research was initially intended to investigate the compressor's performance as a function of run time. However, failure of the compressors prevented conducting more lengthy experiments that were needed for analysis. Previous research by Lipp [4] showed that

EHCs could run for >10,000 hours without significant degradation in performance. Mechanical compressors, in comparison, have a mean time between failure around 900 hrs [46]. The significantly longer mean time between failure for EHCs suggests that operation, maintenance, and repair cost savings over mechanical compressors may prove to offset the slightly lower efficiencies witnessed during this study.

THIS PAGE INTENTIONALLY LEFT BLANK

IV. DISCUSSION

A. NAVY PHOTOVOLTAIC INFRASTRUCTURE

The Navy and Marine Corps have installed approximately 405 photovoltaic arrays worldwide over the last 30 years. The estimated value of this investment is $1.9B (Plant Replacement Value). However, Figure 39 shows most of this investment has been made in the past ten years. Plant Replacement Value is an estimate of the cost to design and construct a replacement facility at the same location meeting current code requirements. This metric is used throughout the DOD as a measurement of size, to calculate condition ratings, and to estimate long-term recapitalization requirements. The estimate is calculated using the equation outlined in Unified Facilities Criteria (UFC) 3–701-01 Chapter 3, Unit Costs for DOD Facilities Cost Models [47]. Since the Department of the Navy has already made substantial investments in photovoltaic arrays, it makes sense to take efforts to increase reliability and resiliency of these systems. One method of increasing resiliency is to incorporate energy storage capability with the renewable energy generation. Only a few demonstration projects have been planned in the DOD for renewable energy storage. The Navy Resilient Energy Program Office is working on microgrids in Connecticut and Arizona that incorporate battery storage, as well as two battery storage stations in California. The other services are also investing in microgrids with energy storage and energy storage stations. So far, all of these demonstration projects have relied on battery technology for their energy storage.

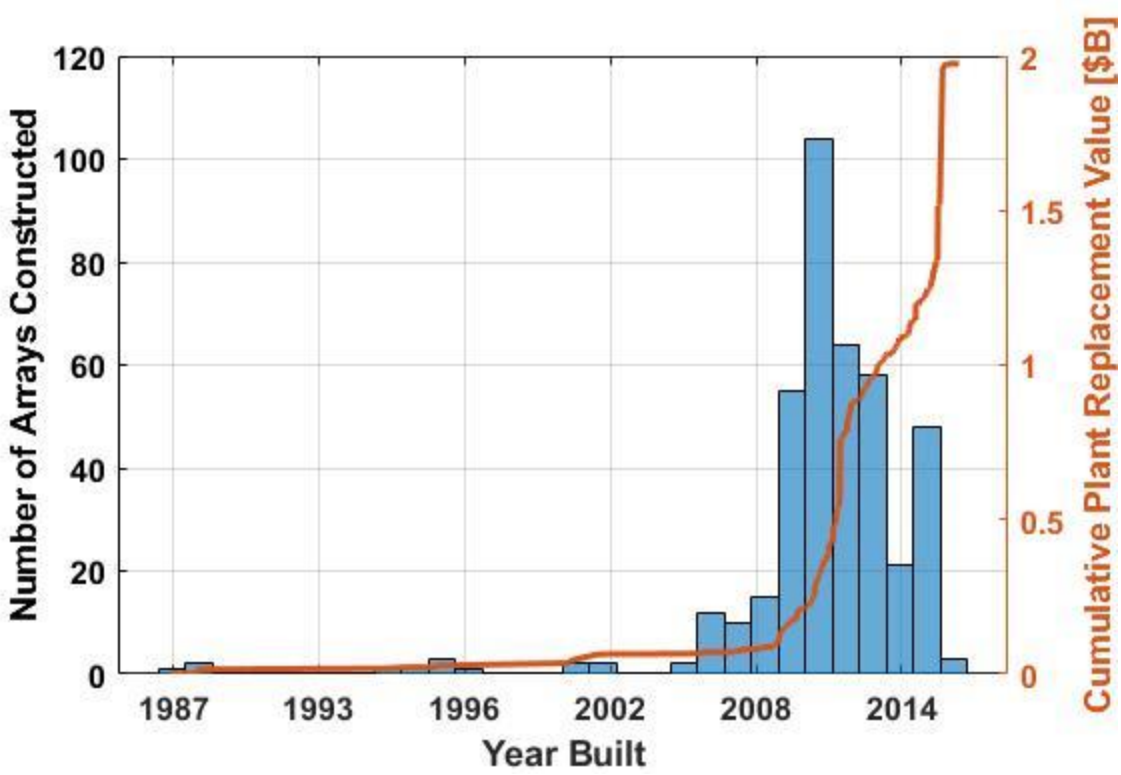

Figure 39. Department of the Navy Photovoltaic Facility Investment. Source: [48].

Over half of the photovoltaic arrays installed by the Department of the Navy are located in California where the grid operators are battling a growing oversupply problem. The oversupply results from an increase of solar and wind generation during periods of low demand that has forced grid operators like California Independent System Operator (CAISO) to curtail renewable energy production. Figure 40 shows the renewable curtailment CAISO has had to enact over the past few years and highlights an increasing trend.

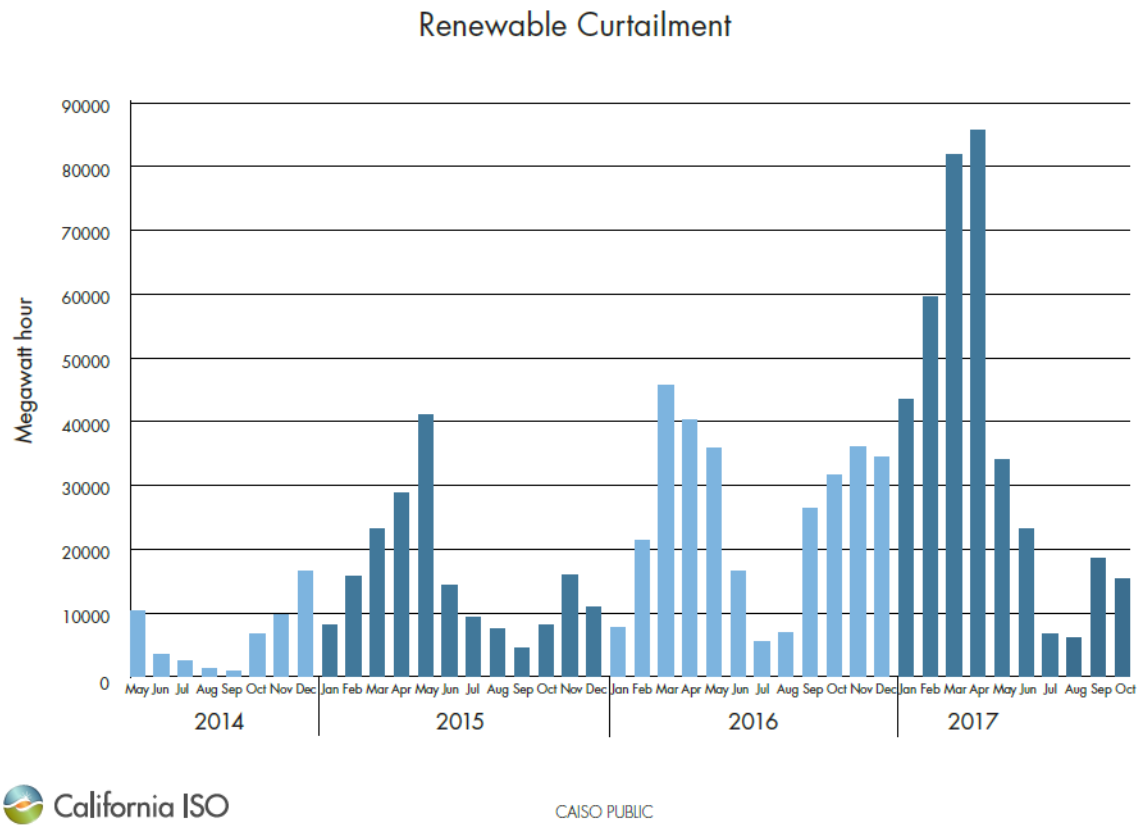

Figure 40. California Independent System Operator (CAISO) Renewable Curtailment Totals (2014 – 2015). Source: [49].

Adding hydrogen generation and storage to existing photovoltaic facilities could serve to increase the diversity of energy storage technologies in the Navy's portfolio of renewable energy investments. Investing in only one technology, batteries, will make it more challenging to conduct life cycle comparisons between the different shore energy storage technologies available. Additional demonstration projects that incorporate hydrogen generation and storage should be pursued to allow realistic comparisons. Selection criteria for candidate sites could include potential users of the hydrogen alternative fuel, local utility rate structures, and existing local grid reliability.

B. OPPORTUNITIES

1. Stationary Installations

The European Union is investing heavily in Hydrogen and Fuel Cell technology. The Fuel Cell and Hydrogen Joint Undertaking has funded approximately 532M€ ($622M) for 170 major projects relating to hydrogen and fuel cell technologies [50]. Lessons learned from these projects can provide insight and guidance for any DOD agency seeking to implement a hydrogen energy storage station into a microgrid or remote outpost. For instance, the 2011–2014 ELYGRID (electrolyzer to grid) project concluded long returns on investment and complex site-specific power and gas markets contribute to slow adoption of using electrolyzers in grid-scale applications [51]. One other European Union project to note is the "Combined Hybrid Solution of Multiple Hydrogen Compressors for Decentralized Energy Storage and Refueling Stations" project in Germany. This 3-year, 2.5M€ ($2.9M) project started in January 2017 and will focus on integrating small, silent, low-cost compressors with traditional mechanical compressors in decentralized environments [52]. Decentralized environments include both small-scale refueling and hydrogen storage facilities on islands. The same scope of effort could be applied to Navy installations in the Pacific.

2. Expeditionary Application

In his white paper, "The Future Navy," the Chief of Naval Operations outlined the need to increase forward presence of persistent, self-sufficient platforms to execute long-term U.S. strategy [53]. Among these platforms, he specifically mentions the "increasing numbers of unmanned air vehicles" and asserts "[t]here is no question that unmanned systems must also be an integral part of the future fleet" [53]. A hydrogen production, compression, and storage system modeled after the one built during this research project could fuel forward deployed unmanned systems without long fuel logistics lines of communication. A small-scale, reliable hydrogen station coupled with persistent unmanned Command, Control, Communications, Computers, Intelligence, Surveillance and Reconnaissance (C4ISR) assets could meet the demand for self-sustaining assets worldwide.

Multiple unmanned aerial vehicle manufacturers are already demonstrating commercially available hydrogen fuel cell powered drones. Last year, for instance, Intelligent Energy demonstrated their Unmanned Aerial Vehicle (UAV) Fuel Cell Module proving it could fly for longer durations and farther distances than battery-only units [54]. Longer flight times, farther travel distance, and greater lift capacity are the key advantages advertised by manufacturers. If these claims are proven correct, using renewably produced hydrogen to fuel squadrons of unmanned aerial vehicles is a possibility worth investigating.

A site visit to Lithuania was conducted during this research to investigate the performance of a hybrid power generation and management system built for North Atlantic Treaty Organization (NATO) deployed forces. The demonstration station, shown in Figure 41, managed three different types of power generators (wind, solar, diesel), a battery energy storage bank, and 150kW of intermittent loads. The entire system fits into two 6 m (20ft) ISO containers for rapid transport and deployment. A 35% savings in fuel usage was demonstrated during a field exercise supporting 70 tents and 500–600 troops [55]. The battery energy storage utilized expensive lithium-ion batteries that required a separate chiller plant to maintain low temperatures in the field. Similar systems could be built with hydrogen storage that offered peak shaving like the one demonstrated in Lithuania, as well as, hydrogen fuel for vehicles in the field.

Figure 41. NATO Camp Hybrid Power Station

Aside from military C4ISR applications, hydrogen fueling infrastructure can also support UAVs used for installation surveying, inspection, and assessments. An ongoing Energy Systems Technology Evaluation Program (ESTEP) demonstration project by Naval Facilities Engineering Command (NAVFAC) Engineering and Expeditionary Warfare Center (EXWC) is using UAVs to survey and inspect existing electric utility infrastructure in remote areas to reduce manning requirements and personnel safety risks [56]. These surveying and inspection UAVs could be used for many routine inspections of building envelopes, critical infrastructure, real estate and protected environmental areas. In 2015, the Minnesota Department of Transportation successfully proved this concept in their "Unmanned Aerial Vehicle Bridge Inspection Demonstration Project" concluding the UAVs offered a cost-effective and safe means of gathering detailed visual and infrared data on bridges, waterways, and embankments [57].

3. Hydrogen at Sea

Most progress in fuel cell powered unmanned vehicles has been made in aerial applications. However, if the Navy invested in hydrogen stations, unmanned subsurface and surface vehicles could also benefit from having their fuel generated locally in remote regions using renewable sources of energy. EHCs like the ones tested during this research

could be used to significantly reduce the overall size and weight of the compression stations needed to fuel such unmanned vehicles. Their compactness would also benefit sea-based energy strategies such as the novel “energy ship” concept proposed by Dr. Maximilian Platzer. He proposed using sailing ships to harvest wind energy through hydrokinetic turbines, converting the turbine shaft energy into electricity, using the electricity to generate hydrogen, and then using the hydrogen to power shore installations and transport vehicles [58] and [59]. This concept requires compressed hydrogen storage onboard the sailing vessels. Reducing weight through storage is unlikely since storage at high pressures requires heavy cylinders due to hydrogen’s physical properties and tendency to cause embrittlement. Saving weight by reducing the compressor size is more achievable, and EHCs offer a means of reducing overall system weight significantly.

THIS PAGE INTENTIONALLY LEFT BLANK

V. CONCLUSION

The purpose of this research was to design, build, and test a renewably powered hydrogen gas compression and storage station incorporating an electrochemical hydrogen gas compressor. The station designed, constructed, and tested during this research has confirmed that EHCs operate as advertised and can be used in energy storage applications. The solid-state operation alleviates the problem of expensive operations and maintenance costs associated with mechanical hydrogen compressors. However, the breakdown of both EHCs tested during this research highlight a significant reliability concern. Additionally, EHCs are still in an early design and development state and require additional engineering before they can compete with mechanical compressors. The EHCs used during this research lacked NFPA/NEC compliant connections, automated passive and active safety devices, and industrial controls. If manufacturers can correct both reliability deficiencies and design deficiencies, EHCs could serve in multiple Navy environments for a wide range of hydrogen applications.

Experimental performance data was obtained for two EHCs with different rated flow capacities. This data was analyzed based on three different operating principles: Nernst electrochemical process efficiency, comparison to ideal adiabatic operation of mechanical compressors, and ideal isothermal compression efficiency. The tests indicate EHCs do not necessarily follow the ideal isothermal compression cycle and will be less efficient than the ideal case. A maximum isothermal efficiency can be determined experimentally at specific compressor outlet pressures. The smaller EHC's efficiency peaked at 21% when the outlet pressure reached 14 Bar. The larger EHC failed before its efficiency could be determined.

THIS PAGE INTENTIONALLY LEFT BLANK

APPENDIX A. VACUUM/PRESSURE PURGING CALCULATIONS

The purge station was designed to deliver at least 34 atm (500 psi) nitrogen using a commercial-off-the-shelf gas cylinder header and regulator. The vacuum pump available for use by the laboratory was capable of delivering a maximum of 711 mm (28 in) Hg (gauge) vacuum (0.064 atm).

The number of vacuum/pressure purge cycles required is calculated according to the formula found in [27] as follows:

$$N \geq \frac{\ln\left(\frac{C_{safe}}{C_{air}}\right)}{\ln\left(\frac{P_{Low}}{P_{High}}\right)} = \frac{\ln\left(\frac{0.01}{0.21}\right)}{\ln\left(\frac{P_{Low}}{P_{High}}\right)}, \qquad (17)$$

$$N = 1, 2, 3, \ldots$$

where,

C_{safe} = Safe concentration of residual oxygen, 1% per CGA G-5.4

C_{air} = Initial concentration of oxygen in air, 21%

P_{Low} = Absolute pressure after vacuum

and,

P_{High} = Purging pressure of inert gas, 34 atm N_2 (500 psi) maximum.

The total mass of N2 required for the vacuum/pressure purge process is calculated as follows:

$$m = n \times M = \frac{\left(P_{High} - P_{Low}\right) \cdot V}{R \cdot T} \times \frac{M}{1000\left(g / kg\right)}, \qquad (18)$$

where,

n = Moles of purge gas added to the station, mol

M = Molar Mass of Nitrogen, 28.0134 $\frac{g}{mol}$

V = Total Volume of vessels, 0.2592 m^3

R = Universal Gas Constant, 8.314 $\frac{J}{mol \cdot K}$

T = normal temperature, 298.15 K (25 °C).

Table 11 provides list of optimum vacuum/pressure combinations to conserve purge gas.

Table 11. Optimum Vacuum/Pressure Purge Regimes

P_{Low}, atm	P_{High}, atm	N	Total Mass of N_2 Required, kg
0.064	1.7	1	0.5
0.332	1.7	2	0.8
0.064	1.3	2	0.8
0.332	1.3	3	0.9
0.666	2.0	3	1.2
0.666	3.4	2	1.6
1.0	3.0	3	1.8
0.332	7.1	1	2.0
1.0	4.7	2	2.2
0.666	14.3	1	4.0
1.0	21.0	1	6.0

APPENDIX B. PIPE WALL THICKNESS CALCULATIONS

The minimum tube wall thickness is calculated using the following formula from [37]:

$$t_m = t + c \tag{19}$$

Where c = sum of the mechanical allowances (thread or groove depth) plus corrosion and erosion allowances. A value of 0.0762 mm (0.003 in) was used because negligible corrosion and erosion are expected during the stations short period of operation.

D = outside diameter of pipe as listed in tables of standards or specifications, or as measured. A value of 12.7±0.0762mm (0.5±0.003 in) was provided by the manufacturer.

d = inside diameter of the pipe.

E = quality factor from Table IX-3B Longitudinal Joints Factors for Pipeline Materials. A value of 1.0 is listed for all seamless piping.

M_f = material performance factor that addresses the loss of material properties associated with hydrogen gas service. Austenitic stainless steels do not have a material performance factor listed. A value of 1.0 was used.

P = internal design pressure gauge pressure. A maximum of 2.0684×10^7 Pa (3,000 psi) was used.

S = stress value for material from Table IX-1A. 1.15142450×10^8 Pa (16.7 ksi) is listed for 316L at 37.7778 °C (100°F).

T = pipe wall thickness (measured or minimum per purchase specification)

t = pressure design thickness, not less than that calculated in accordance with either equation below. For straight pipe under internal pressure with t < D/ 6=2.1167±0.0127 mm (0.0833±0.0005 in):

$$t = \frac{PD}{2\left(SEM_f + PY\right)} = \frac{2.0684\times10^7 \cdot \left(12.7 \pm 0.0762\right)}{2\left(1.15142450\times10^8 \cdot 1 \cdot 1 + 2.0684\times10^7 \cdot 0.4\right)}$$

$$= 1.0642 \pm 0.0064 mm$$

$$t = \frac{PD}{2\left[SEM_f + P(1-Y)\right]} = \frac{2.0684\times10^7 \cdot \left(12.7 \pm 0.0762\right)}{2\left(1.15142450\times10^8 \cdot 1 \cdot 1 + 2.0684\times10^7 \cdot \left(1-0.4\right)\right)}$$

$$= 1.0297 \pm 0.0062 mm$$

A value of 1.0706 mm was used for *t*.

Therefore, $t_m = t + c$ = 1.0706 + 0.0762 = 1.1468 mm (0.0452 in). The minimum thickness is less than the standard tube size selected for the ½" OD tubing, and there is no need for thicker wall tubing.

APPENDIX C. PIPING AND IDENTIFICATION (P&ID) DIAGRAM

Filename: Deimos - E:\FOSSON\Drawings and Sketches\ Compression P&ID (Draft).vsd

December 1, 2017	NPS Hydrogen Gas Compression & Storage Station P&ID

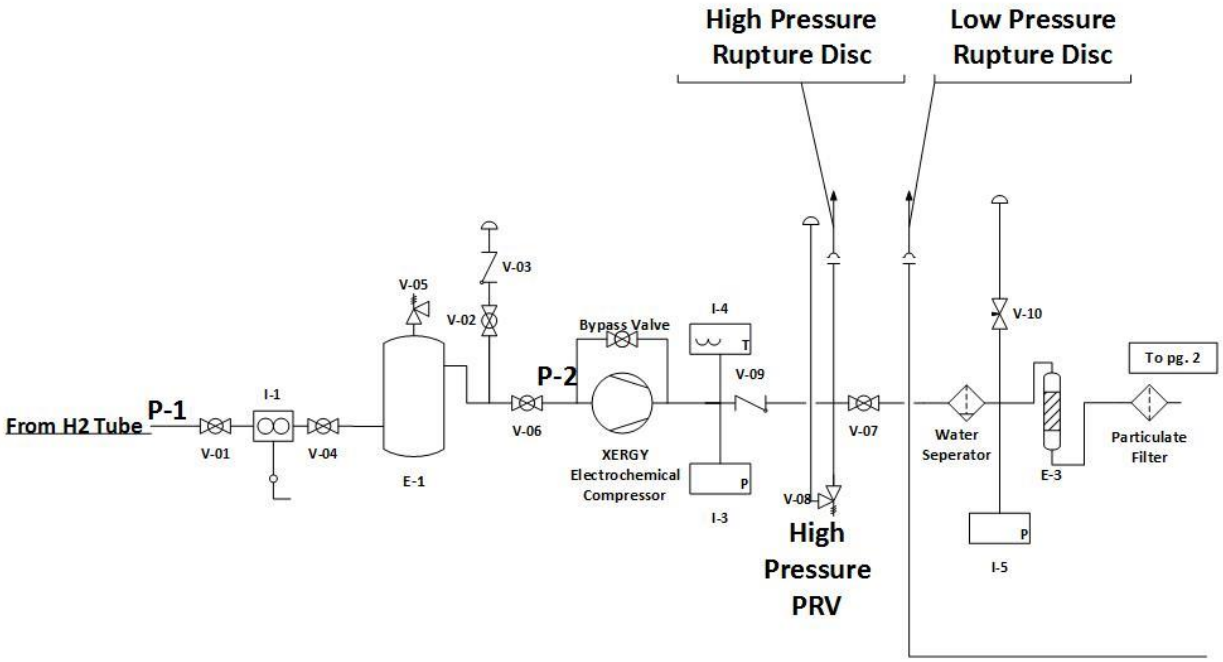

December 1, 2017	NPS Hydrogen Gas Compression & Storage Station P&ID

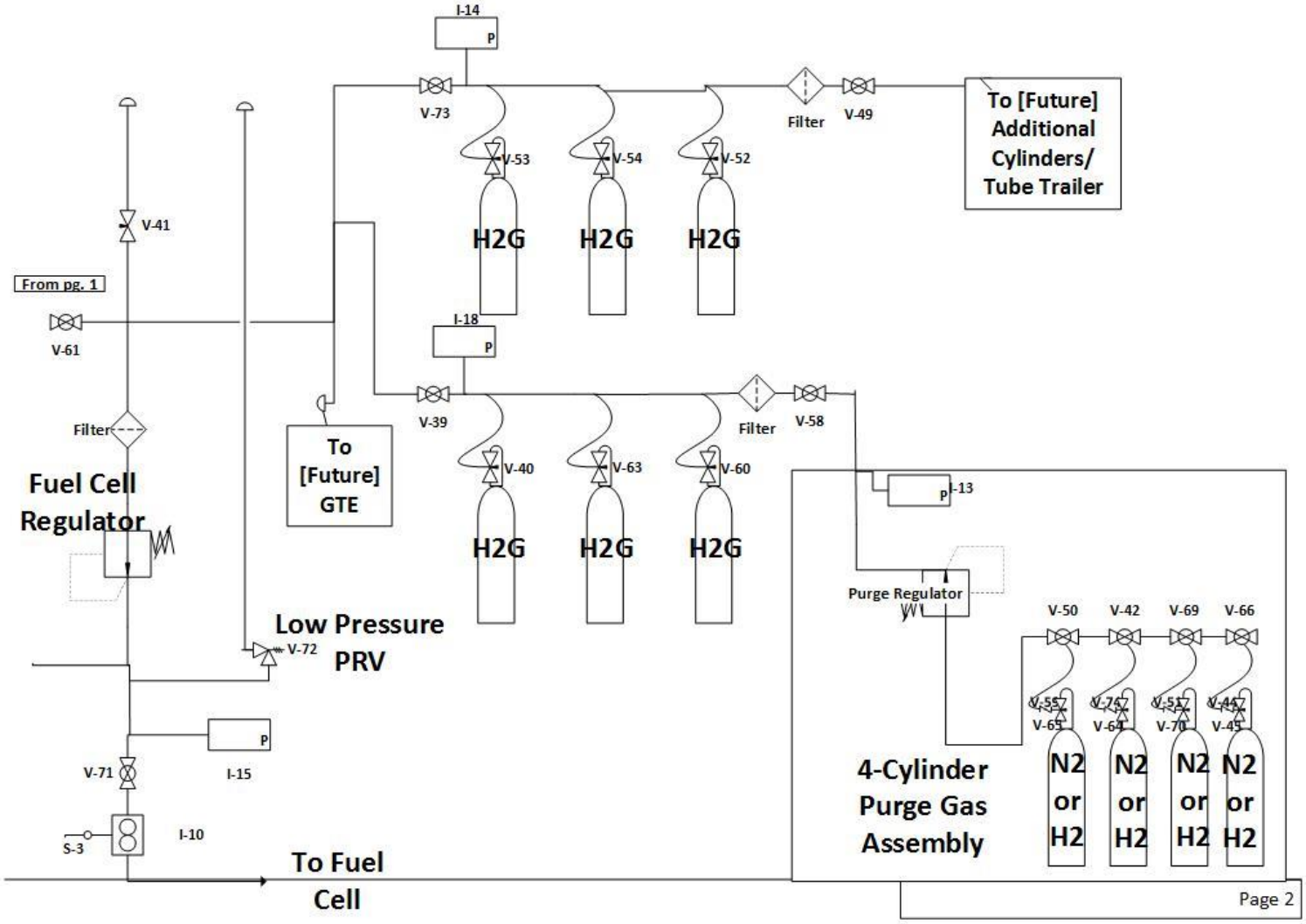

Valve List

Displayed Text	Description	Line Size	Valve Class	Manufacturer	Model
V-01	PFA Tubing Ball Valve				
V-02	PFA Tubing Ball Valve				
V-03	Poppet Check Valve				
V-04	PFA Tubing Ball Valve				
V-05	Relief Valve				
V-06	316 SS Ball Valve	1/4" T	40G Series	Swagelok	SS-43GS4
V-07	316 SS Ball Valve	1/4" T	40G Series	Swagelok	SS-43GS4
V-08	300psi 316L SS Relief Valve	1/4" T	PRV Series	Swagelok	PRV2-N2F-02-0-VV
V-09	316 SS Poppet Check Valve	1/4" T	CP Series	Swagelok	SS-4CP4-1/3
V-10	316 SS Needle Valve	1/4" T	1 Series	Swagelok	SS-1RS4
V-11	316 SS Ball Valve	1/4" T	40G Series	Swagelok	SS-43GS4
V-12	316 SS Needle Valve	1/4" T	1 Series	Swagelok	SS-1RS4
V-13	50 psi 316 SS Relief Valve	1/4" T	R Series	Swagelok	SS-RL3S4
V-14	316 SS Ball Valve	1/4" T	40G Series	Swagelok	SS-43GS4
V-15	316 SS Ball Valve	1/2" T	40G Series	Swagelok	SS-43GS8
V-16	316 SS Ball Valve	1/2" T	40G Series	Swagelok	SS-43GS8
V-17	316 SS Ball Valve	1/2" T	40G Series	Swagelok	SS-43GS8
V-18	316 SS Ball Valve	1/2" T	40G Series	Swagelok	SS-43GS8
V-19	316 SS Ball Valve	1/2" P	54 Series Manifold	Matheson Gas	54-48V
V-20	316 SS Ball Valve	1/2" P	54 Series Manifold	Matheson Gas	54-48V
V-21	316 SS Ball Valve	1/2" P	54 Series Manifold	Matheson Gas	54-48V
V-22	316 SS Ball Valve	1/2" P	54 Series Manifold	Matheson Gas	54-48V
V-23	Brass Cylinder Valve	13/16"	CGA350	Norris Cylinder	Model 8BC250
V-24	Brass Cylinder Valve	13/16"	CGA350	Norris Cylinder	Model 8BC250
V-25	Brass Cylinder Valve	13/16"	CGA350	Norris Cylinder	Model 8BC250
V-26	Brass Cylinder Valve	13/16"	CGA350	Norris Cylinder	Model 8BC250
V-27	Brass Cylinder Valve	13/16"	CGA350	Norris Cylinder	Model 8BC250
V-28	Brass Cylinder Valve	13/16"	CGA350	Norris Cylinder	Model 8BC250
V-29	Integrated Pigtail Check Valve	13/16"	CGA350	Matheson Gas	54-48V
V-30	Integrated Pigtail Check Valve	13/16"	CGA350	Matheson Gas	54-48V
V-31	Integrated Pigtail Check Valve	13/16"	CGA350	Matheson Gas	54-48V
V-32	Integrated Pigtail Check Valve	13/16"	CGA350	Matheson Gas	54-48V
V-33	Brass Cylinder Valve	13/16"	CGA350	TBD	TBD
V-34	Brass Cylinder Valve	13/16"	CGA350	TBD	TBD
V-35	Brass Cylinder Valve	13/16"	CGA350	TBD	TBD
V-36	Brass Cylinder Valve	13/16"	CGA350	TBD	TBD
V-37	316 SS Ball Valve	1/4" T	40G Series	Swagelok	SS-43GS4
V-38	316 SS Needle Valve	1/4" T	1 Series	Swagelok	SS-1RS4

Instrument List

Description	Connection Size	Service	Manufacturer	Model
Flowmeter	1/4" NPT M	Normal	Alicat	
Flowmeter	1/4" NPT M	Normal	Alicat	
Pressure Gage	1/4" NPT M	Normal	McDaniel Controls Inc.	2.5" SS Model KN 0-3000 PSI
Themometer	1/2" NPT M	Normal	Swagelok	T48L-040-DS-08-G-8-NTSS
Pressure Gage	1/4" NPT M	Normal	McDaniel Controls Inc.	2.5" SS Model KN 0-3000 PSI
Pressure Gage	1/4" NPT M	Normal	McDaniel Controls Inc.	2.5" SS Model KN 0-3000 PSI
Pressure Gage	1/2" NPT M	Normal	NoShok	4" SS Model 40-500-3000-psi-CC
Pressure Gage	1/2" NPT M	Normal	NoShok	4" SS Model 40-500-3000-psi-CC
Pressure Gage	1/2" NPT M	Normal	NoShok	4" SS Model 40-500-3000-psi-CC

Pipeline List

Displayed Text	Description	Line Size	Schedule	Design Pressure [psig]	Design Temperature [F]	Quantity
P-1	PFA Tubing	1/4 OD x 0.062"	Hose	275	400	1
P-2	316 SS Seamless Tubing	1/4 OD x .049"	Tube	4 800	100	5
P-3	316 SS Seamless Tubing	1/2 OD x .049"	Tube	4 800	100	5
P-4	316 SS Tubing	1/2 OD	Tube	3 000	100	1
P-5	PFA Tubing	1/4 OD x 0.062"	Hose	275	400	2
						59

Equipment List

Displayed Text	Description	Manufacturer	Material	Model
E-1	Water Bubler		PVC	
XERGY Electrochemical Compressor	Electrochemical Compressor	Xergy		X-CELL
Water Seperator	High Pressure Service Water Seperator With Drain	Parker	316 SS	SJN2L-100WSY
E-3	Activated Charcoal Filter With Drain	Parker	316 SS	SJN2L-AWCY
Particulate Filter	High Pressure Service Particulate Filter With	Parker	316 SS	SJN2S-4CWCY
Filter	40 Micron, 7 Micorn, 2	Swagelok	316 SS	SS-4TF-SS-8TF-
Purge Regulator	0-500 PSI	Matheson	316 SS	3510A
Fuel Cell Regulator	0-50 PSI	TESCOM	316 SS	44-2260-241-1532

APPENDIX D. MATLAB SCRIPT FOR EXPERIMENT DATA COLLECTION

Filename: Deimos - E:\FOSSON\NI cDAQ Tests and Scripts\TestScript.m

```
%% Hydrogen Compression Station Data Acquisition Using NI CompactDAQ
9184
% (1)  Verify COM port for Alicat Flow Meter using Device Manager
% (2)  Open NI MAX and test CompacDAQ Chasis to verify communications
% (3)  Enter filename below
filename='20171017'
%% Reset NI DAQ
daqreset
devices = daq.getDevices
s = daq.createSession('ni')
%%
% Establish Communications with Alicat Flow Meter
flowMeter=serial('COM3','TimeOut',2,'BaudRate',19200,'Terminator','CR')
;
fopen(flowMeter);
% Preallocate Data Arrays
runtime = 60; %seconds
time = zeros(1,runtime);
NIdata = zeros(8,runtime);
timerecord=zeros(1,runtime);
inletflowrate=zeros(1,runtime);
inletpressure=zeros(1,runtime);
inlettemp=zeros(1,runtime);

% Temperature Measurement
% Add Thermocouples and Configure
%%
addAnalogInputChannel(s,'cDAQ9185-1C7CD98Mod1',0:2, 'Thermocouple');
%%
tc1 = s.Channels(1);
set(tc1);
tc1.ThermocoupleType = 'K';
tc1.Units = 'Celsius';
tc2 = s.Channels(2);
set(tc2);
tc2.ThermocoupleType = 'K';
tc2.Units = 'Celsius';
tc3 = s.Channels(3);
set(tc3);
tc3.ThermocoupleType = 'K';
tc3.Units = 'Celsius';
%%
% Voltage Measurement
% Add Analog Input Channels
addAnalogInputChannel(s,'cDAQ9185-1C7CD98Mod3', 0:1, 'Voltage');
addAnalogInputChannel(s,'cDAQ9185-1C7CD98Mod4', 0:2, 'Voltage');
%%
for i=1:runtime % # of samples to collect data for
```

```
    tic
    time(i)=now;
    fprintf(flowMeter,'A');
    IN=fscanf(flowMeter);

[OUT.ID,OUT.pressure,OUT.temp,OUT.LPM,OUT.SLPM,OUT.gas]=strread(IN,...
        '%s%f%f%f%f%s', 'delimiter', ' ');
    inletflowrate(i)=OUT.SLPM;
    inletpressure(i)=OUT.pressure;
    inlettemp(i)=OUT.temp;
    NIdata(:,i) = s.inputSingleScan;
%     yyaxis left
%     hold on
%     plot(i,inletflowrate(i),'.')
%     plot(i,NIdata(4,i),'.',i,NIdata(5,i),'.')
%     yyaxis right
%     plot(i,NIdata(6,i),'.',i,NIdata(7,i),'.')
    toc
    pause(2-toc)
end
datestr(time);
%
%% Clean up the serial object
fclose(flowMeter);
delete(flowMeter);
clear flowMeter;
%% Write data to file
A=[time',inletflowrate',inletpressure',inlettemp',NIdata'];
xlswrite(filename,A)
%% Read data in file
B=xlsread(filename)

% plot(time,data(:,3),time,data(:,4),time,data(:,5),time,data(:,6), ...
% time,data(:,7),time,data(:,8),time,data(:,9),time,data(:,10));
% xlabel('Time (secs)');
% ylabel('Voltage')
% figure
% plot(time, data(:,1),time,data(:,2))
% xlabel('Time (secs)');
% ylabel('Temperature (Celcius)');
```

APPENDIX E. SENSOR SPECIFICATIONS

A. NATIONAL INSTRUMENTS CDAQ 9185 SPECIFICATIONS [60]

SPECIFICATIONS

cDAQ™-9185

4-Slot, Extended Temperature, Ethernet CompactDAQ Chassis

Definitions

Warranted specifications describe the performance of a model under stated operating conditions and are covered by the model warranty.

Characteristics describe values that are relevant to the use of the model under stated operating conditions but are not covered by the model warranty.

- *Typical* specifications describe the expected performance met by a majority of the models.
- *Nominal* specifications describe parameters and attributes that may be useful in operation.

Specifications are *Typical* unless otherwise noted.

Conditions

Specifications are valid at 25 °C unless otherwise noted.

Analog Input

Input FIFO size	127 samples per slot
Maximum sample rate[1]	Determined by the C Series module or modules
Timing accuracy[2]	50 ppm of sample rate
Internal base clocks	80 MHz, 20 MHz, 13.1072 MHz, 12.8 MHz, 10 MHz, 100 kHz
Number of channels supported	Determined by the C Series module or modules

[1] Performance dependent on type of installed C Series module and number of channels in the task.
[2] Does not include group delay. For more information, refer to the documentation for each C Series module.

NATIONAL INSTRUMENTS

B. ALICAT M-SERIES MASS FLOW METER SPECIFICATIONS [61]

Technical Data for Alicat M-Series Mass Flow Meters
0 – 0.5 sccm Full Scale through 0 – 5000 slpm Full Scale

ALICAT SCIENTIFIC
Tel: 888-290-6060
www.alicat.com/m

Standard Specifications (Contact Alicat for available options.)

Performance	M-Series Mass Flow Meter
Accuracy at calibration conditions after tare	± (0.8% of Reading + 0.2% of Full Scale)
High Accuracy at calibration conditions after tare	± (0.4% of Reading + 0.2% of Full Scale) High Accuracy option not available for units ranged under 5 sccm or over 500 slpm.
Accuracy for Bidirectional Meters at calibration conditions after tare	± (0.8% of reading + 0.2% of total span from positive full scale to negative full scale)
Repeatability	± 0.2% Full Scale
Zero Shift and Span Shift	0.02% Full Scale / ºCelsius / Atm
Operating Range / Turndown Ratio	0.5% to 100% Full Scale / 200:1 Turndown
Maximum Measurable Flow Rate	up to 128% Full Scale (Gas Dependent)
Typical Response Time	10 ms (Adjustable)
Warm-up Time	< 1 Second

Operating Conditions	M-Series Mass Flow Meter
Mass Reference Conditions (STP)	Field-selectable, defaults to 25°C & 14.696 psia unless requested otherwise
Operating Temperature	−10 to +60 ºCelsius
Humidity Range (Non–Condensing)	0 to 100%
Maximum Internal Pressure (Static)	145 psig
Maximum Allowable Instantaneous Differential Pressure Across Device (Inlet to Outlet)	75 psid
Proof Pressure	175 psig
Mounting Attitude Sensitivity	None
Ingress Protection	IP40
Wetted Materials	303 & 302 Stainless Steel, Viton®, Heat Cured Silicone Rubber, Glass Reinforced Polyphenylene Sulfide, Heat Cured Epoxy, Aluminum, Gold, Silicon, Glass. If your application demands a different material, please contact Alicat.

Communications / Power	M-Series Mass Flow Meter
Monochrome LCD or Color TFT Display with integrated touchpad	Simultaneously displays Mass Flow, Volumetric Flow, Pressure and Temperature
Digital Output Signal[1] Options	RS-232 Serial / RS-485 Serial / Modbus / EtherNet IP / DeviceNet / PROFIBUS
Analog Output Signal[2] Options	0-5 Vdc / 1-5 Vdc / 0-10 Vdc / 4-20 mA
Optional Secondary Analog Output Signal[2]	0-5 Vdc / 1-5 Vdc / 0-10 Vdc / 4-20 mA
Electrical Connection Options	8 Pin Mini-DIN / 9-pin D-sub (DB9) / 15-pin D-sub (DB15) / 6 pin locking
Supply Voltage	7 to 30 Vdc (15-30 Vdc for 4-20 mA outputs)
Supply Current	0.040 Amp (+ output current on 4-20 mA)

1. The **Digital Output Signal** communicates Mass Flow, Volumetric Flow, Pressure and Temperature
2. The **Analog Output Signal** and **Optional Secondary Analog Output Signal** communicate your choice of Mass Flow, Volumetric Flow, Pressure or Temperature

Features	M-Series Mass Flow Meter
Gas Select™ 5.0	**Gas Select™ 5.0** provides **98 Preloaded Gas Calibrations: See the following page for a complete list.** If your application calls for a gas not on this list, please let us know. We can also calibrate to a wide variety of complex gas mixtures involving up to eight gas constituents. **For corrosive gases and refrigerants see Alicat's MS-Series meters (*www.alicat.com/ms*).**
COMPOSER™	**COMPOSER™ is a feature of Gas Select™ 5.0 that allows users to defines up to 20 user gas compositions with up to 5 constituent gases per mix (*www.alicat.com/composer*).**

Range Specific Specifications

Full Scale Flow Mass Meter	Pressure Drop at FS Flow (psid) venting to atmosphere[1]	Mechanical Dimensions[2]	Process Connections[3]
0.5 sccm to 1 sccm	1.0	3.9"H x 2.4"W x 1.1"D	M-5 (10-32) Female Thread (Shipped with M-5 (10-32) Male Buna-N O-ring face seal to 1/8" Female NPT fittings.)
2 sccm to 50 sccm	1.0		
100 sccm to 20 slpm	1.0	4.1"H x 2.4"W x 1.1"D	1/8" NPT Female
50 slpm	2.0	4.4"H x 4.0"W x 1.6"D	1/4" NPT Female
100 slpm	2.5		
250 slpm	2.1	5.0"H x 4.0"W x 1.6"D	1/2" NPT Female
500 slpm	4.0	5.0"H x 4.0"W x 1.6"D	3/4" NPT Female (A 1-1/4" NPT Female optional process connection is available for 2000 slpm meters.)
1000 slpm	6.0		
1500 slpm	9.0		
2000 slpm	5.0	5.3"H x 5.2"W x 2.9"D	
3000 slpm	7.1	5.3"H x 5.2"W x 2.9"D	1-1/4" NPT Female
4000 slpm	2.7	7.6"H x 5.2"W x 2.9"D	2" NPT Female
5000 slpm	3.4	6.3"H x 5.2"W x 3.9"D	

1. Lower Pressure Drops Available, please see our **WHISPER-Series** mass flow controllers at ***www.alicat.com/whisper***.
2. See drawings for metric equivalents
3. Compatible with Swagelok® tube, Parker®, face seal, push connect and compression adapter fittings. VCR and SAE connections upon request.

C. CR MAGNETICS DC CURRENT TRANSDUCER SPECIFICATIONS [62]

DC Current Transducer

DIN RAIL / PANEL MOUNT, RMS

SPECIFICATIONS

Basic Accuracy:	1.0 %	MTBF:	Greater than 100 K hours
Linearity:	10% to 100% FS	Output Load:	4-20 mADC - 0 to 300 Ω
Thermal Drift:	500 PPM/°C		0-5 VDC - 2K Ω or Greater
Operating Temperature:	0°C to +50°C	Relative Humidity:	5% to 95%, Non-Condensing
Installation Category:	CAT II	Supply Current:	
Vibration Tested To:	IEC 60068-2-6,1995	CR5210:	Typical 35mA Max 40mA
Pollution Degree:	2	CR5210S:	Typical 30mA Max 35mA
Response Time:	250 ms	CR5220:	Typical 60mA Max 100mA
Altitude:	2000 meter max.	CR5220S:	Typical 40mA Max 50mA
Insulation Voltage:	2500 VDC	Torque Specs.:	3.0 inch lbs. (0.4Nm)
Supply Voltage:	24 VDC ±10%	Weight:	0.5 lbs.
Frequency Range:	DC Only		
Cleaning:	Water-dampened cloth		

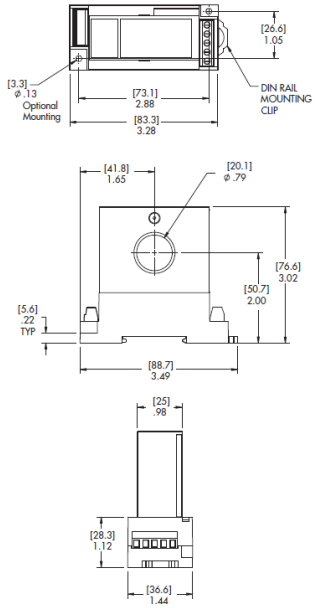

OUTLINE DRAWING

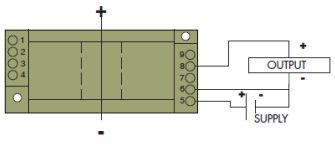

CR5210 5 VDC Output
CR5211 10 VDC Output

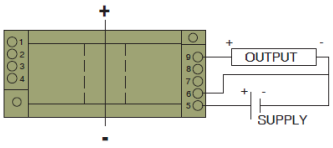

CR5220 4 - 20 mADC Output

CONNECTION DIAGRAM

NOTE: The building installation must have a switch or circuit-breaker that is in close proximity and within easy reach of the operator. The switch or circuit breaker shall be marked as the disconnecting device for the equipment.

The Professional Energy Monitoring Company
CR MAGNETICS
ISO 9001:2008 Quality Management System
3500 Scarlet Oak Blvd. St. Louis MO USA 63122 V: 636-343-8518 F: 636-343-5119
Web: http://www.crmagnetics.com 47 E-mail: sales@crmagnetics.com

C Transducers

D. NOSHOK INC ANALOG PRESSURE GAUGE SPECIFICATIONS [63]

NOSHOK

CERTIFICATE OF CALIBRATION

Traceable to N.I.S.T.

Customer:

McMaster-Carr Supply Company

9630 Norwalk Blvd

Santa Fe Springs CA 90670

UNITED STATES

Technician: dsabol

PO Number: FC-50441730

Sales Order Number: 528791

Certification Number: 70111592

Certification Date: 1/11/2017

Installation Date*: _____

**Date calibration cycle begins. Filled in by user based on installation date and users' QA program*

Calibration Due Date:** _____

***Date gauge is to be recertified. Filled in by user when gauge is installed*

Part Number:	40-500-3000-psi-CC-McMaster	**Accuracy:**	± 1% FS
UUT (psi)	**Actual Pressure**	**Hysteresis**	**Error (% of FS)**
500	515.77	0.00	-0.53%
1000	1013.16	0.00	-0.44%
1500	1521.13	0.00	-0.70%
2000	2026.38	0.00	-0.88%
2500	2522.98	0.00	-0.77%
3000	3015.76	0.00	-0.53%
2500	2514.14	-8.83	-0.47%
2000	2022.54	-3.84	-0.75%
1500	1520.68	-0.46	-0.69%
1000	1014.79	1.63	-0.49%
500	501.18	-14.59	-0.04%

Calibration Parameters:

Test Temperature: 70° ± 2°F

Test Humidity: Less than 70% RH

Pressure Media: Water / Alcohol Mix

Calibration Standard:

Model Number: 640-3000-2-35-2-47

Serial Number: 2243383

Accuracy: ±0.052% FS

Cal Due Date**: 8/1/2017

Approved: _____

**Applies only to calibration standard used for this certification

NOSHOK, Inc. | 1010 West Bagley Road | Berea, OH 44017 | Ph 440.243.0888 | Fax 440.243.3472 | www.noshok.com

ISO 9001:2015 REGISTERED

E. HONEYWELL MLH SERIES PRESSURE TRANSDUCER SPECIFICATIONS [64]

Heavy Duty Pressure Transducers

MLH Series, 6 bar to 550 bar | 50 psi to 8000 psi

Table 1. Pressure Range Specifications[1] (At 25 °C [77 °F] and at rated excitation unless otherwise specified.)

bar			psi		
Operating Pressure	Proof Pressure	Burst Pressure	Operating Pressure	Proof Pressure	Burst Pressure
6	18	60	50	150	500
10	30	100	100	300	1000
16	48	160	150	450	1500
25	75	250	200	600	2000
40	80	400	250	750	2500
60	120	600	300	900	3000
100	200	1000	500	1500	5000
160	320	1600	1000	2000	10000
250	500	2068	2000	4000	20000
350	700	2068	3000	6000	30000
500	750	2068	5000	7500	30000
550	825	2068	8000	12000	30000

[1] Comparable metric units follow same proof and burst specifications.

Table 2. Electrical Specifications

Characteristic	Output Signal					
	Ratiometric (A)	Current (B)	Regulated (C)	Regulated (D)	Regulated (E)	Regulated (G)
Zero output	0.5 Vdc	4 mA	1 Vdc	0.25 Vdc	0.5 Vdc	1 Vdc
Full scale span (FSS)	4 Vdc (0.5 Vdc to 4.5 Vdc)	16 mA (4 mA to 20 mA)	5 Vdc (1 Vdc to 6 Vdc)	10 Vdc (0.25 Vdc to 10.25 Vdc)	4 Vdc (0.5 Vdc to 4.5 Vdc)	4 Vdc (1 Vdc to 5 Vdc)
Excitation	5 Vdc (6 Vdc max.)[1]	9.5 Vdc to 30 Vdc[2]	8 Vdc to 30 Vdc[2]	14 Vdc to 30 Vdc[2]	7 Vdc to 30 Vdc[2]	8 Vdc to 30 Vdc[2]
Supply current	4 mA typ., 8 mA max.	N/A	5 mA typ., 17 mA max.	5 mA typ., 17 mA max.	5 mA typ., 17 mA max.	5 mA typ., 17 mA max.
Source (nominal)	1 mA	N/A	1 mA	1 mA	1 mA	1 mA
Sink (nominal	1 mA at zero output	N/A	1 mA at zero output	1 mA at zero output	1 mA at zero output	1 mA at zero output
Supply rejection ratio	90 dB	90 dB	90 dB	90 dB	90 dB	90 dB
Output impedance	25 Ohm max.	N/A	25 Ohm max.	25 Ohm max.	25 Ohm max.	25 Ohm max.

[1] Maintains ratiometricity at 5 ±0.25 Vdc excitation. Product can tolerate 6 Vdc excitation without damage.

[2] See Figures 1 and 2 for more information regarding maximum excitation voltage vs. operating temperature.

Table 3. Environmental and Mechanical Specifications

Characteristic	Parameter
Material in contact with media: port diaphragm	 stainless steel 304L Haynes 214 alloy
Housing material	black plastic – Amodel AS-4133 HS – PPA
Weight (typical for Metri-Pack 150 and 1/8 NPT pressure port types)	57.0 g [2.0 oz]
Shock	100 g peak [11 ms]
Vibration	MIL-STD-810C, Figure 514.2-5, Curve AK, Table 514.2-V, Random Vibration Test (overall g rms = 20.7 min.)
Compensated and operating temperature range: 0.5 Vdc to 4.5 Vdc ratiometric output all regulated and 4 mA to 20 mA outputs	 -40 °C to 125 °C [-40 °F to 257 °F] -40 °C to 125 °C [-40 °F to 257 °F] (See Figures 1 and 2 for operating area details.)
Storage temperature range	-40 °C to 125 °C [-40 °F to 257 °F]
Approvals	RoHS, CE, UL Component Recognition for USA and Canada: File No. E258956

Table 4. Performance Specifications (At 25 °C [77 °F] and under unless otherwise noted.)

Characteristic	Parameter
Response time	<2 ms
Accuracy[1]: ≥100 psi ≤100 psi	 ±0.25 %FSS ±0.50 %FSS
Total Error Band[2]: Gage: <300 psig ≥300 psig Sealed gage: ≥300 psis without **L, M, P** electrical connector types: 100 psis to 299 psis (-40 °C to 85 °C [-40 °F to 185 °F]) 100 psis to 299 psis (>85 °C to 125 °C [>185 °F to 257 °F]) ≥300 psis (-40 °C to 125 °C [-40 °F to 257 °F]) with **L, M, P** electrical connector types: 100 psis to 299 psis (-40 °C to 65 °C [-40 °F to 149 °F]) 100 psis to 299 psis (>65 °C to 125 °C [>149 °F to 257 °F]) ≥300 psis (-40 °C to 65 °C [-40 °F to 149 °F]) ≥300 psis (>65 °C to 125 °C [>149 °F to 257 °F])	 ±3 %FSS ±2 %FSS ±2 %FSS ±3 %FSS ±10 %FSS ±2 %FSS ±10 %FSS ±15 %FSS ±5 %FSS ±15 %FSS

[1] Includes pressure non-linearity (BFSL), pressure hysteresis and non-repeatability. Thermal errors are not included.

[2] Includes zero error, span error, thermal effect on zero, thermal effect on span, thermal hysteresis, pressure-non-linearity, pressure hysteresis and non-repeatability.

Figure 1. Operating and Temperature Compensation for All Regulated Output Options

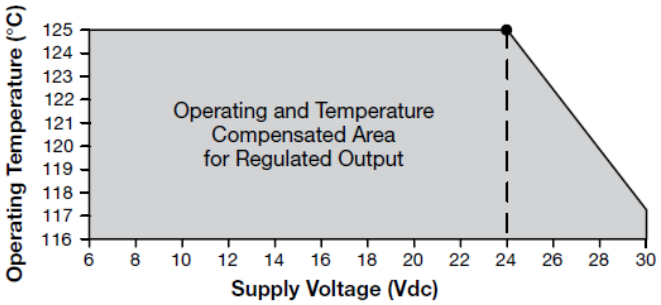

Note: Dot indicates the maximum operating temperature of 125 °C [257 °F] with a 24 V supply.

Figure 2. Operating and Temperature Compensation for 4 mA to 20 mA Output

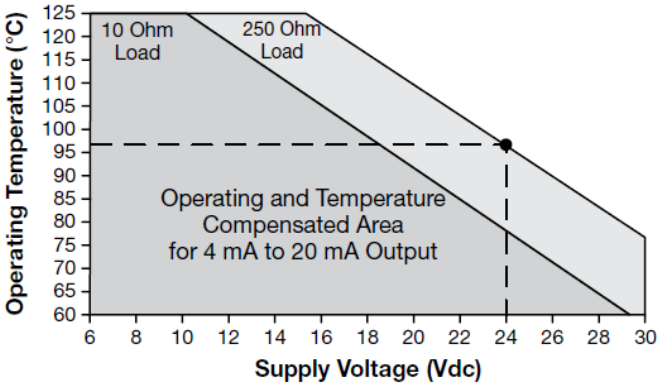

Note: The operating area is extended with a 250 Ohm resistor. Higher loads extend the operating area. Dot indicates the maximum operating temperature when using a 24 V supply and a 250 Ohm resistor.

F. WIKAI ANALOG TEMPERATURE GAUGE/BIMETAL THERMOMETER SPECIFICATIONS [65]

Certificate Number: SO00060907-1-1
Calibration Date: 9/15/2017
Date Entered Into Service:
Re-Calibration Date:

Pressure and Temperature Measurement
WIKA Instrument, LP
1000 Wiegand Boulevard
Lawrenceville, Georgia 30043

Tel. 770-513-8200
Fax. 770 338-5118
www.wika.com
info@wika.com

CERTIFICATE OF CALIBRATION

Customer: # Swagelok Co Region 4

WIKA S/O : # SO00060907 LINE 1

WIKA Model No:	T48L-040-DS-08-G-8-NTSS
Model Description:	TI.31 4.0 " 50/300 °F/C Glass 1/2"NPT DM NIST 316SS
Accuracy:	ASME B40.3 GRADE A
Tag-Number:	N/A
Serial Number:	81000F5G

Reference Standard:

Laboratory Standard:	DC 30 # 4	Accuracy:	0.01° C
Serial Number:	CN BC 1090	Calibration Date:	7/10/2017
		Calibration Due Date:	7/10/2018
Laboratory Standard:	DC 30 # 4	Accuracy:	0.01° C
Serial Number:	CN BC 1090	Calibration Date:	7/10/2017
		Calibration Due Date:	7/10/2018
Laboratory Standard:	4201 C	Accuracy:	0.025° C
Serial Number:	4201-C	Calibration Date:	7/5/2017
		Calibration Due Date:	7/5/2018

The thermometer described above was manufactured and tested in accordance with all applicable specifications as stated in ASME B40.3 and/or EN 13190 and was calibrated by comparison to laboratory standards traceable to the National Institute of Standards and Technology (NIST).

Standard Temperature	Thermometer Reading	Correction To Reading	
Celsius		Celsius	Pass/Fail
20	20.0	0.0	Pass
80	80.5	0.5	Pass
140	139.0	-1.0	Pass

Calibration Lab Tech: Janja Tadic

Quality Assurance: Erving Rivera

Page 1 of 1

ISO 9001 Certified

G. TYPE K THERMOCOUPLE PROBE SPECIFICATIONS [66]

Threaded Thermocouple Probe for Liquids & Gases

Type K, 3" Long

In stock
$67.03 E
1245N1

Type	K
Temperature Range	32° to 900° F
Probe	
Length	3"
Diameter	3/16"
Accuracy	±0.75%
Response Time	1 sec.
Cable Length	4 ft.
For Use With	Liquids, Gases
Connection Type	Wire Leads
Mount Type	Threaded
Sensor Type	Grounded
Probe Connection	
Pipe Size	1/2
Thread Type	NPT
Gender	Male
Maximum Pressure	Not Rated
Cable Material	Fiberglass
Probe Material	Stainless Steel
Maximum Cable Temperature	900° F
Wire	
Lead Length	3"
Gauge	24
RoHS	Compliant

For easy installation in thermowells, tanks, pipes, and other closed vessels, these thermocouples have an NPT male probe connection.

H. NATIONAL INSTRUMENTS NI 9211 ANALOG THERMOCOUPLE INPUT MODULE SPECIFICATIONS [67]

Input Characteristics

Number of channels	4 thermocouple channels, 1 internal autozero channel, 1 internal cold-junction compensation channel
ADC resolution	24 bits
Type of ADC	Delta-Sigma
Sampling mode	Scanned
Voltage measurement range	±80 mV
Temperature measurement ranges	Works over temperature ranges defined by NIST (J, K, T, E, N, B, R, S thermocouple types)
Conversion time	70 ms per channel; 420 ms total for all channels including the autozero and cold-junction channels
Common-mode voltage range	
Channel-to-COM	±1.5 V
COM-to-earth ground	±250 V
Common-mode rejection ratio (0 Hz to 60 Hz)	
Channel-to-COM	95 dB
COM-to-earth ground	>170 dB
Input bandwidth (-3 dB)	15 Hz
Noise rejection (at 50 Hz and 60 Hz)	85 dB minimum
Overvoltage protection	±30 V between any input and COM
Differential input impedance	20 MΩ
Input current	50 nA
Input noise	1 µVrms
Gain error (at -40 °C to 70 °C)	0.06% typical, 0.1% maximum
Offset error (with autozero channel on)	±15 µV typical, ±20 µV maximum
Gain error from source impedance	Add 0.05 ppm per Ω when source impedance >50 Ω
Offset error from source impedance	Add ±0.05 µV typical, ±0.07 µV maximum per Ω when source impedance >50 Ω

Cold-junction compensation sensor accuracy	
0 °C to 70 °C	±0.6 °C typical, ±1.3 °C maximum
-40 °C to 70 °C	±1.7 °C maximum
MTBF	633,012 hours at 25 °C; Bellcore Issue 2, Method 1, Case 3, Limited Part Stress Method

Temperature Measurement Accuracy

Measurement sensitivity[1]	
With autozero channel on	
Types J, K, T, E, N	<0.07 °C
Type B	<0.25 °C
Types R, S	<0.60 °C
With autozero channel off	
Types J, K, T, E, N	<0.05 °C
Type B	<0.20 °C
Types R, S	<0.45 °C

The following figures show the typical and maximum errors for each thermocouple type when used with the NI 9211 over the full temperature range and autozero on. The figures account for gain errors, offset errors, differential and integral nonlinearity, quantization errors, noise errors, and isothermal errors. The figures do not account for the accuracy of the thermocouple itself.

Figure 2. Thermocouple Type J and N Errors

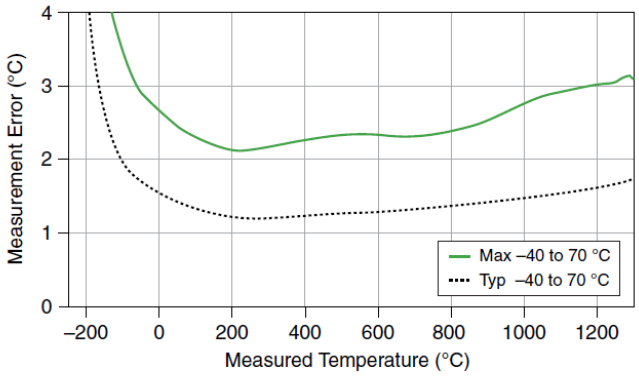

[1] Measurement sensitivity represents the smallest change in temperature that a sensor can detect. It is a function of noise. The values assume the full measurement range of the standard thermocouple sensor according to ASTM E230-87.

Figure 3. Thermocouple Type K Errors

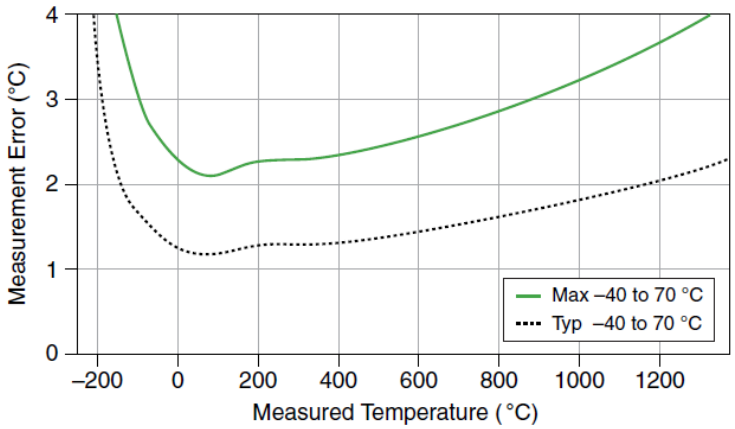

Figure 4. Thermocouple Type T and E Errors

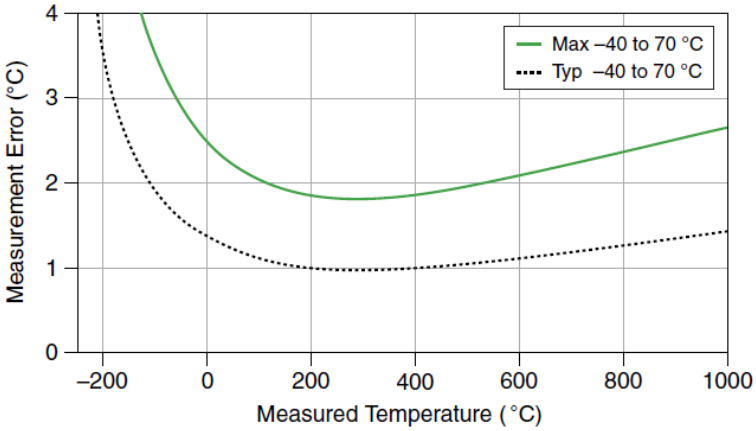

Figure 5. Thermocouple Type B Errors

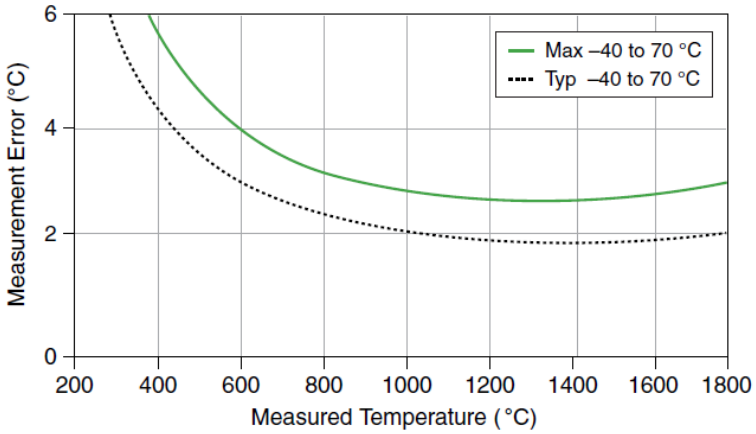

I. NATIONAL INSTRUMENTS NI 9215 ANALOG VOLTAGE INPUT SPECIFICATIONS [68]

NI 9215 Input Circuitry

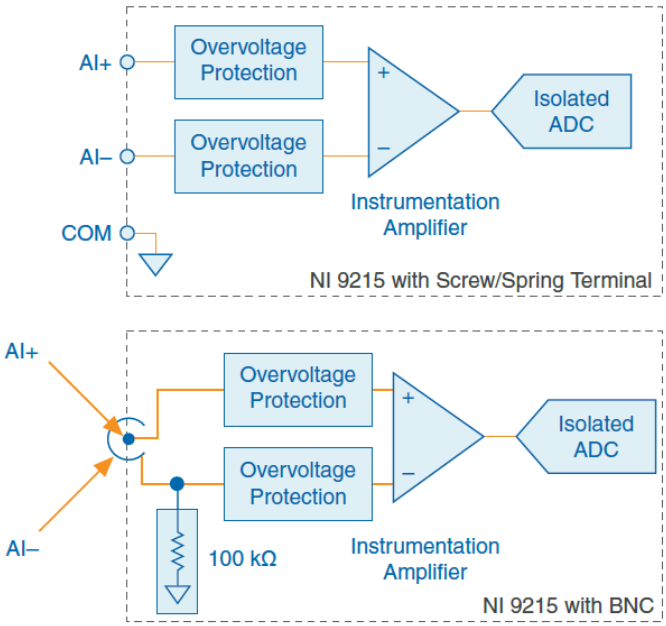

- Input signals on each channel are buffered, conditioned, and then sampled by an ADC.
- Each AI channel provides an independent track-and-hold amplifier, enabling you to sample all channels simultaneously.

NI 9215 Specifications

The following specifications are typical for the range -40 °C to 70 °C unless otherwise noted.

Caution Do not operate the NI 9215 in a manner not specified in this document. Product misuse can result in a hazard. You can compromise the safety protection built into the product if the product is damaged in any way. If the product is damaged, return it to NI for repair.

Input Characteristics

Number of channels	4 analog input channels
ADC resolution	16 bits
Type of ADC	Successive approximation register (SAR)
Input range	±10.0 V

Input Voltage Ranges	
Measurement Voltage, AI+ to AI-	
Minimum[1] (V)	±10.2
Typical (V)	±10.4
Maximum (V)	±10.6
Maximum Voltage (Signal + Common Mode)	
NI 9215 with screw terminal	Each channel must remain within ±10.2 V of common.
NI 9215 with spring terminal	Each channel must remain within ±10.2 V of common.
NI 9215 with BNC	All inputs must remain within 10.2 V of the average AI- inputs.
Overvoltage protection	±30 V
Conversion time	
Channel 0 only	4.4 µs
Channels 0 and 1	6 µs
Channels 0, 1, and 2	8 µs
Channels 0, 1, 2, and 3	10 µs

Table 1. Accuracy

Measurement Conditions		Percent of Reading (Gain Error)	Percent of Range[2] (Offset Error)
Calibrated	Maximum (-40 °C to 70 °C)	0.2%	0.082%
	Typical (23 °C ±5 °C)	0.02%	0.014%
Uncalibrated[3]	Maximum (-40 °C to 70 °C)	1.05%	0.82%
	Typical (23 °C ±5 °C)	0.6%	0.38%

Stability	
Gain drift	10 ppm/ºC
Offset drift	60 µV/ºC

[1] The minimum measurement voltage range is the largest voltage the NI 9215 is guaranteed to accurately measure.

[2] Range equals ±10.4 V.

[3] Uncalibrated accuracy refers to the accuracy achieved when acquiring in raw or unscaled modes where the calibration constants stored in the module are not applied to the data.

CMRR (f_{in} = 60 Hz)	73 dB min
Input bandwidth (-3 dB)	420 kHz minimum
Input impedance	
Resistance	
NI 9215 with screw terminal (AI-to-COM)	1 GΩ
NI 9215 with spring terminal (AI-to-COM)	1 GΩ
NI 9215 with BNC (Between any two AI- terminals)	200 kΩ
Input bias current	10 nA
Input noise	
RMS	1.2 LSB_{rms}
Peak-to-peak	7 LSB
Crosstalk	-80 dB
Settling time (to 2 LSBs)	
NI 9215 with screw terminal	
10 V step	10 µs
20 V step	15 µs
NI 9215 with spring terminal	
10 V step	10 µs
20 V step	15 µs
NI 9215 with BNC	
10 V step	25 µs
20 V step	35 µs
No missing codes	15 bits guaranteed
DNL	-1.9 to 2 LSB
INL	±6 LSB maximum
MTBF	1,167,174 hours at 25 °C; Bellcore Issue 6, Method 1, Case 3, Limited Part Stress Method

THIS PAGE INTENTIONALLY LEFT BLANK

LIST OF REFERENCES

[1] Aviles, A., 2016,"Renewable production of water, hydrogen, and power from ambient moisture," Masters Thesis, Department of Mechanical Engineering, Naval Postgraduate School, accessed April 15, 2017, https://calhoun.nps.edu/handle/10945/51584.

[2] U.S. Department of the Navy, 2012, "Department of the Navy Energy Program for Security and Independence Roles and Responsibilities," SECNAVINST 4101.3, Washington, DC, p.2.

[3] U.S. Department of Defense, 2014, "DOD Energy Policy," DoDD 4180.01, Washington, DC, p.1.

[4] Lipp, L., 2012, "Electrochemical Hydrogen Compressor." Final Scientific/Technical Report Under DOE Award Number DE-EE003727, FuelCell Energy, Inc.

[5] Parks, G., Boyd, R., Cornish, J., and Remick, R., 2014, "Hydrogen Station Compression, Storage, and Dispensing Technical Status and Costs," Technical Report NREL/BK-6A10-58564, p. 9, https://www.nrel.gov/docs/fy14osti/58564.pdf.

[6] Borgnakke, S., 2013, *Fundamentals of Thermodynamics* Seventh Edition, John Wiley and Sons, University of Michigan, Table 15.3.

[7] Dunlap, R., 2014, *Sustainable Energy* Cengage Learning Engineering, Stamford, CT, 1 ed., Table 20.3.

[8] Alternative Fuels Data Center, 2014, Data Chart, accessed September 9, 2017, https://www.afdc.energy.gov/fuels/fuel_comparison_chart.pdf.

[9] Parkash, S., 2010, *Petroleum Fuels Manufacturing Handbook: Including Specialty Products and Sustainable Manufacturing Techniques*, McGraw-Hill, Columbus, OH, p.1.

[10] Avallone, E., Baumeister III, T., and Sadegh, A., 2007, *Marks' Standard Handbook for Mechanical Engineers*, Eleventh Edition. McGraw-Hill, Columbus, OH, Table 7.1.8.

[11] Avallone, E., Baumeister III, T., and Sadegh, A., 2007, *Marks' Standard Handbook for Mechanical Engineers*, Eleventh Edition. McGraw-Hill, Columbus, OH, para 7.1.2.

[12] Avallone, E., Baumeister III, T., and Sadegh, A., 2007, *Marks' Standard Handbook for Mechanical Engineers,* Eleventh Edition. McGraw-Hill, Columbus, OH, Table 7.1.7.

[13] U.S. Department of Energy, 2017, *DOE Technical Targets for Fuel Cell Systems and Stacks for Transportation Applications,* Fuel Cell Technologies Office, Accessed September 9, 2017. https://energy.gov/eere/fuelcells/doe-technical-targets-fuel-cell-systems-and-stacks-transportation-applications.

[14] Reddy, T., 2011, *Linden's Handbook of Batteries*, Fourth Edition, McGraw-Hill, Columbus, OH, Table 1.2.

[15] Dunlap, R., 2014, *Sustainable Energy Cengage Learning Engineering,* Stamford, CT, 1 ed., Table 19.1.

[16] Avallone, E., Baumeister III, T., and Sadegh, A., 2007, *Marks' Standard Handbook for Mechanical Engineers,* Eleventh Edition. McGraw-Hill, Columbus, OH, Section 9.1.12.

[17] U.S. Department of Energy, Fuel Cell Technologies Office, Hydrogen Storage website, Accessed 25 October 2017, https://energy.gov/eere/fuelcells/hydrogen-storage.

[18] Dawson, V., and Bowles, M., 2004, Taming Liquid Hydrogen: The Centaur Upper Stage Rocket 1958–2002, National Aeronautics and Space Administration, Washington, DC, pp.v-vii.

[19] Stetson, N., 2017, Hydrogen Storage Program Overview, U.S. Department of Energy, FY 2016 Annual Progress Report, Washington, DC, p.7.

[20] U.S. Naval Observatory, 2017, "Monterey, California Rise and Set for the Sun for 2017," Astronomical Applications Department, Washington, DC, accessed April 20, 2017, http://aa.usno.navy.mil/cgi-bin/aa_rstablew.pl?ID=AA&year=2017&task=0&state=CA&place=monterey.

[21] Yu, S., 2017, "Analysis of an Improved Solar-Powered Hydrogen Generation System for Sustained Renewable Energy Production," Masters Thesis, Department of Mechanical Engineering, Naval Postgraduate School, Monterey, CA.

[22] Capstone Turbine Corp., 2016, "DOE Funds Argonne National Lab to Test Capstone Microturbines with Hydrogen and Synthetic Fuels," Press Release, Chatsworth, CA, accessed October 15, 2017, https://ir.capstoneturbine.com/press-releases/detail/3506/doe-funds-argonne-national-lab-to-test-capstone.

[23] Capstone Turbine Corp., 2002, "Technical Specifications and Descriptions for a Single Capstone Microturbine," Product Specification, Chatsworth, CA, accessed October 15, 2017, http://www.capstone.ru/imgcompany/capstone/pdf/ProductSpecification.pdf.

[24] Darrow, K., Tidball, R., Wang, J., and Hampson, A., 2017, "Catalog of CHP Technologies Section 5. Technology Characterization – Microturbines," U.S. Environmental Protection Agency Combined Heat and Power Partnership, accessed October 19, 2017, https://www.epa.gov/sites/production/files/2015-07/documents/catalog_of_chp_technologies_section_5._characterization_-_microturbines.pdf.

[25] American Institute of Chemical Engineers, *Center for Chemical Process Safety, 2009, Inherently Safer Chemical Processes: A Life Cycle Approach,* John Wiley and Sons, Inc., New York, p.9.

[26] Compressed Gas Association Inc., 2011, "CGA G-5-2011 Hydrogen," Chantilly, VA, p.1.

[27] Crowl, D., 2003, *Understanding Explosions*, Center for Chemical Process Safety, New York, New York, pp.122-125.

[28] Compressed Gas Association Inc., 2012, "CGA G-5.4-2012 Standard for Hydrogen Piping Systems at User Locations," Chantilly, VA, p.7.

[29] Crowl, D., 2012, Minimize the Risks of Flammable Materials, American Institute of Chemical Engineers, CEP, p.30.

[30] Early, M., Coache, C., Cloutier, M., Moniz, G., and Vigstol, D., 2016, *National Electrical Code Handbook*, Fourteenth Edition, National Fire Protection Association, Quincy, Massachusetts, p.587.

[31] National Fire Protection Association, 2016, *NFPA 2 Hydrogen Technologies* Code 2016 Edition, Quincy, MA, pp. 2–45.

[32] Compressed Gas Association Inc., 2012, "CGA G-5.4-2012 Standard for Hydrogen Piping Systems at User Locations," Chantilly, VA, p.2.

[33] Nayyar, M., 2000, *Piping Handbook,* Seventh Edition. McGraw-Hill Professional, Columbus, OH, Section B8.4.

[34] National Institute of Standards and Technology, "NIST Reference Fluid Thermodynamic and Transport Properties Database (REFPROP)," Version 8.0, accessed April 24, 2017. https://h2tools.org/hyarc/data/hydrogen-properties.

[35] Avallone, E., Baumeister III, T., and Sadegh, A., 2007, *Marks' Standard Handbook for Mechanical Engineers,* Eleventh Edition. McGraw-Hill, Columbus, OH, Chapter 8.7 Pipe, Pipe Fittings, and Valves.

[36] Swagelok, 2017, "Tubing Data," product specifications, pp.4-5, accessed October 10, 2017, https://www.swagelok.com/downloads/webcatalogs/en/MS-01-107.pdf.

[37] American Society of Mechanical Engineers, 2015, "ASME B31.12 Hydrogen Piping and Pipelines," New York, NY, IP-5.5.3 Tubing Joints, p.95.

[38] National Fire Protection Association, 2016, *NFPA 2 Hydrogen Technologies Code* 2016 Edition, Quincy, MA, pp.2-27.

[39] National Fire Protection Association, 2016, NFPA 2 *Hydrogen Technologies Code* 2016 Edition, Quincy, MA, pp.2-27. pp. 2–38-2-45.

[40] Pratt, J., Terlip, D., Ainscough, C., Kurtz, J., and Elgowainy, A., 2015, "H2First Reference Station Design Task Project Deliverable 2–2," National Renewable Energy Laboratory Technical Report, NREL/TP-5400-64107, p.34.

[41] RIX Industries, 2016, "Hydrogen Compressors Sales Sheets," accessed 20 November 2016, http://www.rixindustries.com/industrial-compressors/hydrogen-compressors.

[42] PDC Machines,2016, "Diaphragm Compressor Brochure," accessed 20 November 2016, http://www.pdcmachines.com/diaphragm-compressors/brochure.

[43] Hydro-PAC, Inc, 2016, "Compressor Brochure," accessed 20 November 2016, http://www.hydropac.com/literature.html.

[44] Tzimas, E., Filiou, C., Peteves, S.D., and Veyret, J.-B, 2003, Hydrogen Storage: State-of-the-art and Future Perspective, European Commission, Directorate General Joint Research Center, Institute for Energy, Petten, The Netherlands, p. 29.

[45] Parker Hannifin Corp, "High Pressure Filters," Catalog, Filtration and Separation Division Bulletin 1300–997/USA, Oxford, MI, p.24.

[46] National Renewable Energy Laboratory (NREL), 2016, "Hydrogen Compressor Reliability Investigation and Improvement," Cooperative Research and Development (CRADA) Final Report CRD-13-514, p.1.

[47] U.S. Department of Defense, 2017, DOD Facilities Pricing Guide, Unified Facilities Criteria (UFC) 3–701-01, Washington, DC, pp. 6–7, accessed November 6, 2017, https://www.wbdg.org/ffc/dod/unified-facilities-criteria-ufc/ufc-3-701-01.

[48] Naval Facilities Engineering Command, 2017, Internet Navy Facilities Asset Data Store (iNFADS), Database, query date August 16, 2017.

[49] California Independent System Operator, 2017, "Historical Curtailment," graphic, accessed November 7, 2017, http://www.caiso.com/informed/Pages/ManagingOversupply.aspx.

[50] Fuel Cells and Hydrogen Joint Undertaking, 2017, Projects Key Figures, website, accessed November 6, 2017, http://www.fch.europa.eu/page/key-figures.

[51] Fuel Cells and Hydrogen Joint Undertaking, 2015, "ELYGRID," Final Report, accessed November 6, 2017, http://www.fch.europa.eu/sites/default/files/project_publisheable_reports/278824_ELYGRID_Final_Report-12_20150218_125803_CET.3-24.pdf.

[52] European Commission, 2016, "FCH-01-8-2016 - Development of innovative hydrogen compressor technology for small scale decentralized applications for hydrogen refuelling or storage," program summary, accessed November 6, 2017, http://cordis.europa.eu/programme/rcn/700839_en.html.

[53] Richardson, J., 2017, "The Future Navy," White Paper, Washington, DC, p. 6, accessed November 6, 2017, http://www.navy.mil/navydata/people/cno/Richardson/Resource/TheFutureNavy.pdf.

[54] Intelligent Energy P.L.C., 2017, "UAV Fuel Cell Module," brochure, Loughborough, GB, accessed November 6, 2017, http://www.intelligent-energy.com/uploads/product_docs/Final_UAV_brochure_web_version.pdf.

[55] North Atlantic Treaty Organization (NATO) Energy Security Center of Excellence, June 29, 2017 briefing.

[56] Richards, L., 2017, "Energy, Utility, and Emergency Response Solutions Using Unmanned Aerial Systems," proposal made at ESTEP Program Review, Naval Postgraduate School, July 27, 2017.

[57] Lovelace, B., 2015, "Unmanned Aerial Vehicle Bridge Inspection Demonstration Project," Research Project Final Report 2015–40, Minnesota Department of Transportation, Office of Transportation System Management, accessed November 6, 2017, http://www.dot.state.mn.us/research/TS/2015/201540.pdf.

[58] Platzer, M., and Sarigul-Klijn, N., 2015, Energy Ships and Plug-in Hybrid Electric Vehicles: Are they the Key for a Rapid Transition to and Emission-Free Economy?, ASME 2015 International Mechanical Engineering Congress and Exposition Proceedings IMECE2015-50652, Houston, TX.

[59] Pelz, P., Holl, M., and Platzer, M., 2015, Analytical Method Towards and Optimal Energetic and Economical Wind-Energy Converter, Energy, 95.

[60] National Instruments, 2017, “cDAQ™-9185,” Specifications, accessed December 4, 2017, http://www.ni.com/pdf/manuals/376606a.pdf.

[61] Alicat, 2017, “Technical Data for Alicat M-Series Mass Flow Meters,” Specifications, accessed December 4, 2017, http://www.alicat.com/documents/specifications/Alicat_Mass_Meter_Specs.pdf.

[62] CR Magnetics, 2017, “DC Current Transducer,” Specifications, accessed December 4, 2017, http://www.crmagnetics.com/Assets/ProductPDFs/CR5200%20Series.pdf.

[63] NOSHOK, 2017, “400/500 Series All Stainless Steel Pressure Gauges,” Specifications, accessed December 4, 2017, http://www.noshok.com/400-500-series-ss-specs.shtml.

[64] Honeywell, 2017, “Heavy Duty Pressure Transducers,” Specifications, accessed December 4, 2017, https://sensing.honeywell.com/honeywell-sensing-heavy-duty-pressure-transducers-mlh-series-datasheet-008118-8-en.pdf.

[65] Wikai, 2017, “Bimetal Thermometer,” Specifications, accessed December 4, 2017, http://www.wika.us/upload/DS_TMTI_31_en_us_16144.pdf.

[66] McMaster-Carr, 2017, “Threaded Thermocouple Probe for Liquids & Gases,” Specifications, accessed December 4, 2017, https://www.mcmaster.com/#1245n12/=1ag1nx0.

[67] National Instruments, 2017, “NI 9211 Analog Thermocouple Input,” Specifications, accessed December 4, 2017, http://www.ni.com/pdf/manuals/373466a_02.pdf.

[68] National Instruments, 2017, “NI 9215 Analog Voltage Input,” Specifications, accessed December 4, 2017, http://www.ni.com/pdf/manuals/373779a_02.pdf.

INITIAL DISTRIBUTION LIST

1. Defense Technical Information Center
   Ft. Belvoir, Virginia

2. Dudley Knox Library
   Naval Postgraduate School
   Monterey, California